



THESIS
2
2008

This is to certify that the
dissertation entitled

MODIFICATION OF POLYLACTIDE BIOPLASTIC USING
HYPERBRANCHED POLYMER BASED
NANOSTRUCTURES

presented by

Rahul Bhardwaj

has been accepted towards fulfillment
of the requirements for the

Ph.D. degree in Packaging



Amar Kumar Mohanty

Major Professor's Signature

12-19-2007

Date

PLACE IN RETURN BOX to remove this checkout from your record.
TO AVOID FINES return on or before date due.
MAY BE RECALLED with earlier due date if requested.

DATE DUE	DATE DUE	DATE DUE
APR 12 2011 03 10 11		

•
**MODIFICATION OF POLYLACTIDE BIOPLASTIC USING HYPERBRANCHED
POLYMER BASED NANOSTRUCTURES**

By

Rahul Bhardwaj

A DISSERTATION

**Submitted to
Michigan State University
in partial fulfillment of the requirements
for the degree of**

DOCTOR OF PHILOSOPHY

School of Packaging

2008

ABSTRACT

MODIFICATION OF POLYLACTIDE BIOPLASTIC USING HYPERBRANCHED POLYMER BASED NANOSTRUCTURES

By

Rahul Bhardwaj

Poly lactide (PLA) is the most well known renewable resource based biodegradable polymer. The inherent brittleness and poor processability of PLA pose considerable technical challenges and limit its range of commercial applications. The broad objective of this research was to investigate novel pathways for polylactide modification to enhance its mechanical and rheological properties. The focus of this work was to tailor the architecture of a dendritic hyperbranched polymer (HBP) and study its influence on the mechanical and rheological properties of PLA bioplastic. The hyperbranched polymers under consideration are biodegradable aliphatic hydroxyl-functional hyperbranched polyesters having nanoscale dimensions, unique physical properties and high peripheral functionalities.

This work relates to identifying a new and industrially relevant research methodology to develop PLA based nanoblends having outstanding stiffness-toughness balance. In this approach, a hydroxyl functional hyperbranched polymer was crosslinked in-situ with a polyanhydride (PA) in the PLA matrix during melt processing, leading to the generation of new nanoscale hyperbranched polymer based domains in the PLA matrix. Transmission electron microscopy and atomic force microscopy revealed the “sea-island” morphology of PLA-crosslinked HBP blends. The domain size of a large portion of the crosslinked HBP particles in PLA matrix was less than 100 nm. The presence of crosslinked hyperbranched polymers exhibited more than 500% and 800%

improvement in the tensile toughness and elongation at break values of PLA, respectively, with a minimal sacrifice of tensile strength and modulus as compared to unmodified PLA. The toughening mechanism of PLA in the presence of crosslinked HBP particles was comprised of shear yielding and crazing. The volume fraction of crosslinked HBP particles and matrix ligament thickness (inter-particle distance) were found to be the critical parameters for the toughening of PLA. The maximum average matrix ligament thickness was 114 nm for a toughened polylactide nanoblend and correlated well with the theoretical prediction of the matrix ligament thickness.

Fourier transform infrared spectroscopy and dynamic mechanical thermal analysis proved the crosslinking of the HBP phase in the PLA matrix. The crosslinked HBP was effective at hydroxyl (-OH) to anhydride molar ratios of: 2:1, 1:1 or 1:2. The glass transition temperature values of the crosslinked HBP phase at these molar ratios were observed to deviate from the predictions made by the Fox equation. The hydrophilic nature of the hyperbranched polymer was altered to hydrophobic by incorporation of polyanhydride crosslinker, as demonstrated by the increase in the contact angle with water. Rheological studies showed that there was a network formation in the PLA matrix after in-situ crosslinking of HBP. The HBP was found to reduce the melt viscosity of PLA dramatically and this effect was maintained even after its in-situ crosslinking in the PLA matrix.

Finally, the current research unwraps the new opportunities provided by the unique physical and chemical properties of highly functional hyperbranched polymers in generating new nanostructured multiphase polymer systems with enhanced properties.

To my Parents, and Brother Rajiv

ACKNOWLEDGEMENTS

It is giving me an immense pleasure to express my gratitude to all, who have contributed and supported me in the completion of this dissertation. First of all, I like to express my sincere thanks to my advisor: Dr. Amar K. Mohanty for enabling me to achieve this feat. Your constant motivation, support and confidence in my abilities have propelled me to finish this piece of research work. Your astute comments and inputs have been a remarkable contribution to this work. I am thankful to my committee members: Dr. Lawrence Drzal, Dr. Susan E. Selke and Dr. Bruce Harte for their thorough reviews, suggestions, and constructive criticism that helped immensely in improving the scope of this dissertation. I am thankful to US National Science Foundation for providing me the financial support for my research under NSF award DMI-0400296. I am also thankful to college of agriculture and natural resources (CANR) and the graduate school at MSU for awarding me the dissertation completion fellowship.

I am thankful to Dr. Manjusri Misra for her constant support and inputs during my doctoral work. I am extremely thankful to my friends and colleagues from Dr. Mohanty's research group: Sanjeev Singh, Yash Parulekar, Edward Drown, Dinesh Aithani, Mariappan Chidambarakumar, Dr. Hiroaki Miyagawa, Dr. Qiangxian Wu, Abhishek Singh, Ajay Kathuria, and Dhiraj Hasija for their help in experiments and engaging in several discussions on my research. I am also thankful to Alicia Pastor-Lecha, Ewa Danielewicz, Carol Flegler, Per Askeland, Mike Rich, Brian Rook, Hazel-Ann Hosein and Kelby Thayer for their assistance in several processing and characterization techniques. I want to express my special thanks to my friends: Mahesh, Raj, Rajesh, Tejveer, and Anand for their constant motivation and support.

Finally, thanks or gratitude is just not suitable word to express my appreciation to my parents. Their unparalleled support and motivation have enabled me to achieve beyond my capabilities. I am especially thankful to the pillar of my family, my brother: Rajiv for standing by me during my journey to this dissertation and many more things. I am thankful to my sister, brother-in-law, and sister-in-law for providing me the encouragement. I am also thankful to my fiancé Gaytri for being a moral support to me. Last but not the least, I am grateful to my loving niece Saachi for being a stress buster during the ups and down of my research.

Rahul Bhardwaj

East Lansing, MI

December 18, 2007

TABLE OF CONTENTS

LIST OF TABLES.....	x
LIST OF FIGURES.....	xii
KEY TO SYMBOLS OR ABBREVIATIONS.....	xvi
Chapter 1: Introduction.....	1
1.0 Introduction.....	1
1.1 Thesis Structure.....	5
1.2 References.....	7
Chapter 2: Literature Review.....	10
2.0 Preparation and Structure of Polylactides.....	10
2.1 Properties and Deformation of Polylactides.....	15
2.2 Rheology of Polylactides.....	21
2.3 Current Methods to Modify Polylactide Properties.....	23
2.3.1 Copolymerization.....	23
2.3.2 Plasticization.....	24
2.3.3 Blending.....	27
2.3.4 Polylactide based Nanocomposites.....	34
2.4 Hyperbranched Polymers (HBP).....	42
2.5 Toughening of Polymers.....	46
2.5.1 Rubber Toughening.....	49
2.5.2 Toughening Mechanism.....	50
2.5.3 Brittle to Ductile Transition (BDT) Criteria.....	52
2.6 Alternate Ways of Toughening of Polymers.....	54
2.6.1 Interpenetrating Networks.....	54
2.6.2 Nanostructure Blending.....	55
2.7 References.....	58
Chapter 3: Modification of Brittle Polylactide (PLA) by Novel Hyperbranched Polymer based Nanostructures.....	73
3.0 Introduction.....	73
3.1 Experimental Section.....	75
3.1.1 Materials.....	75
3.1.2 Reactive Extrusion.....	76
3.1.3 Testing and Characterization.....	79
3.1.3.1 Ultracentrifugation.....	79
3.1.3.2 Fourier Transform Infrared Microscopy (FTIR).....	80
3.1.3.3 Dynamic Mechanical Thermal Analysis (DMTA).....	81
3.1.3.4 Parallel Plate Rheology.....	81
3.1.3.5 Transmission Electron Microscopy (TEM).....	81

3.1.3.6 Atomic Force Microscopy (AFM).....	81
3.1.3.7 Tensile Properties.....	82
3.1.3.8 Scanning Electron Microscopy (SEM).....	82
3.2 Results and Discussion.....	82
3.2.1 Solvent Extraction, Morphology and Fourier Transform Infrared Spectroscopy.....	82
3.2.2 Dynamic Mechanical Thermal Analysis.....	86
3.2.3 Rheological Evidence of Networked Interface between PLA and Crosslinked HBP.....	88
3.2.4 Complex Viscosity.....	89
3.2.5 Transmission Electron Microscopy (TEM).....	91
3.2.6 Atomic Force Microscopy (AFM).....	94
3.2.7 Tensile Properties.....	96
3.2.8 Mode of Deformation of PLA-crosslinked HBP Blend under Tensile Loading.....	98
3.2.9 Scanning Electron Microscopy (SEM).....	104
3.3 References.....	106

Chapter 4: Effect of the Concentration of Crosslinker on the Properties of PLA/in-situ Crosslinked HBP Blends.....109

4.0 Introduction.....	109
4.1 Experimental Section.....	110
4.1.1 Materials.....	110
4.1.2 Preparation of PLA-cHBP Blends.....	111
4.1.3 Testing and Characterization.....	112
4.1.3.1 Dynamic Mechanical Analysis.....	112
4.1.3.2 Ultracentrifugation and Fourier Transform Infrared Spectroscopy.....	112
4.1.3.3 Tensile Testing.....	113
4.1.3.4 Transmission Electron Microscopy (TEM).....	113
4.1.3.5 Contact Angle Measurements.....	113
4.1.3.6 Gel Permeation Chromatography (GPC).....	114
4.2 Results and Discussion.....	114
4.2.1 Dynamic Mechanical Thermal Analysis.....	114
4.2.2 Ultra-Centrifugation and Fourier Transform Infrared Spectroscopy of Crosslinked HBP.....	118
4.2.3 Tensile Properties.....	121
4.2.4 Transmission Electron Microscopy (TEM).....	124
4.2.5 Contact Angle Measurements.....	127
4.2.6 Effect of Processing, Presence of HBP and Crosslinked HBP on the Molecular Weight of PLA.....	129
4.3 References.....	131

Chapter 5: Phase Morphology and Brittle-to-Ductile Transition in PLA-crosslinked HBP Blends.....133

5.0 Introduction.....	133
-----------------------	-----

5.1 Experimental Section.....	135
5.1.1 Reactive extrusion for fabrication of PLA-cHBP Blends.....	135
5.1.2 Testing and Characterization.....	136
5.1.2.1 Transmission Electron Microscopy (TEM).....	136
5.1.2.2 Particle Size Analysis.....	136
5.1.2.3 Density and Volume Fraction of Crosslinked HBP Particles.....	137
5.1.2.4 Tensile Properties.....	138
5.1.2.5 Scanning Electron Microscopy (SEM).....	138
5.2 Results and Discussions.....	138
5.2.1 Phase morphology of PLA-crosslinked HBP Blends.....	138
5.2.2 Mechanical Properties and Deformation Mechanism of PLA-crosslinked HBP Blend.....	143
5.2.3 Particle Size Analysis.....	151
5.2.4 Brittle-to-Ductile Transition in PLA-crosslinked HBP Blend.....	153
5.3 References.....	159
Chapter 6: Conclusions and Recommendations for Future Work.....	161
6.1 Conclusions.....	161
6.2 Recommendations for Future Work.....	163
7: Appendix: Density of NaCl Salt Solutions of Different Concentrations.....	165

LIST OF TABLES

Table 2.1	Comparison of mechanical and thermo-mechanical properties of PLAs with conventional polymers; here M_v – molecular weight (Adopted after ref. no. 3, 13-17).....	16
Table 2.2	Properties of PLA and some other biopolymers. (After ref. no. 2, 18-23).....	17
Table 2.3	Typical differences in the characteristics of a linear and dendritic polymer (After ref. 130).....	43
Table 3.1	Processing parameters of neat PLA and its blend with hyperbranched polymer (HBP), in-situ crosslinked HBP and poly(anhydride) (PA).....	79
Table 3.2	The solution behavior of PLA and its blends after dissolving in methylene dichloride.....	83
Table 3.3	Mechanical properties of neat PLA and its blends.....	97
Table 4.1	Processing parameters of neat PLA and its blends.....	111
Table 4.2	Estimation of amount of crosslinked hyperbranched polymer (using equation 4.1) formed in various PLA blends after in-situ crosslinking of hyperbranched polymer with different concentration of poly(anhydride).....	119
Table 4.3	Effects of HBP/PA ratio on the tensile properties of PLA-cHBP blends.....	122
Table 4.4	Contact angle of various materials with water	128
Table 5.1	Details of various PLA based compositions and their processing parameters.....	135
Table 5.2	Effects of amount of crosslinked hyperbranched polymer of OH /anhydride ratio (1:1) on the tensile properties of PLA-cHBP Blends.....	144
Table 5.3	Particle size characteristics of crosslinked HBP particles in PLA-cHBP blends.....	151

Table 5.4	Comparison of experimental matrix ligament thickness with theoretical values for toughened nanoblends; here type A: PLA/HBP/PA (88/9.7/2.3. type B: PLA/HBP/PA (92/6.4/1.6).....	157
-----------	--	-----

LIST OF FIGURES

Figure 2.1	General chemical structure of PLA.....	10
Figure 2.2	Stereochemical structures: A: Lactic acid; B: Lactides.....	11
Figure 2.3	The schematic of formation of a PLA prepolymer, lactide and conversion of lactide in PLA. (redrawn after ref. no.7).....	12
Figure 2.4	Conversion of lactide in to PLA via coordination insertion mechanism in presence of tin octoate, Sn (Oct) ₂ , here R= growing polymer chain (redrawn after ref. no.7).....	12
Figure 2.5	A typical stress-strain curve of poly (L-lactide), PLLA obtained at a crosshead speed of 15.4 mm/min at ambient conditions (25°C).....	18
Figure 2.6	Schematic representation of the difference in the morphology of dendrimer (monodisperse) and Hyperbranched polymer (polydisperse). Redrawn after ref. 133. Here (●) represents central core and (△) represents end groups.....	44
Figure 2.7	Schematic of Matrix Ligament Thickness. (Redrawn after ref. 162).....	52
Figure 2.8	Schematic of stress volume sphere around a rubber particle. Here shaded area represents a rubber particle. (Redrawn after ref. 146).....	53
Figure 2.9	Schematic representation of method of preparation of conventional blends and nanostructure blends. (Redrawn after Ref. 178).....	57
Figure 3.1	(A) Chemical structure of the chief constituent of hyperbranched polymer (HBP). (B) Chemical structure of polyanhydride (PA)....	77
Figure 3.2	Schematic illustrations of in-situ crosslinking of hyperbranched polymer (HBP) in PLA melt with the help of a polyanhydride (PA). (After ref. 25).....	78
Figure 3.3	SEM photomicrographs of extracted crosslinked HBP particles.....	84
Figure 3.4	FTIR spectrum: A: Neat PLA; B: HBP-PA particles (Extracted), C: HBP-PA particles (Outside); D: Hyperbranched polymer (HBP); E: Polyanhydride (PA).....	84
Figure 3.5	Temperature dependence of the loss modulus (E'') of: (A) neat PLA, (B) PLA/HBP (92/08), and (C) PLA/HBP/PA (92/5.4/2.6) blends.....	87

Figure 3.6	Behavior of storage modulus, G' of neat PLA and its blend as a function of oscillatory frequency (ω).....	88
Figure 3.7	Variation of complex viscosity, η^* , of neat PLA and its blend as function of oscillatory frequency (ω).....	90
Figure 3.8	Transmission electron micrograph of PLA having 8 wt.% of pristine HBP. (Scale bar: 50 nm).....	92
Figure 3.9	Transmission electron micrographs of PLA having crosslinked HBP 3.8A: Scale bar: 200 nm; 3.8B: Scale bar: 100 nm.....	93
Figure 3.10	Tapping mode AFM phase image of PLA/HBP/PA(92/5.4/2.6)blend 3.10A: Scan size: 10 μm ; 3.10B: Scan size: 5 μm	95
Figure 3.11	Stress-strain curves obtained at a crosshead speed of 15.4 mm/min.....	96
Figure 3.12	Tensile specimens after testing to failure at 15.4 mm/min under uniaxial tension.....	99
Figure 3.13:	TEM photomicrograph of deformed region of neat PLA. The arrow indicates the tensile load direction (Scale bar: 2 μm).....	100
Figure 3.14	TEM photomicrograph of deformed region of modified PLA; 3.14A: Extension of crazes; 3.14 (scale bar: 2 μm); 3.14B: Extension of crosslinked HBP. The arrow indicates the tensile load direction.(scale bar: 500nm).....	101
Figure 3.15	Schematic illustration of different stages of mechanical deformation process of PLA in presence of crosslinked HBP particles.....	103
Figure 3.16	Scanning electron micrographs of tensile fractured surfaces: 3.16A: Neat PLA; 3.16B: PLA/HBP (92/08); 3.16C: PLA/HBP/PA (92/5.4/2.6).....	105
Figure 4.1	Effect of OH to anhydride molar ratio on the glass transition temperature of crosslinked HBP phase in PLA blends where, A: OH/anhydride (4:1); B: OH/anhydride (3:1); C: OH/anhydride (2:1); D: OH/anhydride (1:1) and E: OH/anhydride (1:2).....	115
Figure 4.2	Temperature dependency of loss modulus of neat PLA and its blends with HBP and in- situ crosslinked HBP: (A) Neat PLA; (B) PLA/HBP (92/08); (C) PLA/HBP/PA (92:7.1:0.9) OH to anhydride 2:1; (D) PLA/HBP/PA (92:7.1:0.9) OH to anhydride 1:1; (E): PLA/HBP/PA (92:7.1:0.9)	

	OH to anhydride 1:2.....	117
Figure 4.3	FTIR spectrum: A: Polyanhydride; B: HBP, C: Extracted HBP-PA (2:1); D: Extracted HBP-PA (1:1); E: Extracted HBP-PA (1:2); F: Neat PLA.....	120
Figure 4.4	Effect of weight of crosslinked HBP particles on the elongation at break value of PLA-cHBP blends.....	123
Figure 4.5	TEM photo-micrographs (Scale bar: 500 nm) A: PLA/HBP/PA (92:7.55:0.45) OH to anhydride, 4:1 B: PLA/HBP/PA (92:7.4:0.6) OH to anhydride, 3:1.....	125
Figure 4.6	TEM photo-micrographs (Scale bar: 500 nm) A: PLA/HBP/PA (92:7.1:0.9) OH to anhydride, 2:1 B: PLA/HBP/PA (92:6.4:1:6) OH to anhydride, 1:1.....	126
Figure 4.7	TEM photomicrograph (Scale bar: 500 nm)of PLA/HBP/PA (92/5.4/2.6).....	127
Figure 4.8	Molecular weight and polydispersity of PLA in various processing conditions, and in presence of HBP and crosslinked HBP: A: Neat PLA; B: PLA (3 min.); C: PLA (10min.); D: PLA/HBP (92/08); E: PLA/HBP/PA (92:7.1:0.9) OH to anhydride 2:1; F: PLA/HBP/PA (92:7.1:0.9) OH to anhydride 1:1; G: PLA/HBP/PA (92:7.1:0.9) OH to anhydride 1:2.....	129
Figure 5.1:	Transmission Electron Photomicrograph (Scale bar: 500nm); A: (PLA/HBP/PA(98/1.6/0.4) B: PLA/HBP/PA(96/3.2/0.8).....	139
Figure 5.2	Transmission Electron Photomicrograph (Scale bar: 500 nm) A: PLA/HBP/PA (92/6.4/1.6) B: PLA/HBP/PA (88/9.7/2.3).....	140
Figure 5.3	TEM photomicrograph (Scale bar: 500 nm) of PLA/HBP/PA (84/12.9/3.1).....	141
Figure 5.4	Stress – strain curves of neat PLA and various PLA-cHBP blends obtained at a strain rate of 15.4 mm/mm min; A: Neat PLA; B: PLA/HBP/PA (98/1.6/0.4); C: PLA/HBP/PA (96/3.2/0.8); D: PLA/HBP/PA (92/6.4/1.6); E: PLA/HBP/PA (88/9.7/2.3); F: PLA/HBP/PA (84/12.9/3.1).....	145
Figure 5.5	Effect of concentration of crosslinked hyperbranched polymer on the tensile toughness of neat PLA and PLA-cHBP blends.....	146

Figure 5.6	SEM photomicrograph of tensile fractured samples A: Neat PLA B: (PLA/HBP/PA(98/1.6/0.4) C: PLA/HBP/PA(96/3.2/0.8).....	149
Figure 5.7	SEM photomicrograph of tensile fractured samples A: PLA/HBP/PA (92/6.4/1.6) B: PLA/HBP/PA (88/9.7/2.3) C: PLA/HBP/PA (84/12.9/3.1).....	150
Figure 5.8	Particle size distributions of crosslinked HBP particles. (A) PLA/HBP/PA (92/6.4/1.6); (B) PLA/HBP/PA (88/9.7/2.3).....	152
Figure 5.9	Schematic of Matrix Ligament Thickness. Redrawn after ref. 7.....	153
Figure 5.10	Effect of volume fraction on the inter-particle distance of crosslinked HBP particles in PLA-cHBP Blends.....	155
Figure 5.11	Effect of inter-particle distance on the tensile toughness of PLA-cHBP blends.....	156

KEY TO SYMBOLS OR ABBREVIATIONS

<i>Symbols</i>	<i>Key</i>
T_g	Glass Transition Temperature
T_m	Melt Temperature
T	Temperature
\pm	Standard deviation
®	Registered
°C	Degrees Celcius
°F	Degrees Fahrenheit
°K	Degrees Kelvin
Å	Angstrom
cc	cubic centimeter
m	meter
mm	millimeter
nm	nanometer
μm	micron meter
ϵ	Epsilon
Π	Pi
ρ	Density

Σ	Summation
φ	Volume fraction
ω	Frequency
MPa	Megapascal
GPa	Gigapascal
Hz	Hertz
J	Joules
Pa	Pascal
DMA	Dynamic mechanical analysis
GPC	Gel Permeation Chromatography
TEM	Transmission Electron Microscopy
SEM	Scanning Electron Microscopy
AFM	Atomic Force Microscopy
PLA	Poly(lactide) or Poly(lactic acid)
HBP	Hyperbranched Polymers
cHBP	Crosslinked Hyperbranched Polymer
PA	Polyanhydride
BDT	Brittle to Ductile Transition
LDPE	Low density polyethylene
LLDPE	Linear low-density polyethylene
HDPE	High density polyethylene
HIPS	High-impact Polystyrene
ABS	Acrylonitrile butadiene styrene

PS	Polystyrene
PBAT	Polybutylene adipate-co-terephthalate
PBS	Poly(butylene succinate)
PCL	Poly(ϵ -caprolactone)
PEO	Polyethylene Oxide
PHA	Polyhydroxyalkanoate
PHB	Polyhydroxybutyrate
PHBV	Polyhydroxybutyrate-co-valerate
PU	Polyurethanes
US	United States

Chapter 1: Introduction

1.0 Introduction

Synthetic polymers such as polyethylene (PE), polypropylene (PP), polystyrene (PS), polyethylene terephthalate (PET) and polyvinyl chloride (PVC) share a major chunk of commodity plastics^[1]. The non-renewability, staggering waste problem, emissions of greenhouse gases during production and incineration of synthetic polymers are making a serious dent on the versatility of these polymers. In the last couple of decades, there was a paradigm shift in developing biobased polymers, blends and composites as potential candidates to replace or substitute conventional polymers for real world applications. Biomass/ agricultural feedstocks offer an ample opportunity for utilization of abundant carbon-neutral renewable resources for the production of bioenergy and biomaterials, which can facilitate a transition from nonrenewable carbon sources to renewable bioresources^[2]. A popular approach involves the use of biological processes to produce chemical commodities from agricultural feedstocks.

The biodegradable polymers especially obtained from renewable resources have shown much promise to overcome the problems associated with conventional polymers. The global biodegradable plastic market was more than 100 million pounds in 2005 and is likely to increase to 200 million pounds by 2010^[3]. The green polymers like polylactides, PLA; polyhydroxyalkanoates, PHAs; starch plastics; biobased poly(trimethylene terephthalate), and functionalized vegetable/plant oil-based resins are some examples of biologically derived materials that are moving rapidly towards mainstream applications^[4-6].

Poly lactides are the leading biodegradable polymers, which are looked upon as sustainable alternative to petroleum based plastics. The primary interest in these polymers originated due to the production of their precursor, i.e. lactic acid, from renewable resources such as corn, sugar beet, sugarcane, cellulosic waste, and rice starch^[7-11]. The polymerization of lactic acid was first introduced by Carothers et al. in 1932^[12]. But the major breakthrough in pilot production of PLA was achieved by Cargill in 1992. Currently NatureWorks LLC owned by Cargill is independently producing PLA from corn based feedstock in its plant at Blair, Nebraska, USA^[13]. NatureWorks, with a PLA production capacity of 140,000 t per annum, is the single largest producer of PLA bioplastic^[14]. The other producers of PLA are Toyota (Japan), Biomer (Germany) and Hycail (Netherlands)^[15-17]. PLA has been used in biomedical applications for many years but its use as a commercial commodity thermoplastic was pursued only in the last two decades. Wal-Mart, the world's largest retailer, started using PLA in packaging applications in the beginning of November 2005^[18]. The current applications of PLA bioplastic are in packaging, textiles and electronics.

The inherently poor properties of PLA such as poor impact strength, low elongation at break, poor melt strength, low heat deflection temperature (HDT), narrow processing window and low thermal stability are impeding its large scale commercial applications. Modification of these properties of PLA is necessary for developing it as a commodity plastic. The properties of PLA heavily depend on the stereochemical makeup of its repeat unit. Polylactide is commonly prepared through the ring-opening polymerization of a cyclic dimer of lactic acid known as lactide. The lactide units are known to exist in three-stereochemical forms i.e. L-lactides, D-lactides and D,L/meso-

lactides^[19]. The choice of lactide dimer and catalyst can provide PLA with a wide range of backbones such as block, alternating or random. PLA made entirely from L-lactide is called as poly (L-lactide), PLLA, and is the most common form of polylactides. High molecular weight PLA is a stiff, colorless and glossy thermoplastic having properties similar to polystyrene (PS) and can be processed by injection molding, fiber spinning, thermoforming and film casting^[19]. Previously, PLA was only modified for biomedical applications but there is a strong increase in the number of research papers and patent applications pertaining to the modification of properties of PLA bioplastics for commodity applications. Several methods such as copolymerization, plasticization, blending, and clay based nanocomposites have been mentioned in the literature to improve the properties of polylactides. These methods are referenced later in related sections of this dissertation. The improvement in the toughness and flexibility of PLA is targeted through copolymerization, plasticization and blending with other tough polymers. Heat deflection temperature, gas barrier and stiffness of polylactides are improved by clay based nanocomposites.

In the midst of these approaches, nanostructure polymer blends having a minority polymer phase with dimensions less than 100 nm, have shown a lot of promise because of their enhanced thermo-mechanical properties, optical transparency and toughness in comparison to conventional polymer blends. Reactive blending, utilizing the concepts of in-situ polymerization, graft and block copolymerization lead to creation of nanostructure blends^[20, 21]. So far the nanostructure blending is restricted to a handful of petroleum based polymers such as polyamide (PA), polypropylene (PP), and poly(vinylidene fluoride) (PVDF)^[20-22].

The emerging hyperbranched polymer (HBP) can help in designing and manipulating new nanoscale morphologies for polymer modification. HBP falls in the category of dendritic polymers, which are gaining attention due to their unique structures and properties. Hyperbranched polymers encompass highly branched nanoscopic structures having high peripheral functionality^[23]. They are polydisperse and can be prepared using one-pot synthesis, unlike dendrimers, making the former less costly. The role of hyperbranched polymers is reported as a processing aid, branching agent and compatibilizer for conventional thermoplastics^[24-26]. But the unique physical properties and high peripheral functionality of HBP offer lot of other opportunities for polymer modifications. The HBP can play a role of novel building blocks for generating new nanostructures inside a polymer matrix, ranging from core-shell to highly networked morphologies. There is a great scope to tailor the architecture of hyperbranched polymers and study their influence on the properties of the host polymer.

In this work, hyperbranched polymers (HBP) are investigated as potential modifiers for PLA bioplastics. The effect of hyperbranched polymer on mechanical and rheological properties of PLA is investigated. A reactive extrusion technique is used to generate new structures based on hyperbranched polymer inside a polylactide matrix. An in-situ crosslinking reaction of HBP is carried out with help of a polyanhydride to generate highly networked particles in a continuous phase of polylactide. The toughening effect of crosslinked HBP particles is investigated. The size, volume fraction and matrix ligament thickness are correlated with the mode of deformation of PLA.

1.1 Thesis Structure

This dissertation is divided into 6 chapters. A brief overview of all remaining chapters is described as follows

Chapter 2 of this dissertation is a review of literature pertaining to polylactide bioplastic, its structure, properties and current methods of its modification. Hyperbranched polymers, their structure and properties are also discussed. A literature review of toughening of polymers, toughening theories and parameters that determine the brittle to ductile transition in multiphase polymer systems are discussed. Alternate toughening methodologies such as interpenetrating networks and nanostructure blending are also discussed.

Chapter 3 describes a new polymer modification technique, in which a hydroxyl functional hyperbranched polymer is in-situ crosslinked in PLA matrix during its melt processing. New nano size HBP based particles are generated, which have a profound toughening effect on PLA without sacrificing much of its modulus and strength. The pristine form of HBP was not effective in improving the ductility of PLA. The toughening mechanism of PLA is investigated. The rheological studies revealed reduction in the melt viscosity of PLA in presence of pristine as well as crosslinked HBP particles.

Chapter 4 incorporates the study of effects of crosslinking of HBP with different amounts of polyanhydride and its effect on the mechanical properties and morphology of PLA-cHBP blend. The Fox equation is applied to correlate the experimental glass transition temperature of crosslinked HBP phase in PLA matrix. The optimized hydroxyl

(OH) to anhydride molar ratio for effective crosslinking of HBP is identified by this study.

Chapter 5 investigates the effects of volume fraction of crosslinked HBP on the toughening of PLA. An understanding of phase morphology of crosslinked HBP particles and its relation with brittle to ductile transition in modified PLA was established. The matrix ligament thickness parameter (distance between two neighboring particles) is investigated as a critical parameter for toughening of PLA. The experimental matrix ligament thickness is correlated with theoretical values.

Chapter 6 discusses the summary of results, conclusions and recommendations for future work.

1.2 References

1. Amass, W., Amass, A., Tighe, B., A Review of Biodegradable Polymers: Uses, Current Developments in the Synthesis and Characterization of Biodegradable Polyesters, Blends of Biodegradable Polymers and Recent Advances in Biodegradation Studies. *Polymer International*, 1998. **47**: p. 89-144.
2. Ragauskas, A. J., Williams, C. K., Davison, B. H., Britovsek, G., Cairney, J., Eckert, C. A., Frederick Jr., W. J., Hallett, J. P., Leak, D. J., Liotta, C. L., Mielenz, J. R., Murphy, R., Templer, R., Tschaplinski, T., The Path Forward for Biofuels and Biomaterials. *Science*, 2006. **311**: p. 484-489.
3. Plastic News February 27, 2006 [cited March 2, 2007]; Available from: <http://www.plasticsnews.com/subscriber/fyi.html?id=1140814250>
4. Gross, R. A., Kalra, B., Biodegradable polymers for the environment. *Science*, 2002. **297**(5582): p. 803-807.
5. Carole, T. M., Pellegrino, J., Paster, M. D., Opportunities in the Industrial Biobased Products Industry. *Applied Biochemistry and Biotechnology*, 2004. **113-116**: p. 871-885.
6. Kurian, J. V., *Sorona Polymer: Present Status and Future Perspectives*. Natural Fibers, Biopolymers, and Biocomposites, ed. A.K. Mohanty, Misra, M., Drzal, L. T. 2005, Boca Raton: CRC Press.
7. Ray E. Drumright, Patrick R. Gruber, and David E. Henton, Polylactic Acid Technology. *Advance Materials*, 2000. **12**(23): p. 1841-1846.
8. Goksungur, Y., Guvenc, U., Batch and continuous production of lactic acid from beet molasses by *Lactobacillus delbrueckii* IFO 3202. *Journal of Chemical Technology and Biotechnology*, 1997. **69**(4): p. 399-404.
9. Timbuntam, W., Sriroth, K., Tokiwa, Y., Lactic acid production from sugar-cane juice by a newly isolated *Lactobacillus* sp. *Biotechnology Letters*, 2006. **28**(11): p. 811-814.
10. Shen, X. L., Xia, L. M., Lactic acid production from cellulosic waste by immobilized cells of *Lactobacillus delbrueckii*. *World Journal of Microbiology & Biotechnology*, 2006. **22**(11): p. 1109-1114.
11. Fukushima, K., Sogo, K., Miura, S., Kimura, Y., Production of D-lactic acid by bacterial fermentation of rice starch. *Macromolecular Bioscience*, 2004. **4**(11): p. 1021-1027.

12. Holten, C. H. , Lactic Acid Properties and Chemistry of Lactic Acid and Derivatives. *Verlag Chemie, Germany*, 1971.
13. <http://www.natureworksllc.com/About-NatureWorks-LLC.aspx> (accessed on February 28, 2007).
14. <http://www.european-bioplastics.org/index.php?id=141> (Accessed On March 5, 2007).
15. Biotechnology and Afforestation Businesses, Environmental Aspects, http://www.toyota.co.jp/en/environmental_rep/06/download/pdf/e_report06_p39_p41.pdf. (Accessed on March 1, 2007).
16. <http://www.biomer.de/>, (Accessed on February 25, 2007).
17. <http://www.hycail.com/> (Accessed on February 27, 2007).
18. Esposito, F. , Retailers face tough resin options. *Plastics News*, October 24, 2005.
19. Garlotta, Donald, A Literature Review of Poly(Lactic Acid). *Journal of Polymers and the Environment*, 2002. **9**(2): p. 63-84.
20. Hu, G. H., Cartier, H., Reactive Extrusion: Toward Nanoblends. *Macromolecules*, 1999. **32**: p. 4713-4718.
21. Ruzette, A. V., Leibler, L., Block copolymers in tomorrow's plastics. *Nature Materials*, 2005. **4**: p. 19-31.
22. Shimizu, H., Li, Y., Kaito, A., and Sano, H. , Formation of Nanostructured PVDF/PA11 Blends Using High-Shear Processing. *Macromolecules*, 2005. **38**: p. 7880-7883.
23. Seiler, M. , Dendritic Polymers-Interdisciplinary Research and Emerging Applications from Unique Structural Properties. *Chem. Eng. Technol*, 2002. **25**(3).
24. Hong, Y., Coombs, S.J., Cooper-White, J.J., Mackay, M.E., Hawker, C.J., Malmstro"m, E., Rehnberg, N. , Film blowing of linear low-density polyethylene blended with a novel hyperbranched polymer processing aid. *Polymer*, 2000. **41**: p. 7705-7713.
25. Jannerfeldt, G., Boogh, L., Manson, J.A.E. , Tailored interfacial properties for immiscible polymers by hyperbranched polymers. *Polymer*, 2000. **41**: p. 7627-7634.

26. Kil, S.B., Augros, Y. . Leterrier, Y., Manson, J.A.E. , Rheological Properties of Hyperbranched Polymer/Poly(ethylene Terephthalate) Reactive Blends. *Polymer Engineering and Science*, 2003. **43**(2).

Chapter 2: Literature Review

2.0 Preparation and Structure of Polylactides

The chemical makeup of polylactides (PLA) (Figure 2.1) consists of repeating units of lactic acid monomer. Lactic acid ($\text{CH}_3\text{CHOHCOOH}$) exists in two stereochemical enantiomers, i.e. L-lactic acid and D-lactic acid, due to the presence of a chiral carbon center (Figure 2.2). The lactic acid is predominantly produced from carbohydrate fermentation using various strains of the genus lactobacilli, which exclusively produce lactic acid^[1]. The lactic acid is converted into polylactides by three predominant routes of polymerization; condensation/coupling, azeotropic dehydration condensation and ring opening polymerization (ROP)^[2]. The cyclic compounds known as lactides are the main precursors of polylactide formation. Lactides are known to exist in three stereochemical forms, i.e. L-lactide, D-lactide and meso/DL-lactide (Figure 2.2)^[3]. The corresponding polylactides are called poly(L-lactide), PLLA; poly(D-lactide), PDLA; and poly(DL-lactide), PDLLA, respectively.

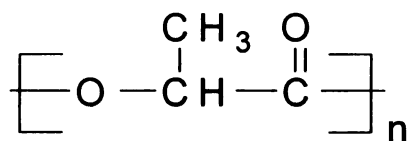


Figure 2.1: General chemical structure of PLA.

The ring opening polymerization of lactides is the most general approach for production of high molecular weight polylactides. A schematic of lactide formation and its polymerization are presented in Figure 2.3^[2]. The possible routes of lactide

polymerization are cationic, anionic and coordination reaction mechanism. Catalyst systems based on tin, aluminum, zinc and lanthanides are used for polymerization of lactides. Tin compounds, especially tin(II) bis-2-ethylhexanoic acid (tin octoate) have been preferred for the bulk polymerization due to their solubility in molten lactide, high catalytic activity and low rate of racemization^[2]. A generalized mechanism of

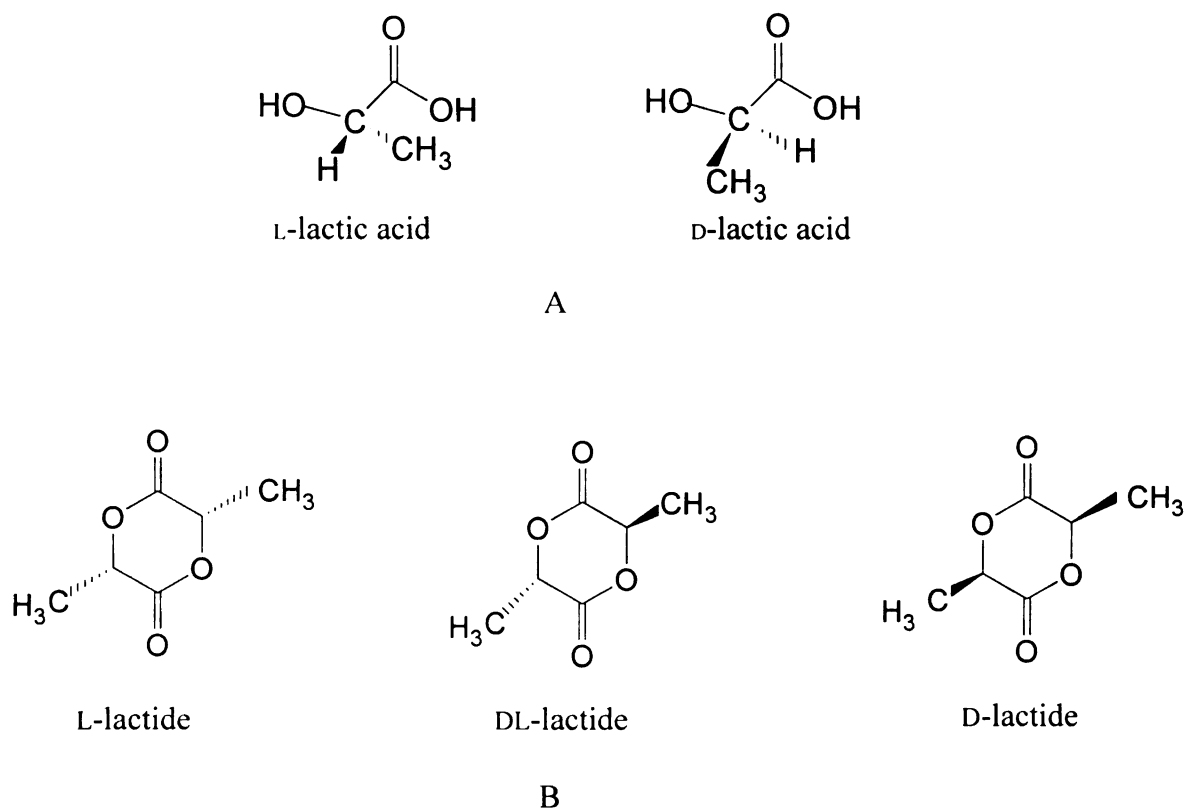


Figure 2.2: Stereochemical structures: A: Lactic acid; B: Lactides

coordination insertion polymerization of lactide to polylactides is shown in Figure 2.4^[2]. Cargill Dow LLC, currently known as NatureWorks LLC has developed an environmentally friendly method for production of polylactides from lactides in the melt state rather than in solution^[2]. The properties of polylactides strongly depend on the stereochemical makeup of the lactide units. The stereochemistry of lactides depends on

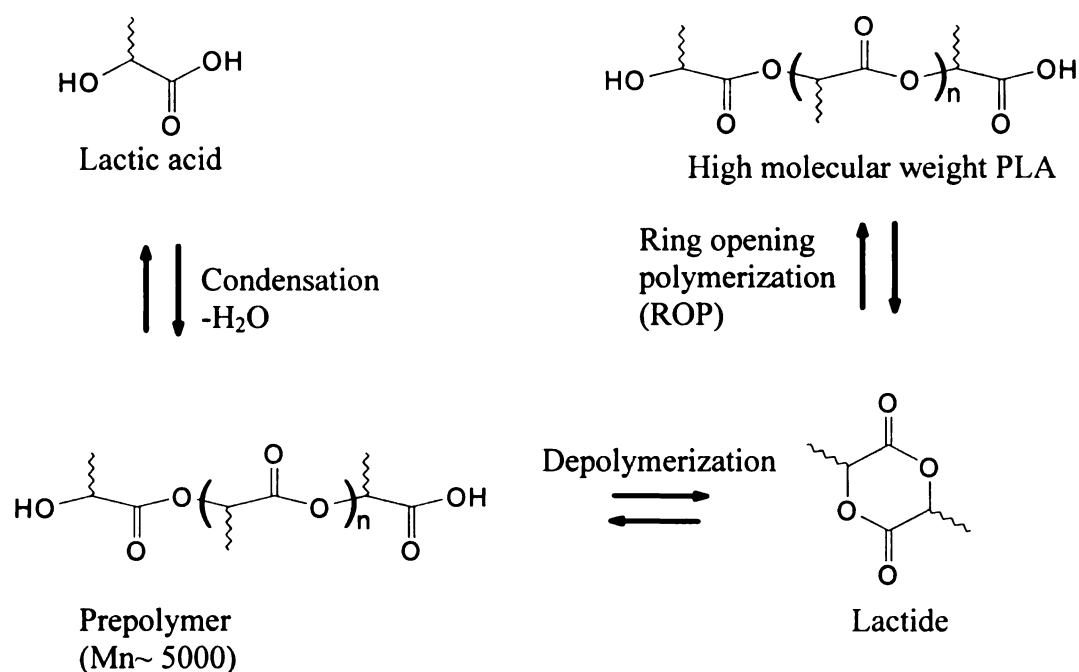


Figure 2.3: The schematic of formation of a PLA prepolymer, lactide and conversion of lactide into PLA (redrawn after ref. no.7)

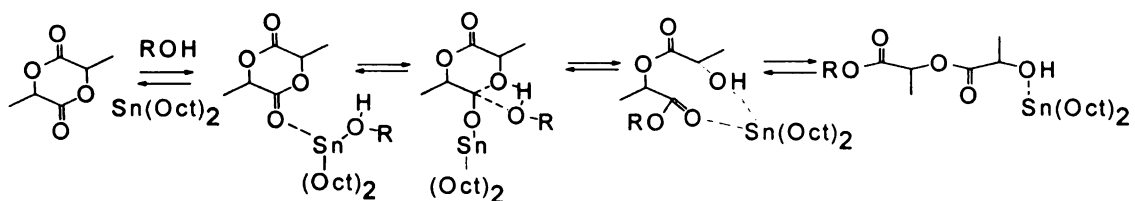


Figure 2.4: Conversion of lactide into PLA via coordination insertion mechanism in presence of tin octoate, Sn (Oct)₂, here R= growing polymer chain (redrawn after ref. no.7)

the feed ratio and stereochemical nature of the lactic acid monomer, temperature and catalyst. In turn the stereochemistry of the lactides will determine the stereochemical makeup of the resulting polymer. The choice of lactide dimer and catalyst can provide PLA with a wide range of backbones such as block, alternating or random copolymer^[4, 5]. The stereochemical composition of the polylactide has a strong influence on the melting point, rate and extent of crystallization of the polymer.

PLA is a semi-crystalline polymer and its mechanical properties depend on the details of crystalline and amorphous regions. The degree of crystallinity, size and arrangement of crystallites has profound effects on the physical and mechanical properties of the polymer. The crystal structure of PLA plays a significant role in determining its physical properties, so it becomes important to discuss the crystal morphology of PLA. PLA can have three crystal structures (α , β and γ forms), depending on the crystallization conditions and drawing. The α form was determined for both optically pure PLLA and PDLA as reported by De Santis and Kovacs^[6]. The crystals were thought to be left handed 10_7 helix for PLLA and right handed 10_3 helix for PDLA. The crystal lattice was an orthorhombic unit-cell having constant values i.e. $a = 1.06$ nm, $b = 0.610$ nm and $c = 2.88$ nm. The ratio of a/b suggested hexagonal close packing of helices. Puiaggali et al.^[7] studied the formation of a frustrated crystal structure of PLLA upon stretching or stroking. Here stroking meant shearing of the PLA film on a glass slide with the help of a razor blade. The frustrated structure consisted of three-fold helices in a trigonal unit cell. The structure accommodated the random up-down orientation of neighboring chains associated with rapid crystallization conditions.

Hoogsteen et al.^[8] reported the α and β crystal form of the solution spun poly (L-lactide), PLLA fibers. The chain conformation of α and β were left handed 10/3 and 3/1 helices respectively. The conformational energies and packing of these two structures were nearly the same, therefore both crystal modifications can co-exist. The α form was comprised of a lamellar folded chain morphology while the β form corresponded to a fibrillar morphology. The transformation from α to β form was possible at high draw temperature and draw ratio. Takahashi et al.^[9] studied the effect of uniaxial tensile drawing on the crystal transformation of the PLLA film. The highly oriented PLLA film having α crystal form was prepared and subjected to various draw ratios (DR), draw temperatures (T_d) and draw stresses. Initially the crystals were oriented in the draw direction and progressively transformed into β form on further drawing. The properties of PLLA based fibers were found to depend on the draw ratio, crystallinity and molecular weight of the PLLA resin. The solution spun fibers showed better tensile strength caused by low entrapment of entangled chain in solution-spun fibers as compared to melt-spun fibers. The tensile strength of the fiber was also correlated with drawing temperatures, which in turn had effects on the two-crystal modification of PLLA^[10]. The temperature dependent variation in the lamellar structure was studied by Cho et al.^[11]. The crystal thickness and long spacing, i.e. distance between the center of adjacent crystallites were minimum at 120°C and increased for both lower and higher crystallization temperatures. Kishore et al.^[12] studied the isothermal melting of PLLA. It was reported that the lamellar thickening occurred during PLA crystallization, with an increase in the annealing time leading to an increase in the melting point and heat of fusion. The high activation energy (828 KJ/mol) obtained from plotting the logarithm of the melting rate versus the

reciprocal temperature, suggested the complex nature of melting and thickening. A proper explanation was not given for this phenomenon. PLA crystal morphology and its crystallization kinetics have been extensively researched but there is a scarcity of literature that correlates the crystal morphology of PLA with its bulk properties. This is probably due to the deformation mechanism of PLA, which is not entirely dependent on the crystalline structure of PLA. The lack of conformational flexibility of PLA and low entanglement density has a major effect on the deformation mechanism and the bulk properties of PLA (discussed in the next section). The correlation of these parameters with the crystalline structure of PLA can provide some interesting information about the bulk property behavior of PLA.

2.1 Properties and Deformation of Polylactides

PLA possesses several good physical properties that make it suitable for commercial applications. PLA has good crease-retention and crimp properties, excellent grease and oil resistance, easy low-temperature heat sealability, and good barrier to flavors and aromas^[2]. A comparison of properties of two different types of PLAs with some conventional polymers is given in Table 2.1^[3, 13-17]. Both types of PLA exhibited good tensile and flexural properties. The low elongation at break, poor impact strength and low heat deflection temperature are some of the inferior properties of PLA. PLA has very similar physical properties as polystyrene (PS), such as tensile modulus and tensile strength. Auras et al.^[14] studied PLA properties with respect to its packaging applications. It was reported that PLA has good heat sealability below its melting point, and lower CO₂, O₂ and water permeability coefficients than polystyrene (PS) but higher than poly(ethylene terephthalate), PET. Other biobased as well as petroleum derived

Table 2.1: Comparison of Mechanical and thermo-mechanical properties of PLAs with conventional polymers; here Mv – molecular weight (Adopted after ref. no. 3, 13-17)

	L-PLA (Mv = 66000)	D, L-PLA (Mv = 114000)	Polystyrene (PS)*	Polyethylene terephthalate (PET)**	Polypropylene (PP)
Tensile Strength (MPa)	59	44	44	50	36
Elongation at break (%)	7.0	5.4	1.5	60-110	-
Modulus of Elasticity (GPa)	3.7	5.4	2.8	2-4	1.2
Flexural Strength (MPa)	70	53	83	70	33
Unnotched Izod Impact (J/m)	106	88	-	-	-
Notched Izod Impact (J/m)	26	18	16	101	30
Rockwell Hardness	88	76	-	106	-
Heat Deflection Temperature (°C)	55	50	88	70	106
Vicat Penetration temperature (°C)	59	52	101	76	-

*Dow STYRON 615APR General Purpose Polystyrene Resin, ** Eastar GN002 glycol modified polyethylene terephthalate (PET)

Table 2.2: Properties of PLA and some other biopolymers. (After ref. no. 2, 18-23).

	PLA (NatureWorks®)	PLA (Biomere® L9000)	Polyhydroxy butyrate, PHB, (Biomere®P226)	Polybutyle -ne adipate terephthal ate, PBAT	Poly(butylene succinate), PBS, Bionolle 1001	Poly- caprolactone , PCL	Poly trimethylene terephthalate, PTT
Density, gm/cc	1.25	1.25	1.25	1.26	1.26	1.14	1.35
Melting point, °C	152	169.2	164	115	114-115	60	225
Glass transition temperature , °C	58	-	0.3	-30	-32	-60	45-75
Tensile modulus, GPa	-	3.6	1.4	0.08	-	0.386	-
Flexural modulus, GPa	3.8	-	-	-	0.656	-	2.7
Tensile strength, MPa	48	70	24-27	25	32	-	67.6
Elongation at break (%)	2.5	3.2	6-9	820	-	800-1000	-
Heat distortion temperature , °C	-	55.4	90	-	97	56/47	59

biopolymers are also emerging parallel to PLA. A comparison of properties of PLA with some of the existing biopolymers is given in Table 2.2^[2, 18-23]. PLA has higher strength and modulus but has lower elongation at break and heat distortion temperature than other biopolymers. The inherent brittleness of PLA is one of the chief culprits for its limited commercial applications. A typical stress-strain curve of poly (L-lactide) is given in Figure 2.5. The curve suggests that PLA had poor plastic behavior and failed in a brittle fashion after exhibiting little strain softening.

The brittleness of PLA is a poorly understood phenomenon. The deformation of a polymer glass is controlled by the entanglement density and chain stiffness^[24]. A polymer is considered as glassy at a temperature, when it exhibits a glass transition at least 10 20°C above that temperature. So, PLA ($T_g \sim 58^\circ\text{C}$)^[3] falls in the category of polymer

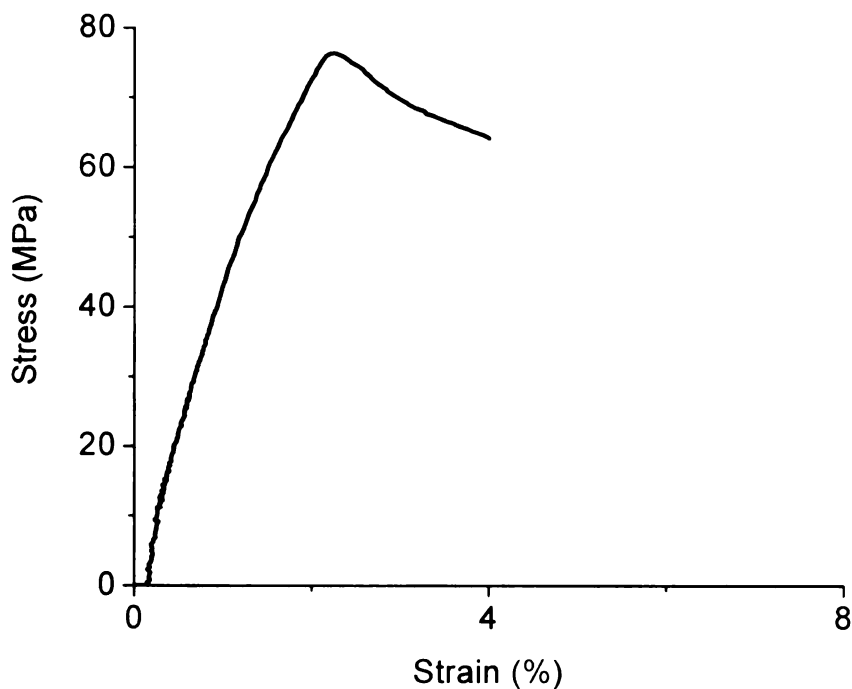


Figure 2.5: A typical stress-strain curve of poly (L-lactide), PLLA obtained at a crosshead speed of 15.4 mm/min at ambient conditions (25°C).

glasses at ambient conditions. Tonelli et al.^[25] studied the conformational statistics of randomly oriented poly (L-lactic acid). The characteristic ratio, C_∞ , a measure of stiffness of a chain, was 2.0 for polylactides. This value of C_∞ suggest that PLLA will deform in ductile manner rather than brittle but the stress-strain behavior suggested the brittle nature of PLLA. Later, Joziasse et al.^[26] studied the chain stiffness of poly(lactide)s and reported higher values of C_∞ for polylactides. The characteristic ratio, C_∞ , increased with an increase in the stereo-regularity of stereo-copolymers of polylactides, while it decreased for stereo-impure polylactide. This decrease in characteristic ratio for stereo-copolymer of PLA was correlated with a decrease in the glass transition temperature of stereo-copolymer with an increase in D-lactide mol.%. The characteristic ratio was 11.8 for isotactic PLLA while it was 9.5 for racemic PDLA. The higher stiffness of PLA chain was explained by geometric isomerism of the ester group of a PLA chain. The ester group in PLA is planer and trans due to the partial double bond character of the skeletal C-O bond. The presence of a smaller valence angle at the skeletal oxygen enhances steric interaction, hindering rotation around the O-C $^\alpha$ bond^[27]. In another study, the higher chain stiffness of isotactic PLLA was explained by the presence of helical sequences^[28].

Grijpma et al.^[29] studied the chain entanglement, drawability and mechanical properties of polylactides. They calculated the molecular weight between entanglements and correlated it with the mechanical properties and drawability of poly (lactide). The characteristic ratio C_∞ , was found to have values, $C_\infty = 11.7$ and $C_\infty = 9.1$ for poly(L-lactide) and L- and D-lactide copolymer, respectively. The high value of characteristic ratio and low entanglement density were deemed responsible for the brittle failure of the amorphous polylactide. The molecular weight between entanglements was 10×10^3 , which

corresponded to a value of characteristic ratio, $C_{\infty}=12$. This suggested the stiffness of the poly(L-lactide) chain. Grijpma et al.^[30] revealed the crazing phenomenon in poly (D,L-lactide) responsible for its brittle behavior. In conventional polymers, polystyrene (PS) is a well known craze forming polymer^[31]. The crazes are the dense array of polymer fibrils that are separated by the voids. The craze volume fraction plays a crucial role in determining the propensity of a craze resulting in a catastrophic failure. The amorphous polylactide has a glass transition temperature of $\sim 55^{\circ}\text{C}$ and fracture of amorphous polylactides was found to occur through crazing mechanism^[32]. The poly(L-lactide) and L/D lactide copolymers behaved as glass at room temperature.

Poly lactides are primarily used for medical applications including drug delivery devices and hard tissue scaffolds. The rate of mass loss and degradation of mechanical properties are very critical in these two cases. The effect of crystallinity on deformation mechanism and bulk properties of polylactides was studied by Renouf-Glauser et al.^[33]. The effect of microstructures on the deformation mechanism of PLA under load was investigated. The amorphous PLA deformed with formation of craze structures. The dry and hydrated PLA samples showed similar deformation through craze formation, while degraded samples showed intermediate behavior. In annealed PLA sample, hydration dramatically changed the bulk properties such as tensile strength, modulus and elongation at break due to the plasticization effect of water. But in crystalline PLA, the deformation occurred by crystal mediated deformation having contributions from cavitation and fibrillated shear process. It was concluded that crystallinity has a huge effect on the bulk and microscopic properties of PLA, more significantly than it did on the micro mechanism of deformation of PLA.

The basic mechanical properties of six different molecular weight amorphous polylactides containing various amount of initial meso-lactide, 10-40%, was studied by Witzke^[34]. The tensile, flexural and Izod impact properties of polylactides were evaluated and compared with high-flow unmodified polystyrene. The unmodified amorphous poly(L-meso-lactide) was a stiff, brittle and strong plastic having properties quite similar to polystyrene (PS). The tensile modulus for amorphous poly(L-co-meso-lactide) was between 549-587 kpsi and was found to increase with molecular weight. The tensile yield strength of amorphous poly(L-co-meso-lactide) decreased with initial meso-lactide fraction i.e. 7700-7800 psi for 10% meso-, and 6600-6800 psi for 34-40% meso-lactide. Flexural strength also decreased with increasing meso-lactide fraction. The flexural modulus, elongation at break and notched Izod impact strength for amorphous poly(L-co-meso-lactide) were independent of initial meso fraction.

2.2 Rheology of Polylactides

The melt rheology of a polymer is an essential element of polymer processing. Processing operations such as fiber spinning, extrusion blown film, thermoforming, and cast films are markedly affected by the rheological properties of a polymer. Dorgan et al.^[35-39] extensively studied the melt rheology of polylactic acid. The melt rheology of PLA was difficult to determine due to the thermal degradation of polylactides. The effects of architectural modification of polylactide on its rheological properties were studied^[35]. The branching of polylactides was pointed out as a good method to control the elasticity and viscosity of this polymer. It was found that branched PLA exhibited higher zero shear viscosity than the linear counterpart. This behavior was caused by the longer relaxation of the polymer chain in the terminal region for the branched polylactide. It was

also found that the branched PLA showed strong shear thinning, resulting in a lower viscosity at a higher shear rate. Melt rheology of high L-content of poly(lactic acid) was studied by Palade et. al.^[40]. The dynamic, shear and transient viscosities of PLA were measured. The polylactide having high L-content could be drawn to large Hencky strain without breaking and showed strain hardening properties. The plateau modulus value for PLA was 5×10^5 Pa. The entanglement molecular weight was approximately 9000 g/mol. An additive, tris (nonylphenyl) phosphite (TNPP) acted as a secondary antioxidant and was found to improve the melt stability of PLA by avoiding its degradation.

Yamane et al.^[41] studied the effect of addition of a small amount of poly (D-lactic acid), PDLA on the melt rheology of poly (L-lactic acid), PLLA. The addition of PDLA produced stereocomplexation in PLLA and acted as a cross-linking point in PLLA resulting in the introduction of long chain branching, leading to an increase in the molecular weight. The zero shear viscosity of PLLA was increased with the addition of PDLA. The addition of high and low molecular weight PDLA caused strong strain hardening character to the PLLA melt. In a study done by Ramkumar et al.^[42], the rheological properties such as complex viscosity, η ; first normal stress coefficient, ψ ; loss modulus, G'' ; and storage modulus, G' were higher for D,L-PLA than L-PLA. The melt elasticity was found to be higher for D,L-PLA as compared to L-PLA and elasticity extends the linear visco-elasticity region to long relaxation time. The entanglement density of D,L-PLA was slightly higher than L-PLA. It was also reported that polylactic acid (PLA) is difficult to test for rheological properties due to its degradation^[42]. The primary reason was the presence of a labile CH proton in the proximity of the carbonyl group, which makes it thermally sensitive. The abstraction of this labile proton was

augmented at higher temperature leading to a free radical chain scission reaction. The ultimate result was a decrease in the molecular weight due to the breakdown of the polymer chains.

2.3 Current Methods to Modify Polylactide Properties

There are several methods mentioned in the literature to modify the properties of polylactides, such as copolymerization, plasticization, blending, clay based nanocomposite. This section discusses these methods and their effect on structure-property relationships of PLA.

2.3.1 Copolymerization

The basic development of the PLA copolymer began for biomedical applications. Crystalline poly(L-lactic acid) is used in biodegradable osteosynthesis and tissue scaffolds, both in animals and humans^[43]. A drawback of this polymer is a poor balance between strength retention and loss of mass. Its high crystalline nature also slows down its resorption. The crystalline debris may even lead to inflammatory reactions. This kind of complication and requirements for tougher polylactides compelled researchers to modify the crystalline and brittle nature of poly(L-lactic acid). Stereocopolymerization of L-lactide with D-lactide and meso-lactide is reported as a method to control the crystallinity and physical properties of polylactides^[32]. Stereocopolymers of L-lactide with D-lactide having comonomer weight ratios varying from 85/15 to 15/85 were amorphous in nature. Grijpma et al.^[32] studied the effect of copolymerization of L-lactide with lactones and cyclic carbonates on the mechanical properties and crystallinity. It was found that lactones and cyclic carbonates reduced the crystallinity of the material.

The entanglement density and the interconnectivity of physical networks influenced the toughness of polylactide. The tensile and impact properties of poly(D,L-lactide) were improved when it was oriented at a temperature close to its glass transition temperature^[30]. The orientation helped in reducing the crazing behavior and caused ductile energy dissipation. The copolymers of PLA with polyethylene oxide (PEO), polycaprolactone (PCL) and polyethylene glycol (PEG) are also reported^[44-49].

2.3.2 Plasticization

Plasticization is a common method to improve the flexibility and processability of a stiff and thermally unstable polymer. Low molecular weight compounds having good solubility with the host polymer are generally used as plasticizers. The plasticization of polylactide has been extensively researched to overcome its brittleness and to widen its area of application⁵⁰⁻⁶⁰. Labrecque et al.^[50] studied the effect of citrate esters on the thermal, mechanical and degradation behavior of PLA based extruded films. Triethyl citrate, tributyl citrate, acetyl triethyl citrate, and acetyl tributyl citrate were used as plasticizers. All of these plasticizers were found to decrease the glass transition temperature and improve the elongation at break of PLA. The citrate plasticizers were more effective in improving the elongation at break when present in excess of 10 wt.%. There was ~ 50% drop in tensile yield strength when the plasticizer concentration was around 10 wt.%. The tensile strength at yield of plasticized PLA was less than 10 MPa when plasticized with 20- 30 wt.% of plasticizers. The tensile yield strength of neat PLA was 51.7 MPa. The loss of citrate plasticizers during extrusion was also observed due to their high volatility. The enzymatic degradation of the plasticized PLA was increased with addition of low molecular weight citrate esters as compared with the unplasticized

PLA^[50]. Jacobsen et al.^[51] used poly (ethylene glycol), glucose monoesters and partial fatty acid esters for plasticizing poly(lactide), PLA. This research reported the improvement in elongation at break and impact resistance when poly(ethylene glycol) was used as plasticizer, while in case of glucose monoesters and partial fatty acid esters, elongation at break of polylactide improved but impact resistance was decreased. Stress whitening was observed in samples which contained 10 wt% of glucose monoesters and fatty acid esters. Glycerol, citrate ester, polyethylene glycol (PEG) of different molecular weight, PEG monolaurate and oligomeric lactic acid have also been reported as plasticizers for PLA^[52]. These plasticizers were found to decrease the glass transition temperature of PLA and improve its elongation at break. The maximum elongation at break, i.e. 200%, was exhibited by polylactide based composition plasticized with 20% of oligomeric lactic acid (OLA). But there was about 28 to 65% decrease in the modulus depending upon the type and amount of plasticizer used. There was enhancement in the percent crystallinity of polylactide on plasticization. This trend was explained by the fact that the plasticization of thermoplastic facilitates increased chain mobility, leading to the increase in crystallizing ability of a polymer. The crystallization temperature of plasticized PLA also decreased due to the lowering of glass transition temperature and increase in the PLA chain mobility. Ljungberg et al.^[53-57] have extensively studied the effects of different plasticizers on thermo-mechanical properties, aging and film extrusion of poly(lactic acid). The poly(lactic acid) was plasticized with monomeric and oligomeric plasticizers such as tributyl citrate (TBC), diethyl bishydroxymethyl malonate (DBM), TBC-oligoesters, DBM-oligoesters and DBM-oligoestermides^[53]. All of these plasticizers were found to improve the flexibility of poly(lactic acid). But the physical aging of

plasticized PLA revealed that PLA plasticized with oligomeric plasticizer exhibited better morphological stability than with monomeric plasticizers. This research showed that the use of high molecular weight plasticizers can help in eliminating the problems such as phase separation, physical aging and migration in plasticized PLA films. In another study^[54], triacetine, tributyl citrate, triethyl citrate, acetyl tributyl citrate and acetyl triethyl citrate were investigated as potential plasticizers for polylactic acid. The evaluation of dynamic mechanical and thermal properties showed that triacetine and tributyl citrate were the most effective plasticizers as they exhibited the largest depression in the glass transition temperature of PLA. Both these plasticizers have a solubility parameter difference of $< 1 \text{ (Jcm}^{-3}\text{)}^{1/2}$ with PLA. It was found that phase separation occurred when these plasticizers were present in excess of 25 wt.%. Phase separation also occurred when the plasticized PLA was heat treated at 50°C. Increase in the crystallinity of plasticized PLA was deemed responsible for the plasticizers' phase separation. Tributyl citrate oligomers were synthesized and used as plasticizers for polylactide^[55]. These oligomers were able to plasticize the PLA and improved its flexibility. But there was partial phase separation when the plasticized PLA was aged over 4 months. The morphological stability of plasticized PLA was enhanced when the plasticizer concentration was 10-15 wt.%. Oligomeric malonate esteramides were synthesized and reported as efficient plasticizers for polylactide^[56]. The oligomer synthesis was based on a plasticizer, diethyl bishydroxymethyl malonate (DBM). The benefits of DBM-based oligomers were intended to avoid the phase separation and to obtain long term phase stability of plasticized PLA based film. It was also proposed that the presence of polar amide groups in oligomeric malonate esteramides would be able to

interact with the PLA chains and improve the compatibility between the plasticizer and PLA. But again the problem of plasticizer phase separation was reported when the plasticized PLA was aged above the glass transition temperature of the blend. It was found that the cold crystallization of plasticized PLA was absent when it was aged at ambient conditions and the plasticized PLA maintained its flexibility. Ljungberg et al.^[57] studied the film extrusion and weldability of poly(lactic acid) plasticized with triacetine and tributyl citrate. It was found that storage of plasticized film caused an increase in crystallinity and reduced the constant heat (CH) welding capability of the film. Hu et al.^[58-60] studied the crystallization, phase separation and aging of poly(lactic acid) plasticized with poly(ethylene glycol), PEG. The crystallization of slowly cooled PLA/PEG blend suggested that the morphology of PLA/PEG blend consisted of large spherulites dispersed in a homogenous matrix.

2.3.3 Blending

Polymer blending is considered as the most benign modification technique in the field of polymer science and engineering. Two or more different polymers are blended to obtain synergism of properties in the resultant blend compared to the individual polymers. Blends may be miscible or immiscible depending on the chemical nature and compatibility of the two polymers. Since, PLA is a biodegradable polymer, the natural choice is to blend it with some other biodegradable tough polymers. Biodegradable blends of PLA with various polyhydroxyalkanoates (PHAs), poly(ϵ -caprolactone) (PCL), poly(butylene succinate) (PBS), and poly(butylene adipate terephthalate) (PBAT), are reported in the literature⁶¹⁻⁸². PLA has also been blended with polyethylene (PE)⁸³⁻⁸⁶, and rubber⁸⁷⁻⁸⁹ in an attempt to improve its toughness.

Blends of PLA with polyhydroxybutyrate (PHB) have been investigated for miscibility, crystallization and morphology of the blends^[61]. It was found that PLA and PHB were immiscible in an amorphous state and exhibited two glass transition temperatures corresponding to the respective components. There was some evidence of miscibility when samples were prepared at higher temperatures. There was transesterification between PLA and PHB leading to the formation a PLA-PHB copolymer, which enhanced the compatibility between the PLA and PHB. Other work^[62] reported that low molecular weight PLA was miscible with PHB over the whole composition range, while high molecular weight PLA showed phase separation when blended with PHB. Ohkoshi et al.^[63] reported the miscibility of PLA with atactic PHB having molecular weight (Mw) ranging from 9400 to 140,000. The result showed that PLLA was miscible with atactic PHB having low molecular weight. The compatibility between PLA and PHB blends was very much dependent on the molecular weight of the components.

Park et al.^[64] studied the uniaxial drawing and mechanical properties of blends of poly(L-lactic acid) (PLLA) with two kinds of PHB having different molecular weights. The blends were prepared through a solvent casting method. The blends were immiscible at all compositions. The drawing of the blends was carried out at two temperatures, one at the T_g of PHB, i.e. 2°C and other at the T_g of PLA, i.e. 60°C. It was observed that the PLA domains in the PHB rich phase was unstretched when PHB had a low molecular weight, but the PLA was able to orient when it was present as a dispersed phase in the continuous phase of ultrahigh molecular weight PHB. PLLA was blended with a PHB based copolymer poly (3-hydroxybutyrate-co-3-hydroxyvalerate) (PHBV), in order to

improve the toughness of PLLA^[65]. The blends were incompatible and showed different glass transition temperatures by differential scanning calorimetry (DSC) and dynamic mechanical analysis (DMA). There was an elastic deformation of the blend under tensile loading with the addition of PHBV.

The properties of PLA, especially brittleness and low impact strength, were improved by blending it with medium chain length poly(3-hydroxy alkanates) (Mcl-PHA) and epoxidized poly(3-hydroxyalkanoates) (ePHA)^[66]. Mcl-PHAs had a side alkyl chain of C₆-C₁₄ carbons. Mcl-PHAs had higher rubber like properties besides being biocompatible. It was hypothesized that the blend of PLA and Mcl-PHA would behave similarly to polystyrene (PS) / acrylonitrile-butadiene-styrene (ABS) blend. The blends of Mcl-PHA and ePHA with PLA were immiscible. The Mcl-PHA and ePHA were present as a dispersed phase in the PLA matrix and enhanced the impact toughness of the blend by a mechanism similar to rubber toughening. The ePHA was more effective in improving the toughness of PLA due to the presence of epoxy groups, which interacted with the PLA phase. The domain size of ePHA in PLA matrix was 0.1-1 μ m. Polylactic acid was also blended with another branched bacterial polyester copolymer comprised of 3-hydroxybutyrate (3HB) and other 3-hydroxyalkanoate unit (3HA) having alkyl side chains of C₃ or more carbon atoms^[67]. These polymers are known as the NodaxTM copolymers. The toughness of PLA was substantially increased when blended with 20 wt.% of this PHA copolymer. The PHA was not able to crystallize at this concentration and existed as a rubbery amorphous phase in the PLA matrix. The finely dispersed phase of the PHA copolymer helped in the dissipation of energy and improved the toughness of the blend.

PLA has been blended with other non-renewable resource based biodegradable polymers for improving its toughness. Blends of PLA with poly (ϵ -caprolactone) (PCL)^[68-75], polybutylene succinate (PBS)^[76-79], poly(butylene succinate adipate) (PBSA)^[80], and poly(butylene adipate terephthalate) (PBAT)^[81] have been reported. BASF, a Germany company, has recently developed a PLA based biodegradable blend called Ecovio[®]^[82]. The blend consists of 45 percent PLA and the rest is BASF's existing biodegradable plastic Ecoflex[®], which is an aliphatic–aromatic polyester derived from petrochemicals. The target applications for Ecovio[®] include flexible plastic bags and other packaging applications. Broz et al.^[68] studied the structure and mechanical properties of PLA-PCL blends. The tensile modulus, strain at failure, and ultimate tensile strength could be tuned through varying the blend composition. A percolation model was used to explain the observed mechanical properties. The percolation threshold in mechanical properties was achieved around the PLA mass fraction of 50%. The blends were immiscible but some adhesion was predicted when the blend had a PCL rich phase. In another study, Semba et al.^[69] studied the effect of crosslinking on the mechanical properties of PLA-PCL blends. The aim of this research was to improve the compatibility between PLA-PCL blends and ultimately improve the tensile strain of the blends. Dicumyl peroxide (DCP) was used as a crosslinking agent for the PLA-PCL blends. It was observed that the blend showed a yield point and ductile behavior when a small concentration of DCP was added. The optimum blend composition was 70 wt.% PLA and 30 wt.% PCL with a DCP concentration of 0.3 phr. The improved compatibility between PLA and PCL was originated through the formation of crosslinks initiated by the peroxide along with the interactions of the ester groups. The dispersed PCL phase in a

continuous phase of PLA extended under tensile loading, thus delaying the failure of the blend. Wang et al.^[70] studied the properties of a reactive blend of PLA with PCL using a branching and coupling agent.

Chen et al.^[76] studied the role of twice functionalized organoclay (TFC) as a compatibilizer in an immiscible PLA-PBS blend. Poly(butylene succinate) (PBS) is a petroleum-derived tough biodegradable polymer. TFC was prepared by treating an organo-clay i.e. Cloisite 25A, with (glycidoxypropyl) trimethoxy silane. Effect of different amounts of TFC on the compatibility of a PLA-PBS blend having 75/25 weight ratio was studied. It was observed that when the TFC content was 5 wt.% or more in the PLA-PBS blend, it acted as a compatibilizer via formation of a PLA-silicate-PBS hybrid and helped in reducing the domain size of the dispersed PBS phase. Tensile modulus and elongation at break of PLA-PBS blends were found to increase in the presence of TFC. Park et al.^[77] studied the phase behavior and morphology of PLA-PBS blends. The blends were classified as semicrystalline/semicrystalline blends due to the presence of two distinct melting peaks in the DSC thermograms of blends over the entire composition range. The interaction parameter between PLA and PBS obtained from the Flory–Huggins equation showed a value of -0.15. Small-angle X-ray scattering revealed that the PBS component was expelled out of the interlamellar region leading to the decrease of the long period and amorphous layer thickness of PLA. A significant crystallization-induced phase separation was observed when PBS weight content was greater than 40 wt.%. In another study, Park et al.^[78] used synchrotron wide angle X-ray scattering (WAXS) and small angle X-ray scattering (SAXS) techniques to study the crystallization behavior and morphological changes of PLA-PBS blends during heating. The

synchrotron WAXS exhibited absence of co-crystallization between PLA and PBS; they crystallized independently of each other. The lamella formation in the blend followed the dual lamellar stack model, which was indicative of formation of PLA and PBS lamellae at different locations.

Blending of polylactide (PLA) with polyethylene (PE) is reported in the literature^[83-86]. PLA-LDPE blends are immiscible in nature and require compatibilizers for toughness improvement of PLA. Synthesis of polyethylene- poly(L-lactide) diblock copolymer (PE-b-PLLA) and its role in compatibilizing the PLA-LDPE blend was studied^[83]. The role of the microstructure of PLA in compatible blends with linear low-density polyethylene (LLDPE) is also reported^[84]. The polylactide-polyethylene (PLLA-PE) block copolymers were used as compatibilizers. It was found that amorphous PLA was toughened only in the presence of PLLA-PE block copolymer, while the toughness of semicrystalline PLA was obtained without the compatibilizer. The PLLA-PE copolymer compatibilizer was effective when the individual polymers had a molecular weight above their entanglement molecular weight. The impact strength of PLLA was improved from 20 to 660 J/m when blended with 20 wt.% of LLDPE in the presence of 5 wt.% of PLLA-PE block copolymer compatibilizers. Anderson et al.^[85] studied the interfacial properties and dispersed phase properties of LDPE on the toughening of PLLA. It was observed that using a block copolymer with varying ability to crystallize could alter the interfacial adhesion. For the lowest modulus of PE dispersed phase, the block copolymer that gave the strongest adhesion was effective in toughening the PLA, while the block copolymer that gave the weakest interfacial adhesion was instrumental in toughening of PLA with the stiffest PE. On other hand, in blends of PLA with

intermediately stiff PE, the copolymer causing intermediate adhesion was most effective in improving the toughness of PLA. The immiscible blend of poly (L-lactide) and low density polyethylene was reactively compatibilized with glycidyl methacrylate (GMA) grafted PE (PE-GMA)^[86]. The compatibility was believed to originate from the in-situ reaction of epoxy groups of PE-GMA with the –OH end groups of PLA. PE-GMA significantly reduced the domain size of the LDPE dispersed phase and improved the elongation at break for the PLA –LDPE blend.

Rubber toughening of PLA has also been used to overcome its brittleness^[87-89]. PLLA was blended with poly(cis-1,4-isoprene) (PIP), a major ingredient of natural rubber^[87]. The PLLA-PIP blend was incompatible and the blend compatibility was improved by grafting a vinyl acetate monomer on the PIP (PIP-g-PVAc). Although there was phase separation in this system but the decrease in the T_g of PLLA with increase in graft copolymer content indicated the mixing of the PVA moiety of PIP-g-PVA with PLLA. There was an increase in the toughness of the resulting blend compared to neat PLLA. A model polyisoprene (PI)-polylactide (PLA) copolymer was synthesized to obtain a toughened PLA^[88]. A PI-OH prepolymer was synthesized with living anionic polymerization followed by the coordination insertion ring opening polymerization with lactides to produce PI-PLA diblock copolymer. Differential scanning calorimetry (DSC) and small angle X-ray scattering (SAXS) suggested that the block copolymers were micro-phase separated. In another relevant study, polybutadiene-polylactide diblock copolymers were also synthesized^[89]. The study focused on the kinetics and mechanism of synthesis of the diblock copolymer. The mechanical properties of these copolymers were not reported.

2.3.4 Polylactide based Nanocomposites

Inclusion of nano-structures in polymeric matrices is looked upon as a unique approach to create revolutionary material combinations. In polymer nanocomposites, the commonly used reinforcements are nanoclay, cellulose nanowhiskers, graphite nanoparticles and carbon nanotubes. Polymer-clay nanocomposites have been the most extensively studied. Clay is a silicate mineral consisting of octahedral sheets of aluminum or magnesium hydroxide sandwiched between two tetrahedral sheets of silicon hydroxide^[90]. The individual clay platelet has a thickness of 1 nm and lateral dimension of 100-1000 nm. The exceptionally high aspect ratio and nanoscale dimensions of clay enables the polymer-clay nanocomposites to exhibit improved mechanical, thermal and barrier properties without the loss of toughness and optical transparency^[91]. “Green” nanocomposites, having either a renewable or nonrenewable resource based biodegradable polymer matrix are the next generation of materials^[92]. Polylactide based nanocomposites having organo-clay as reinforcement are the most extensively researched^[92-123].

Ogata et al.^[93] reported the first PLA-clay nanocomposite in 1997. The purpose of this research was to develop environmentally friendly benign nanocomposites. A PLA-clay blend was prepared using chloroform as a solvent. The montmorillonite clay was modified with distearyldimethylammonium chloride (DSAC). The paper reported inadequate dispersion of clay in the PLA matrix by this method, which was evidenced by presence of clay tectoids, which consist of a stack of several monolayers of clay platelets. There was only a small improvement in the Young’s modulus of PLA-clay nanocomposites. This result was attributed to an absence of intercalation geometry in

PLA-clay nanocomposites. Sinha Ray et al.^[94-103] extensively studied the fabrication, characterization and properties of PLA-layered silicate nanocomposites. In one of the research efforts^[94], montmorillonite (MMT) clay modified with trimethyl octadecylammonium cation was used as organically modified clay for a PLA nanocomposite fabrication. The modified clay was termed C₁₈- MMT. There was a significant improvement in flexural modulus, storage modulus, heat distortion temperature and a decrease in oxygen permeability of neat PLA after incorporation of C₁₈-MMT clay. The biodegradation of neat PLA was enhanced in the presence of C₁₈-MMT. The increase in biodegradation was attributed to the absorption of water by clay from the compost, which triggered the heterogeneous hydrolysis of PLA.

The first successful preparation of intercalated PLA-layered silicate nanocomposites was reported by Sinha Ray et al.^[95]. The paper reported the melt extrusion of PLA and C₁₈-MMT clay to prepare the nanocomposite. The role of oligo-(ϵ -caprolactone) (o-PCL) as a compatibilizer in a PLA/clay nanocomposite was also investigated. The presence of a compatibilizer (0.2 to 3 wt.%) improved the mechanical properties of nanocomposite to a great extent. The hydroxyl functional compatibilizers helped in generation of a flocculated clay structure by enhancing hydroxylated edge-edge interaction of the silicate layers. The PLA/layered silicate nanocomposites exhibited improved material properties in both solid and melt states as compared to the matrix without clay. Sinha Ray et al.^[104] also studied the melt rheology of PLA-clay nanocomposites. The nanocomposites had clay loadings of 2, 3 and 4.8 wt.% of C₁₈-MMT clay. The nanocomposites showed pseudo-solid like behavior, revealed by the smaller terminal region slope values of storage moduli, $G'(\omega)$, and loss moduli,

$G''(\omega)$ as compared to neat PLA. The nanocomposite also exhibited shear independency of $G'(\omega)$ and $G''(\omega)$ values in lower frequency ($a_T \cdot \omega$) regime. This behavior occurred due to the formation of a spatially-linked structure of clay platelets in PLA matrix which caused the preventive relaxation of PLA chain occurring from the physical jamming polymer chains. The flow activation energy and complex viscosity of PLA increased in the presence of MMT clay. The important observation of this research was the tendency of PLA-clay nanocomposites to show strain-induced hardening behavior under uniaxial elongation flow. This property of PLA-clay nanocomposite was exploited in fabrication of foam using carbon dioxide (CO_2) as a blowing agent. The PLA nanocomposite showed smaller cell size and larger cell density as compared to the neat PLA foam. The nucleating effect of clay was instrumental in the formation of uniform cells. The same research group^[105] also reported a separate research article on PLA based nanocellular foam prepared by a batch process using supercritical CO_2 as blowing agent. The nanocomposites of PLA were also foamed by using a mixture of carbon dioxide (CO_2) and nitrogen (N_2) as blowing agent in a batch foaming process^[106]. PLA nanocomposite foams revealed reduced cell size and increased cell density at very low organoclay content. The cell size of foams decreased while both cell density and foam density increased with an increase in the organoclay content.

Maiti et al.^[107] examined the effect of chain length of organic modifiers in three different types of clay: smectite, montmorillonite (MMT), and mica, in PLA based nanocomposites. In PLA-smectite nanocomposites, increase in the chain length of phosphonium ion based organic modifier had a profound effect on the miscibility of organo-clay. There was a decrease in the glass transition temperature of PLA when the

chain length of the modifier increased from C₈ to C₁₆. The melting point of PLA also decreased with an increase in the chain length of the modifier. This suggested that C₁₆ salt had better miscibility with PLA. Properties of PLA-nanocomposites having smectite, montmorillonite (MMT), and mica were also compared. The clays were modified with C₁₆ phosphonium salt. The increase in the storage modulus was greater for smectite nanocomposite than MMT or mica nanocomposite. The better dispersion of smectite clay instead of its lower aspect ratio than MMT and mica, was responsible for this behavior. Smectite nanocomposites also showed better gas barrier properties than the MMT or mica systems. The results indicated the better interaction of smectite clay with PLA caused a stiffer local environment, which helped in improving the modulus and barrier. The effect of clay as a nucleating agent in PLA nanocomposites was researched by Nam and coworkers^[108]. The spherulites in neat PLA and PLA/C-18 MMT showed negative birefringence but the ordering of spherulites for nanocomposites was less than that of neat PLA due to the dispersion of clay platelets inside the spherulites. The crystallization rate of PLA was increased in the presence of clay particles and the researchers concluded that dispersed clay particles acted as nucleating agents for PLA.

Shibata et al.^[109] studied the thermal and mechanical properties of nanocomposites prepared from plasticized polylactide and organo-modified montmorillonites. The plasticized PLA systems contained diglycerine tetracetate (PL-710) and ethylene glycol oligomeric plasticizers. The organo-clays were modified with ammonium salt of octadecylamine (ODA-M) and poly(ethylene glycol) stearylamine (PGS-M). The incorporation of ODA-M clay in PLA and PLA plasticized with PL-710 resulted in an improvement in tensile strength and modulus as compared to PGS-M clay.

PLA plasticized with 10 wt.% PL-710 resulted in a remarkable improvement in elongation at break on incorporation of 3 wt.% of ODA- M clay, while only plasticized system showed no improvement in the said property. The paper did not provide a scientific explanation of this result. In other research^[110], PLA-organically modified clay based nanocomposites were prepared via a solution technique. A lactide emulsion was used to improve the compatibility between the clay and PLA matrix. The storage modulus of the nanocomposite was improved but decreased once the concentrations of silicate were increased. The presence of a large dimension of porosity in PLA-clay nanocomposites having higher silicate content was suggested as a possible reason for this behavior.

The twice functionalization of clay was reported as an effective method of obtaining a exfoliated geometry of clay in a PLA matrix leading to the high mechanical properties of the nanocomposite^[111]. A commercial organo-clay (Cloisite[®] 25A) was functionalized by reacting with (glycidoxypropyl) trimethoxysilane. The resulting clay called twice functionalized clay (TFC), had improved organophilicity. The epoxy group of the silane in TFC reacted with the end groups of PLA and resulted in better compatibility between PLA and TFC. The improvement in tensile modulus, strength and elongation at break for PLLA-TFC nanocomposite was superior to that of PLLA-clay nanocomposites. The effect of addition of polycaprolactone (PCL) on the mechanical properties of a PLA-clay nanocomposite was studied ^[112]. The three different molecular weights of PCL used were 10K, 40K and 70-100K. The addition of PCL to PLA-clay nanocomposites improved the tensile strength and elongation at break. It was also

reported that PCL was not helpful in obtaining exfoliated clay geometries in PLA-organoclay (Cloisite[®] 25A) nanocomposites.

Pluta and coworkers^[113-115] extensively studied the role of organoclays on the physico-chemical properties, aging behavior of plasticized PLA and the effect of processing cycle time on the properties of PLA-clay nanocomposites. Different weight contents of three clays: Cloisite[®] 20A, Cloisite[®] 25A and Cloisite[®] 30B were incorporated in a PLA based composition plasticized with 20 wt.% of polyethylene glycol (PEG)^[113]. The size exclusion chromatography revealed a decrease in the molecular weight with an increase in the filler concentration. This research reported the decreasing affinity of clay towards PLA in order of Cloisite[®] 30B, Cloisite[®] 20A, and Cloisite[®] 25A, respectively. In an extension to this work, Pluta et al.^[114] studied the effect of aging periods (1 and 4 years) on the physical and chemical properties of plasticized PLA nanocomposites. The plasticized PLA and plasticized PLA based nanocomposites were unstable and showed deplasticization after aging. The degradation was more pronounced in the plasticized PLA, where PEG was phase separated and diffused out with aging. The clay helped in restricting the diffusion and was noticeable when the affinity between clay (Cloisite[®] 20A and 30B) and PLA was good. Pluta et al.^[115] also reported the formation of intercalated and exfoliated geometries with an increase in the compounding time. Rheological studies showed pseudo-solid like behavior of PLA nanocomposites. Thermal stability of PLA was found to increase with nano-clay addition. PLA-clay nanocomposite cast film was prepared via a masterbatch method^[116]. An increase in tensile modulus and elongation at break was reported for cast film having 5 wt.% of organically modified montmorillonite clay. Paul et al.^[117, 118]

studied nanocomposites prepared from plasticized PLA. The thermal and morphological properties of the nanocomposites of plasticized PLA having 20 wt.% of polyethylene glycol (PEG 1000) were studied^[117]. The thermal stability of the nanocomposite was reported to be highest when organically modified montmorillonite clay was modified with bis-(2-hydroxyethyl) methyl (hydrogenated tallow alkyl) ammonium cation. The result was related to the better affinity of this clay with PLA owing to the presence of polar interactions. In another study by Paul et al.^[118], both intercalated and exfoliated PLLA/organo modified montmorillonite nanocomposites were synthesized by in-situ ring opening polymerization of L-lactide. Mechanical properties of these nanocomposites were not reported.

Thellen et al.^[119] first reported the fabrication of an extrusion blown film of plasticized PLA based nanocomposites. The effect of processing parameters (screw speeds) on the barrier, thermal, mechanical, and biodegradation properties of the nanocomposites were evaluated and compared to that of neat polymer. There was 48 and 50% improvement in the oxygen barrier and water vapor barrier of the nanocomposite films, respectively, compared to the neat films. The Young's modulus of the nanocomposite was improved by 20%, while the elongation at break was unaffected on nanoclay addition. Tensile strength of the nanocomposites did not change significantly. Thermal stability of the nanocomposite film was enhanced as compared to neat PLA. Tanoue et al.^[120] reported the use of polyethylene glycol (PEG) of different molecular weights as plasticizers for PLA nanocomposites. PEG was not helpful in obtaining an exfoliated clay geometry in the PLA matrix. Chang et al.^[121, 122] studied the thermo-mechanical properties, morphologies, gas permeability and optical translucency of PLA

nanocomposite films. Solution intercalation processing was used for the dispersion of two different kind of clays in PLA^[121]. The organo-clays were montmorillonite modified with hexadecylamine (C16-MMT) and fluorinated-mica modified with hexadecylamine (C16-Mica). One of the important findings of this work was the unaffected optical translucency of nanocomposite film containing organoclay content up to 6 wt%, while the films containing 8 wt% organoclays were slightly cloudier. In another study, Chang et al.^[122] reported the use of hexadecylamine–montmorillonite (C16–MMT), dodecyltrimethyl ammonium bromide–montmorillonite (DTA-MMT), and Cloisite[®]25A organoclays in the preparation of PLA based nanocomposites. An increase in the tensile strength and gas barrier was reported for the nanocomposites.

Gorassi et al.^[123] evaluated the transport properties of PLA based nanocomposites in term of sorption (S) and the zero-concentration diffusion coefficient (D-0). These properties were studied for both exfoliated and intercalated clay geometries in PLA nanocomposites prepared with montmorillonite clays (1, 3, 5, and 10 wt.%) modified with bis-(2-hydroxyethyl)methyl (tallow-alkyl) ammonium cation. The amount of a solvent absorbed i.e. obtained from the linear part of the sorption curve, was lower in the intercalated nanocomposites than the exfoliated nanocomposite at all clay contents. In intercalated samples, the thermodynamic diffusion parameters, D-0, decreased by one order of magnitude with increasing the clay content from 0 to 10 wt%. The exfoliated nanocomposite showed strong lowering in the D-0 value by about two orders of magnitude with respect to all the other samples (unfilled and intercalated). It was found that the exfoliation of the clay platelets was the most vital factor to improve the barrier properties of the material to water vapor. In other research^[124], oxygen barrier properties

of nanocomposites of ethylene-vinyl alcohol copolymer (EVOH) and PLA were studied under dry and humid conditions. Organically modified kaolinite and montmorillonite clays were used for PLA nanocomposite fabrication. The oxygen barrier improved in both nanocomposites but the increase was smaller than that of EVOH nanocomposite. The insufficient compatibility of PLA with these clays was one major reason behind these results. The higher sorption of solvent and slower diffusion kinetics of nanocomposite was predicted as suitable properties for applications such as active packaging. In an effort to develop PLA based bionanocomposites, PLA-cellulose nanowhisker nanocomposites have been explored recently^[125-128].

2.4 Hyperbranched Polymers (HBP)

The polymer science is dominated by the two major molecular architectures linear and crosslinked. The molecular architecture of a polymer has a marked effect on its physical properties. In recent years, macromolecules having dendritic topology are gaining lot of interest due to their nanostructure and unique physical properties. Dendrimers and dendritic polymers such as hyperbranched polymers are at the forefront of this emerging new class of macromolecules^[129]. Some of the characteristic differences in properties of a linear and dendritic architecture are shown in Table 2.3^[130]. The term dendrimers is derived from Greek word dendron (tree) and meros (part). The dendrimers are three dimensional, uniform, monodisperse macromolecules having tree like structures. Their general construction is comprised of a central core or focal point, a well-defined radially symmetrical layer of repeating units, often termed as generation and endgroups, which are also called as terminal or peripheral groups.

Table 2.3: Typical differences in the characteristics of a linear and dendritic polymer. (After ref. 130)

Linear	Dendritic
<ol style="list-style-type: none"> 1. Random Coil Configuration 2. Semicrystalline/crystalline materials: higher glass transition temperature 3. Lower solubility- decrease with molecular weight 4. Entanglement directed rheological properties: shear sensitivity 5. Intrinsic viscosity follows logarithmic- Increase with Mwt 6. Mobility based on reptation: segmental and molecular mobility 7. Anisotropic electronic conductivity 	<ol style="list-style-type: none"> 1. Predictable shape changes as a function of Mwt. and core – robust spheroid; breathing deformability 2. Non-crystalline, amorphous materials: lower glass transition temperatures 3. Increased solubility- Increases with Mwt. 4. Newtonian type rheology- no shear sensitivity, considerably lower viscosity 5. Exhibits viscosity maximum and minimum plateau with Mwt.- low viscosity 6. Mobility involves whole dendrimer as the kinetic flow unit- virtually no reptation 7. Isotropic electronic conductivity.

Tomalia et al.^[129, 131, 132] carried out extensive work in the synthesis of dendrimers and reported the nanoscale dimension of dendrimer (hydrodynamic radii), which increases with the increase in the generation of dendrimers. Hyperbranched polymers (HBP) are extremely branched globular macromolecules that fall in the category of dendritic polymers. They are considered as mutant offspring's of the dendrimers. They are also dendritic in nature but are polydisperse and have irregularity in branching and structure^[133]. Figure 2.6^[134] describes the basic difference in the structure of a dendrimer and a hyperbranched polymer. The major advantage of hyperbranched polymers over dendrimers lies in their one-pot synthesis, which make their synthesis simple and cost

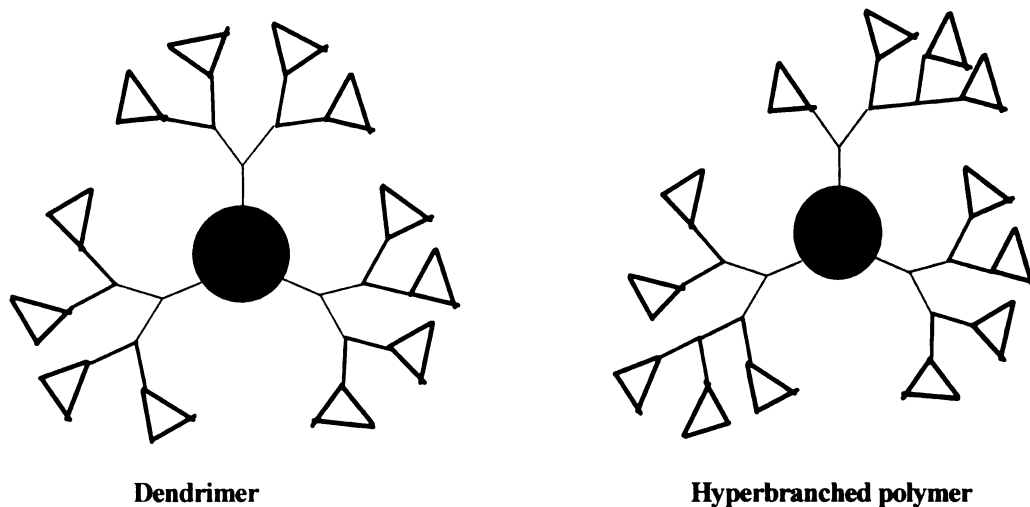


Figure 2.6: Schematic representation of the difference in the morphology of dendrimer (monodisperse) and Hyperbranched polymer (polydisperse). Redrawn after ref. 134. Here (●) represents central core and (△) represents end groups.

effective. On the other hand the synthesis of dendrimers is marred by the protection/deprotection, addition chemistry and purification at every step, making their synthesis extremely costly and time consuming. The hyperbranched polymers possess unique properties like dendrimers in spite of their imperfect molecular architecture. The principal reason for this analogous behavior of HBP is their extensively branched structure and high peripheral functionality. So, the hyperbranched polymers are considered as economical alternates to dendrimers in various application areas. The dendritic and hyperbranched structures can be synthesized in three different ways^[135]:

1. Divergent Approach
2. Mixed Reactivity Approach
3. Convergent approach

In the divergent approach, a multifunctional core is reacted with an equivalent amount of chain extenders depending upon the functional group on the core and reactive

group on the chain extender. Usually an A2B type of chain extender is reacted with central core resulting in molecule having twice the functionality of the core. The similar chain extender can further be used to increase the branching and molecular weight. In the mixed reactivity approach, different chain extenders having selective chemistry can be used to form dendritic structures. For example, in A2B chain extender, the functionality B can react with a central core having functionality C but functionality A cannot react with B or C. Similarly another chain extender C2D can be used for further growth. In this case the functionality D has reactivity with A but C cannot react with either A or D. In the convergent approach, the first step is to produce branches and then connect them to the central core.

The target applications of hyperbranched polymers are as rheological modifiers, additives in process engineering and processing of thermoplastics, lubricants, foams, surface modifiers, toughener for epoxy based resins, plasticizers, and viscosity modifiers for paints^[133]. Some of known examples of hyperbranched polymers are polyphenylenes, aromatic and aliphatic polyesters, polyethers, polyamides, polyurethanes, polycarbonates and polyesteramides^[136]. Hyperbranched polymers especially hydroxyl functional aliphatic polyesters, consist of a polyalcohol core from which branches extend and form a core-shell structure. The core shell structure has abundant hydroxyl groups at the periphery. Perstorp Polyols, a leading company in the manufacturing of hyperbranched hydroxyl functional aliphatic polyesters, use an initial core made up of pentaerythritol or trimethylol propane and uses dimethylol propionic acid as a chain extender^[135]. This results in generation of hydroxyl groups on the periphery of these molecules. The number

of OH groups on the surface will depend on the generation of the hyperbranched polymer. Some properties of hyperbranched polymers are:

- High reactivity due to peripheral functionality
- Nonlinear relationship of viscosity with molecular weight
- High thermal stability
- Variable glass transition temperature

Hyperbranched polymers (HBP) have attracted attention as toughness modifiers for thermosets (e.g. epoxy resins) instead of commercial tougheners such as rubbers and thermoplastics^[137-139]. Their role as compatibilizers and matrix modifiers in polymer blends and composites have also been reported^[140-142]. The current use of hyperbranched polymers as modifiers for linear thermoplastics is not that widespread and is even rare in bioplastics. In the research relevant to polylactides, Wong et al.^[143] reported a significant increase in the interlaminar fracture toughness of PLA based biocomposites in the presence of a hyperbranched polymer. In other research, a dendritic hyperbranched polymer improved the tensile strength and elongation at break of PLA^[144]. It also acted as a nucleating agent and improved the crystallization rate and crystallinity of PLA.

2.5 Toughening of Polymers

The term “toughness” denotes the absorption of energy during deformation of a material, which ultimately leads to fracture. Several applications of polymeric material require that these polymers should have the ability to deform and to sustain loads in various loading modes and should deform in a non-catastrophic way under sudden impact. Toughening of glassy polymers is more frequently achieved by means of incorporation of a dispersed rubbery phase. A polymer is considered glassy at

temperatures 10 to 20°C below its glass transition temperature (T_g)^[24]. A polymer glass usually fails by crazing, yielding or by combination of crazing and yielding. Polymers are classified in two main types: brittle (Type I) and pseudoductile (Type II)^[24]. The brittle polymers usually fail by crazing and have low crack initiation and crack propagation energy. The examples are polystyrene (PS), styreneacrylonitrile (SAN) and polymethylmethacrylate (PMMA). While pseudoductile polymers have propensity to fail by mean of yielding and usually have high crack initiation energy but low crack propagation energy. The examples are polyethylene terephthalate (PET), nylon and polycarbonate (PC).

Wu^[24] showed that brittle/ductile behavior of a polymer glass depends on the two chain parameters i.e. entanglement density and characteristic ratio.

Entanglement density, V_e , and characteristic ratio, C_∞ , a measure of chain stiffness is given by following equations^[24]:

Entanglement density, $V_e = \frac{\rho_a}{M_e}$ 2.1

Characteristic ratio, $C_\infty = \lim_{n \rightarrow \infty} [R_o^2 / nl^2]$ 2.2

Here ρ_a is amorphous mass density and M_e is molecular weight of entangled strand, R_o^2 is the mean square end-to-end distance of an unperturbed chain, n is number of statistical skeletal units, and l^2 is the mean square length of a statistical skeletal unit.

The molecular criteria for craze /yield behavior is shown to depend on the competition between crazing and yielding. When the crazing stress is lower than the yield stress, a polymer fails by crazing and it fails in a ductile mode if the condition is vice versa. The mixed deformation occurs when values of crazing and yield stress are comparable. An equation which gives the molecular criteria of brittle/ductile behavior is given by equation 2.3^[24].

$$\frac{\sigma_z}{\sigma_y} \propto \frac{V_e^{1/2}}{C_\infty} \dots\dots\dots 2.3$$

Here σ_z is the crazing stress and σ_y is the yield stress.

So, polymer having a low entanglement density, V_e , and higher characteristic ratio, C_∞ will tend to craze rather than yield. On other side, a polymer having higher V_e and lower C_∞ will tend to yield rather than craze. Although these criteria for craze/yield behavior is originated strictly for amorphous polymers but it is also known to be applicable for semi-crystalline polymer glasses that don't contain exceedingly high crystallinity. In these polymers amorphous phase is dominating in determining the behavior of the polymer.

A possible route for modification of brittle polymers is to promote large number of local energy absorption process by incorporating a rubbery dispersed phase. It is now well established that thermoplastics can be toughened by adding a suitable amount of rubber^[145]. In these multiphase systems the rubbery second phase initiates the energy absorbing process leading to the enhancement of toughness of the polymer. Several

brittle glassy polymers such as polystyrene (PS), polymethyl methacrylate (PMMA), polycarbonate (PC), and polyvinyl chloride (PVC) have been toughened by elastomeric modification^[146]. Such elastomeric modification approaches is also being extended to semi-crystalline polymers such as polypropylene (PP), polyamide (PA) and other brittle thermoplastics and thermosetts. Besides this modification several other approaches are also available to improve the toughness of brittle polymers. The common approaches are:

1. Rubber toughening
2. Blending with tough polymers
3. Particle filled toughening

Rubber toughening is more relevant to this research and is discussed here.

2.5.1 Rubber Toughening

The existence of rubber toughened plastic has been known for several years and has been researched extensively. The addition of small amount of suitable rubbery material (~10-25%) can provide the enhancement in the toughness of a brittle polymer by several orders of magnitude. The most prominent example is the use of butadiene rubber in polystyrene (PS) and styrene acrylonitrile (SAN) that lead to development of high impact polystyrene (HIPS) and acrylonitrile-butadiene-styrene (ABS) rubber. Other brittle amorphous polymers toughened with rubber particle are PMMA and PC. Among semicrystalline polymers, polypropylene possesses poor impact strength. The impact properties of polypropylene have been improved by the incorporation of rubbery polymers such as natural rubber, and ethylene propylene diene monomer (EPDM) rubber

[147]

2.5.2 Toughening Mechanism

There are several theories developed for the toughening mechanism of a two-phase polymer system in which the rubbery particles form the dispersed phase. The commonly known theories are:

1. Shear yielding
2. Cavitation
3. Multiple crazing
4. Mixed combination of shear yielding, multiple crazing and cavitation.

These theories have been widely applied for toughened amorphous polymer based systems. In case of semicrystalline polymers, the toughening mechanism in the presence of rubbery particles becomes complicated due to the interference of crystalline region. The common phenomena behind these toughening theories are critical ligament thickness, voiding, cavitation and damage competition.

Shear Yielding

The shear yielding phenomenon corresponds to plastic deformation in the localized zones in a polymer matrix. In unfilled polymers, shear yielding usually appears in the form of shear bands but in the case of impact modified systems, usually diffuse regions of plastic deformation appears in addition to the shear bands. Shear yielding is one of common toughening mechanism in several rubber modified blends ^[148, 149]. In the case of multiphase systems, dispersed-phase particles play the role of stress-concentrators which cause three-dimensional stress concentration. This induces the volume-expanding processes of cavitation, interfacial debonding, matrix crazing, and so forth. These mechanisms provide enough opportunity for the matrix around the particles to produce

shear yielding. The stress field caused by neighboring particles will overlap at a certain interparticle distance and the shear-yielding region in the matrix will be expanded further [150].

Cavitation

Dispersing rubbery heterogeneity in a polymer matrix led to creation of several stress centers around the rubbery particles. Stress is usually more at the equatorial plane of dispersed-phase particles under the application of an outside force. So, the interfacial debonding between the matrix and particle will occur first at this place, leading to the formation of microvoids. In another case, if the interfacial adhesion between the particle and matrix is strong, cavitation in the dispersed rubber particle phase occur, owing to the difference in Young's modulus and Poisson's ratio between the dispersed-phase rubber particles and the plastics matrix^[151]. This helps in relieving the triaxial stress state in the matrix, these microvoids/cavities also absorb deformation or fracture energy to produce the brittle to ductile transition. This concept of microvoid toughening in polymers has been studied both theoretically and experimentally^[152-154].

Multiple Crazing

It is well known that several glassy thermoplastics deform in brittle fashion by formation of crazes^[155-157]. Crazes are microvoids interconnected with the help of craze fibrils. The fibrils can sustain considerable plastic strain but the localized nature of crazes cause high stress on them, and instead of causing energy dissipation, they tend to break down, causing the failure of the polymer in a catastrophic manner. In other aspects of crazes, toughness of a glassy polymer can be enhanced by several orders of magnitude by incorporating rubbery particles that promote a large density of crazes^[158-160]. There is a

stress distribution by creation of numerous crazes, which prevent the catastrophic failure of a single craze. The rubber particles acts as passive stress concentrators and tend to initiate crazes around their equatorial region due to difference in the shear modulus of matrix and rubber particles. A certain degree of adhesion between the matrix and the rubbery phase is necessary in order to avoid premature craze failure.

2.5.3 Brittle to Ductile Transition (BDT) Criteria

Concept of Matrix Ligament Thickness and Percolation Model

Wu and coworkers^[24, 161-163] studied the relationship between the chain structure, phase morphology and toughness in polymers and blends. Wu studied the impact strength and rubber content of Nylon- 6/EPDM blends. They derived a brittle to ductile transition (BDT) master curve and proposed a concept of the matrix ligament thickness, τ , which is defined as the nearest distance of the matrix between two neighboring rubber particles (Figure 2.7)^[163], as a critical parameter for toughening of a multi-phase system. When the average ligament thickness is smaller than the critical

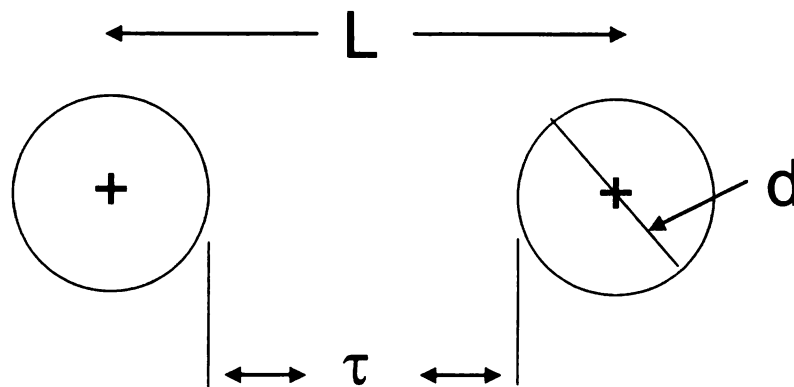


Figure 2.7: Schematic of Matrix Ligament Thickness. (Redrawn after ref. 163)

ligament thickness, τ , the blend will be tough; when greater, it will be brittle. In other words, the BDT will occur at τ . This is because if L is smaller than τ , a plane-strain to plane-stress transition would occur and the ligament would shear-yield, and the blend would be tough. On the other hand, if L is greater than τ , such transition would not occur, and the matrix ligament would fail in a brittle fashion.

Margolina and Wu^[164, 165] proposed a percolation theory for BDT transition. It was proposed the interconnectivity of thin ligaments is needed for facilitating the ductile failure of the matrix by the mechanism of shear yielding. They also put forward the concept of stress volume spheres, in which a percolation in BDT will occur if the stress volume spheres associated with rubber particles will overlap with each other. For this phenomenon to occur the distance between the particles should be below a critical ligament thickness. The schematic of stress volume sphere surrounding a rubber particle is given in Figure 2.8^[147]. Here d is the diameter of the particle. S is the stress volume of the rubber particle and τ is the critical ligament thickness.

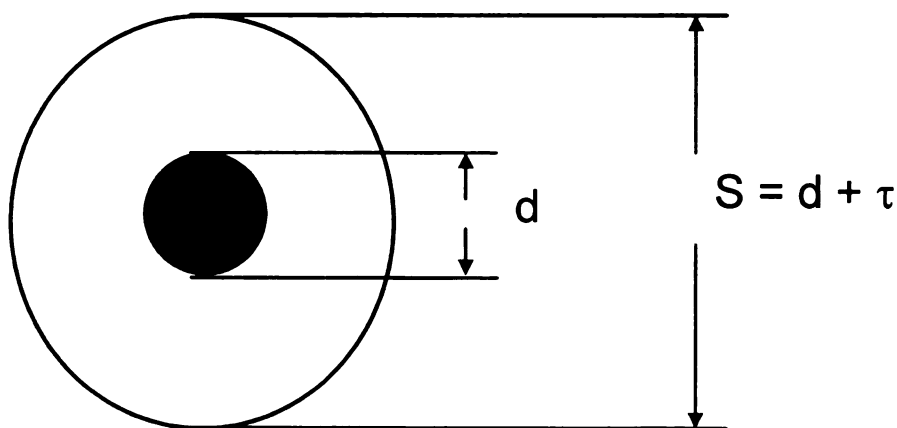


Figure 2.8: Schematic of stress volume sphere around a rubber particle. Here, shaded area represents a rubber particle. (Redrawn after ref. 147)

2.6 Alternate Ways of Toughening of Polymers

2.6.1 Interpenetrating Networks

Interpenetrating networks are novel blends composed of crosslinked polymers. Usually two crosslinked polymer systems are more or less intimately mixed without having covalent bonds between them. There are two popular techniques for producing IPN's ^[166]. In the first type, a polymer of type A is crosslinked and then swollen with a monomer of polymer of type B. This is followed by the in-situ polymerization and crosslinking of polymer B.

In the second approach, linear polymers, prepolymers, or monomers of the two types of polymer, along with their respective crosslinking agents, are taken in some liquid form, e.g. bulk (melt), solution, or dispersion. This is accompanied by the simultaneous polymerization and crosslinking of the two polymers. The normal blending or mixing of polymers is usually affected by the problem of phase separation. The well known reason for this behavior is the large chain length of polymer, which imposes restrictions on the large gain of entropy upon mixing of polymers. However, In the case of IPN the phase separation can be prevented by formation of an interpenetrating network. In a perfect IPN, the only way by which the phase separation can occur, is through breaking of covalent bond. But IPN are also affected by the phase separation, which usually occur well before the crosslinking of polymers take place especially in incompatible polymers. On the other hand, compatible polymers can form perfect IPNs circumventing phase separation completely.

IPN's are classified in several types depending on the mode of their preparation^[167] such as sequential IPN, simultaneous interpenetrating network (SIN) latex

IPN, gradient IPN, thermoplastic IPN, Semi-IPN. The interpenetrating networks have been developed for toughening of thermosets^[168-171]. Among bioplastics, PLLA was successfully toughened by creating a pseudo-semi-interpenetrating network with fullerene end-capped poly(ethylene oxide)^[172, 173]. There was 100 times increase in the strain energy of PLLA for this blend.

2.6.2 Nanostructure Blending

Blends of different polymers can exhibit enhanced mechanical, optical and electro-optical properties, which are not attainable with a single polymer, especially if the blend morphology is formed at submicrometer or nanometer scales. Fabrication and designing of thermodynamically stable polymer blends having structures at submicrometer/nanometer scales poses significant scientific and industrial challenges. These nanostructured materials present a unique combination of properties, which are impossible to achieve with classical blends. For polymer blends processed under typical extrusion conditions, the particle size of the dispersed phase is rarely below 0.1 μ (or 100 nm), irrespective of the compatibilization method employed. Polyethylene and polyamide have been melt blended to obtain new co-continuous morphologies at nanometer scale^[174]. The principle interest in the nanostructured polymer blends is because of the enhanced properties of such materials such as:

- Improved transparency
- Superior toughness
- High heat resistance

- Remarkable creep resistance
- Superior stiffness-toughness balance
- Effective at low concentration of tough polymer
- Retain properties after annealing

In a conventional blending, the micron scale particle of a minority polymer is dispersed in continuous matrix of other polymer. While, the principle aim of nanostructure blending is to obtain nanoscale dimension (less than 100 nm) of the dispersed phase. There are several approaches mentioned for preparation of nanostructure blends. The most common approaches are: ^[175-177]

1. Reactive Extrusion (in situ copolymerization, graft copolymerization)
2. Block copolymerization
3. High shear processing

The nanostructured blends mentioned in the literature are ^[175-177]:

1. Poly(vinylidene fluoride) (PVDF) and polyamide 11 (PA11) blends
2. Polypropylene (PP) and polyamide-6 (PA-6) blends
3. Polyethylene (PE)- polyamide (PA) blends

A graft copolymer having affinity for both polymers is normally used as compatibilizers. When the compatibilizer present above a critical concentration, they tend to reduce the domain size of minority polymer. A schematic representation of difference of micro blend from nanoblend is shown in Figure 2.9^[178].

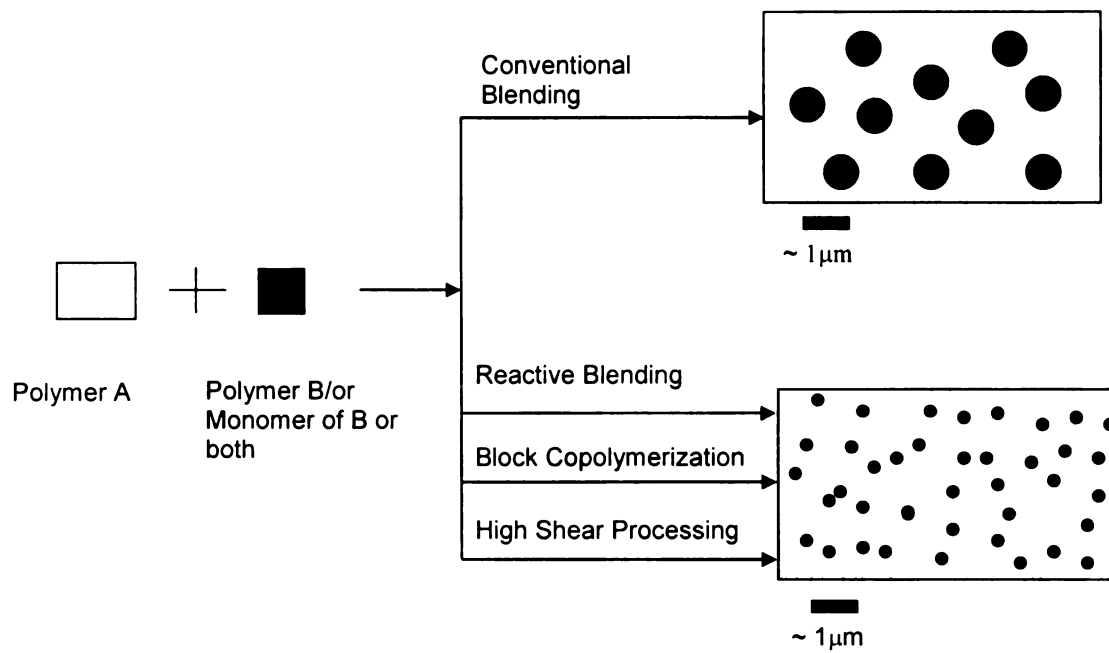


Figure 2.9: Schematic representation of methods of preparation of conventional blends and nanostructure blends. (Redrawn after Ref. 178)

2.7 References

1. Hartmann, M. H., *High Molecular Weight Polylactic Acid Polymers*. Biopolymers from Renewable Resources, ed. D.L. Kaplan. 1998, Berlin: Springer-Verlag. 367-411.
2. Drumright, R. E., Gruber, P. R., Henton, D. E., Polylactic Acid Technology. *Advance Materials*, 2000. **12**(23): p. 1841-1846.
3. Garlotta, Donald, A Literature Review of Poly(Lactic Acid). *Journal of Polymers and the Environment*,, 2002. **9**(2): p. 63-84.
4. Nomura, N., Ishii, R., Akakura, M., Aoi, K. , Stereoselective Ring-Opening Polymerization of Racemic Lactide Using Aluminum-Achiral Ligand Complexes: Exploration of a Chain-End Control Mechanism. *J. Am. Chem. Soc.* , 2002. **124**: p. 5938-5939.
5. Chamberlain, B. M., Cheng, M., Moore, D. R., Ovitt, T. M., Lobkovsky, E. B., Coates, G. W. , Polymerization of Lactide with Zinc and Magnesium -Diiminate Complexes: Stereocontrol and Mechanism *J. Am. Chem. Soc.* , 2001. **123**(14): p. 3229-3238.
6. De Santis, P., Kovacs, A. J., Molecular conformation of poly(S-lactic acid). *Biopolymers* 1968. **6**(3): p. 299-306.
7. Puiggalia, J., Ikadab, Y., Tsujic,H. , Cartiera,L., Okiharaa,T., Lotza,B., The frustrated structure of poly(L-lactide). *Polymer*, 2000 **41**: p. 8921–8930.
8. Hoogesteen, W., Postema, A.R., Pennings, A.J., ten Brinke, G., Zugenmaier, P., Crystal Structure, Conformation and Morphology of Solution –Spun Poly(L-lactide) Fibers *Macromolecules*, 1990. **23** (2).
9. Takahashi, K., Sawai, D., Yokoyama, T., Kanamoto, T., Hyon, S.H., Crystal transformation from the α - to the β -form upon tensile drawing of poly(L-lactic acid) *Polymer* 2004. **45** p. 4969–4976.
10. Eling, B., Gogolewski, S., Pennings, A.J., Biodegradable materials of poly (L-lactic acid) .1. Melt-spun and solution -spun fibers. *Polymer*, 1982. **23**(11): p. 1587-1593.
11. Cho, T.Y.; Strobl, G., Temperature dependent variation in lamellar structure of poly(L-lactide). *Polymer*, 2006. **47**: p. 1036-1043.

12. Kishore, K., Vasanthakumari, R., Pennings, A.J. , Isothermal Melting Behavior of Poly(L-Lactic Acid). *Journal of Polymer Science: Polymer Physics* 1984. **22**: p. 537-542
13. Perego, G., Cella, G. D., Bastioli, C., Effect of molecular weight and crystallinity on poly(lactic acid) mechanical properties. *Journal of Applied Polymer Science*, 1996. **59**(1): p. 37-43.
14. Auras, R., Harte, B., Selke, S., An overview of polylactides as packaging materials. *Macromolecular Bioscience*, 2004. **4**(9): p. 835-864.
15. Dow technical datasheet of STYRON 615APR General Purpose Polystyrene Resin.
16. [cited 03/02/ 2007]; Available from: <http://www.matweb.com/search/SpecificMaterial.asp?bassnum=PE9039>.
17. Huda, M. S., Drzal, L. T., Misra, M., Mohanty, A. K., Williams, K., Mielewski, D. F., A study on biocomposites from recycled newspaper fiber and poly(lactic acid). *Industrial & Engineering Chemistry Research*, 2005. **44**(15): p. 5593-5601.
18. Ave'rous, L., Biodegradable Multiphase Systems Based on Plasticized Starch: A Review. *Journal of Macromolecular Science Part C—Polymer Reviews*, 2004. **C44**(3): p. 231-174.
19. Bhardwaj, R., Mohanty, A. K., Drzal, L. T., Misra, M., *Novel 'Green Composites' from Recycled Newspaper Fiber and Polyhydroxyalkanoates (PHAs): Studies of Thermo-Mechanical Properties*, in *American Society for Composites 20th Annual Technical Conference* September 7-9, 2005: Philadelphia, PA. .
20. Bionolle biodegradable aliphatic polyesters, Technical data sheet, Showa Highpolymer Co. Ltd. .
21. Gross, R. A., Kalra, B., Biodegradable polymers for the environment. *Science*, 2002. **297**(5582): p. 803-807.
22. <http://www.biomer.de/IndexE.html>, <http://www.biomer.de/Huettenberger.pdf> (Accessed on April 19, 2007).
23. Techno-economic Feasibility of Large-scale production of Bio-based Polymers in Europe., <http://www.biomatnet.org/publications/1944rep.pdf> (accessed on April 20, 2007).

24. Wu, S, Chain structure, phase morphology, and toughness relationships in polymers and blends. *Polymer Engineering and Science*, 1990. **30**(13): p. 753-761.
25. Tonelli, A.E., Flory, P.J., The Configuration Statistics of Random Poly (lactic acid) Chains. I. Experimental Results'. *Macromolecules*, 1969. **2**(3): p. 225-227.
26. Joziasse, C. A. P., Veenstra, H., Grijpma, D. W., Pennings, A. J., On the chian stiffness of poly(lactide)s. *Macromol. Chem. Phys.*, 1996. **197**: p. 2219-2229.
27. Brant, D. A., Tonelli, A.E., Flory, P.J., The Configurational Statistics of Random Poly (lactic acid) Chains. 11. Theory. *Macromolecules*, 1969. **2**(3): p. 228-235.
28. Leenslag, J. W., Gogolewski, G.S., Pennings, A.J., Resorbable Materials of Poly(L-lactide). V. Influence of Secondary Structure on the Mechanical Properties and Hydrolyzability of Poly(L-lactide)Fibers Produced by a Dry-Spinning Method. *Journal of Applied Polymer Science*, 1984. **29**: p. 2829-2842.
29. Grijpma, D.W., Penning, J.P., Pennings, A.J., Chain entanglement, mechanical properties and drawability of poly(lactide). *Colloid Polym. Sci.*, 1994. **271**: p. 1068-1081.
30. Grijpma, D.W., Altpeter, H., Bevis, M.J., Feijen, J., Improvement of the mechanical propertes of poly(D,L-lactide) by orientation. *Polymer International*, 2002. **51**: p. 845-851.
31. Donald, A. M. Physics of glassy polymers, ed. R.N. Harward, Young, R. J. 1997: Chapman & Hall.
32. Grijpma, D.W., Pennings, A.J., (Co)polymers of L-lactide, 2^a) Mechanical Properties. *Macromol. Chem. Phys.*, 1994. **195**: p. 1649-1663.
33. Renouf-Glausera, A.C., Roseb, J., Farrarb, D. F., Camerona, R. E., The effect of crystallinity on the deformation mechanism and bulk mechanical properties of PLLA. *Biomaterials* 2005(26): p. 5771–5782.
34. Witzke, D.R., Introduction to properties, engineering and prospects for polylactide polymers, PhD Theses, Michigan State University. 1997.
35. Dorgan, J.R., Lehermeier, H., Mang, M., Thermal and Rheological Properties of Commercial-Grade Poly(Lactic acid)s *Journal of Polymer and the Environment*, 2000. **8**(1): p. 1-9.
36. Dorgan, J.R., Lehermeier, H. J., Palade, L.I., Cicero, J., Polylactides: Properties and Prospects of an Environmentally Benign Plastic from Renewable Resources. *Macromol. Symp.*, 2001. **175**: p. 55-66.

37. Dorgan, J. R., Williams, J. S., Melt rheology of poly(lactic acid): Entanglement and chain architecture effects. *J. Rheol.*, 1999. **43**(5): p. 1141-1155.
38. Dorgan, J. R., Janzen, J., Clayton, M. P., Hait, S. B., Knauss, D. M., Melt rheology of variable L-content poly(lactic acid). *J. Rheol.*, 2005. **49** (3): p. 607-619.
39. Dorgan, J. R., Janzen, Knauss, D. M., Hait, S. B., Limoges, B. R., Hutchinson, M. H., Fundamental Solution and Single-Chain Properties of Polylactides. *Journal of Polymer Science: Part B: Polymer Physics*, 2005. **43**: p. 3100-3111.
40. Palade, L.I., Lehermeier, H.J., Dorgan, J.R., Melt Rheology of High L-Content Poly(lactic acid). *Macromolecules*, 2001. **34**: p. 1384-1390.
41. Yamane, H., Sasai, K., Takano, M., Poly(D-lactic acid) as a rheological modifier of poly(L-lactic acid): Shear and biaxial extensional flow behavior. *J.Rheol.*, 2004. **38**(3): p. 599-609.
42. Ramkumar, D.H.S., Bhattacharya, M., Steady Shear and Dynamic Properties of Biodegradable Polyesters. *Polymer Engineering and Science*, 1998. **38**(9): p. 1426-1435.
43. Bergsma, J.E., Rozema, F.R., Bos R.R.M., de Bruijn, W.C., *J. Oral Maxillofacial Surg.*, 1993. **51**(666-670).
44. Cohn, D., Hotovely-Salomon, A., Biodegradable multiblock PEO/PLA thermoplastic elastomers: molecular design and properties. *Polymer*, 2005. **46**(7): p. 2068-2075.
45. Tew, G. N., Triblock PLA-PEO-PLA hydrogels: Structure and mechanical properties. *Abstracts of Papers of the American Chemical Society*, 2003. **226**: p. U482-U482.
46. Tew, G. N., Bhatia, S. R., Aamer, K., Agrawal, S., DeLong, N. S., Mechanical properties of triblock PLA-PEO-PLA hydrogels. *Abstracts of Papers of the American Chemical Society*, 2005. **229**: p. U970-U970.
47. Tew, G. N., Sanabria-DeLong, N., Agrawal, S. K., Bhatia, S. R., New properties from PLA-PEO-PLA hydrogels. *Soft Matter*, 2005. **1**(4): p. 253-258.
48. Cohn, D., Salomon, A. F., Designing biodegradable multiblock PCL/PLA thermoplastic elastomers. *Biomaterials*, 2005. **26**(15): p. 2297-2305.
49. Li, F., S. M. Li, and M. Vert, Synthesis and rheological properties of polylactide/poly(ethylene glycol) multiblock copolymers. *Macromolecular Bioscience*, 2005. **5**(11): p. 1125-1131.

50. Labrecque, L.V., Kumar, R.A., Dave, V., Gross, R.A., McCarthy, S.P., Citrate Ester as Plasticizers for Poly(lactic acid) *Journal of Applied Polymer Science*, 1997. **66**: p. 1507-1513.
51. Jacobsen, S., Fritz, H.G., Plasticizing Polylactide- The Effect of Different Plasticizers on the Mechanical Properties. *Polymer Engineering and Science*, 1999. **39**: p. 1303-1310.
52. Martin, O., Averrous, L., Poly(lactic acid): Plasticization and Properties of Biodegradable Multiphase Systems. *Polymer*, 2001. **42**: p. 6209-6219.
53. Ljungberg N., Wesslen B., Preparation and Properties of Plasticized Poly(lactic acid) Films *Biomacromolecules*, 2005. **6**: p. 1789-1796.
54. Ljungberg N., Wesslen B., The effects of plasticizers on the dynamic mechanical and thermal properties of poly(lactic acid) *Journal of Applied Polymer Science*, 2002. **86**: p. 1227-1234
55. Ljungberg N., Wesslen B., Tributyl citrate oligomers as plasticizers for poly(lactic acid): thermo-mechanical film properties and aging *Polymer*, 2003. **44**: p. 7679-7688.
56. Ljungberg N., Colombini D., Wesslen B., Plasticization of Poly(lactic acid) with oligomeric malonate esteramides: Dynamic mechanical and thermal film properties *Journal of Applied Polymer Science*, 2005. **96**: p. 992-1002.
57. Ljungberg N., Andersson T., Wesslen B., Film extrusion and film weldability of poly(lactic acid) plasticized with triacetine and tributyl citrate 2003. **88**: p. 3239-3247
58. Hu, Y., Hu, Y.S., Topolkaev, V., Hiltner, A., Baer, E., Crystallization and phase separation in the blends of high stereoregular poly(lactide) with poly(ethylene glycol). *Polymer*, 2003. **44**: p. 5681-5689.
59. Hu, Y., Rogunova, M., Topolkaev, V., Hiltner, A., Baer, E., Aging of poly(lactide)/poly(ethylene glycol) blends. Part 1. Poly(lactide) with low stereoregularity. *Polymer*, 2003. **44**: p. 5701-5710.
60. Hu, Y., Hu, Y.S., Topolkaev, V., Hiltner, A., Baer, E., Aging of poly(lactide)/poly(ethylene glycol) blends. Part 2. Poly(lactide) with high stereoregularity. *Polymer*, 2003. **44**: p. 5711-5720.
61. Zhang, L., Changdong, X., Deng, X., Miscibility, crystallization and morphology of poly(β -hydroxybutyrate)/ poly(*d,l*-lactide) blends. *Polymer*, 1996. **37**(2): p. 235-241.

62. Koyama, N., Yoshiharu, D., Miscibility of binary blends of poly[(R)-3-hydroxybutyric acid] and poly[(S)-lactic acid]. *Polymer*, 1997. **38**(7): p. 1589-1593.
63. Ohkoshi, I., Abe, H., Doi, Y., Miscibility and solid-state structures for blends of poly[(S)-lactide] with atactic poly[(R,S)-3-hydroxybutyrate]. *Polymer* 2000. **41**: p. 5985-5992.
64. Park, J.W., Doi, Y., Iwata, T., Uniaxial Drawing and Mechanical Properties of Poly[(R)-3-hydroxybutyrate]/Poly(L-lactic acid) Blends. *Biomacromolecules*, 2004. **5**: p. 1557-1566.
65. Ferreira, B. M. P., Zavaglia, C. A. C., Duek, E. A. R., Films of PLLA/PHBV: Thermal, Morphological, and Mechanical Characterization. *Journal of Applied Polymer Science*, 2002. **86**: p. 2898-2906.
66. Takagi, Y., Yasuda, R., Yamaoka, M., Yamane, T., Morphologies and Mechanical Properties of Polylactide Blends with Medium Chain Length Poly(3-Hydroxyalkanoate) and Chemically Modified Poly(3-Hydroxyalkanoate). *Journal of Applied Polymer Science*, 2004. **93**: p. 2363-2369.
67. Noda, I., Satkowski, M.M., Dowrey, A.E., Marcott, C., Polymer Alloy of Nodax Copolymers and Poly(lactic acid). *Macromolecular Bioscience*, 2004. **4**: p. 269-275.
68. Broz, M. E., Vanderhart, D. L., Washburn, N. R., Structure and Mechanical Properties of Poly(D, L-lactic acid)/ Poly(ϵ -caprolactone) Blends. *Biomaterials*, 2003. **24**: p. 4181-4190.
69. Semba, T., Kitagawa, K., Ishiaku, U. S., Hamada, H., The Effect of Crosslinking on the Mechanical Properties of Polylactic Acid/Polycaprolactone Blends. *Journal of Applied Polymer Science*, 2006. **10**: p. 1816-1825.
70. Wang, L., Ma, W., Gross R. A., McCarthy, S. P., Reactive Compatibilization of Biodegradable Blends of Poly(lactic acid) and Poly(ϵ -caprolactone). *Polymer Degradation and Stability*, 1998. **59**: p. 161-168.
71. Lostocco, M. R., Borzacchiello, A., Huang, S. J., Binary and ternary poly(lactic acid) poly(ϵ -caprolactone) blends: The effects of oligo- ϵ -caprolactones upon mechanical properties. *Macromolecular Symposia*, 1998. **130**: p. 151-160.
72. Rezgui, F., Swistek, M., Hiver, J. M., G'Sell, C., Sadoun, T., Deformation and damage upon stretching of degradable polymers (PLA and PCL). *Polymer*, 2005. **46**(18): p. 7370-7385.

73. Semba, T., Kitagawa, K., Ishiaku, U. S., Kotaki, M., Hamada, H., Effect of compounding procedure on mechanical properties and dispersed phase morphology of poly(lactic acid)/polycaprolactone blends containing peroxide. *Journal of Applied Polymer Science*, 2007. **103**(2): p. 1066-1074.
74. Stolt, M., Viljanmaa, M., Sodergard, A., Tormala, P., Blends of poly(epsilon-caprolactone-b-lactic acid) and poly(lactic acid) for hot-melt applications. *Journal of Applied Polymer Science*, 2004. **91**(1): p. 196-204.
75. Takayama, T., Todo, M., Tsuji, H., Arakawa, K., Improvement of fracture properties of PLA/PCL polymer blends by control of phase structures. *Kobunshi Ronbunshu*, 2006. **63**(9): p. 626-632.
76. Chen, G. X., Kim, H. K., Kim, E. S., Yoon, J. S., Compatibilization-like effect of reactive organoclay on the poly(L-lactide)/poly(butylene succinate) blends. *Polymer*, 2005. **46**: p. 11829–11836.
77. Park, J. W., Im, S. S., Phase Behavior and Morphology in Blends of Poly(L-lactic acid) and Poly(butylene succinate). *Journal of Applied Polymer Science*, 2002. **86**: p. 647-655.
78. Park, J. W., Im, S. S., Morphological Changes during Heating in Poly(L-lactic acid)/Poly(butylene succinate) Blend Systems as Studied by Synchrotron X-Ray Scattering. *Journal of Polymer Science: Part B Polymer Physics*, 2002. **40**: p. 1931–1939.
79. Shibata, M., Inoue, Y., Miyoshi, Y., Mechanical properties, morphology, and crystallization behavior of blends of poly(L-lactide) with poly(butylene succinate-co-L-lactate) and poly(butylene succinate). *Polymer* 2006. **47**: p. 3557-3564.
80. Lee, S., Lee, J. W., Characterization and processing of Biodegradable polymer blends of poly(lactic acid) with poly(butylene succinate adipate). *Korea-Australia Rheology Journal*, 2005. **17**(2): p. 71-77.
81. Jiang, L., Wolcott, M. P., Zhang, J., Study of Biodegradable Polylactide/Poly(butylene adipate-co-terephthalate) Blends. *Biomacromolecules*, 2006. **7**: p. 199-207.
82. [cited March 5, 2007]; Available from: http://www2.basf.de/basf2/html/plastics/englisch/pages/presse/05_538.htm.
83. Wang, Y., Hillmyer, M.A., Polyethylene-Poly(L-lactide) Diblock Copolymers: Synthesis and Compatibilization of Poly(L-lactide)/Polyethylene Blends. *Journal of Polymer Science Part A: Polymer Chemistry*, 2001. **39**: p. 2755-2766.

84. Anderson, K.S., Shwan, H. L., Hillmyer, M.A. , Toughening of Polylactides by Melt Blending with Linear Low-Density Polyethylene. *Journal of Applied Polymer Science*, 2003. **89**: p. 3757-3768.
85. Anderson, K.S., Hillmyer, M.A., The Influence of Block Copolymer Microstructure on the Toughness of Compatibilized Polylactide/Polyethylene Blends. *Polymer*, 2004. **45**: p. 8809-8823.
86. Kim, F.K., Choi, C.N., Kim, Y.D., Lee, K. Y., Lee, M. S. , Compatibilization of Immiscible Poly(l-lactide) and Low Density Polyethylene Blends. *Fibers and Polymers*, 2004. **5**(4): p. 270-274.
87. Jin, H. J., Chin, I. J., Kim, M. N., Kim, S. H., Yoon, J. S., Blending of poly(L-lactic acid) with poly(cis-1,4-isoprene). *European Polymer Journal*, 2000. **36**: p. 165-169.
88. Schimdt, S. C., Hillmyer, M. A., Synthesis and Characterization of Model Polyisoprene-Polylactide Diblock Copolymers. *Macromolecules*, 1999. **32**: p. 4794-4801.
89. Wang, Y., Hillmyer, M. A., Synthesis of Polybutadiene-Polylactide Diblock Copolymers Using Aluminum Alkoxide Macroinitiators. Kinetics and Mechanism. *Macromolecules*, 2000. **33**: p. 7395-7403.
90. Okamoto, M, *Polymer/clay nanocomposites*, in *Encyclopedia of Nanoscience and Nanotechnology*. 2004, American Scientific Publishers: Valencia, CA p. 791-843.
91. Giannelis, E. P., Polymer Layered Silicate Nanocomposites. *Advanced Materials*, 1996. **8**(1).
92. Ray, S.S., Bousmina, M. , Biodegradable polymers and their layered silicate nanocomposites: In greening the 21st century materials world. *Progress in Materials Science*, 2005. **50**: p. 962-1079.
93. Ogata, N., Jimenez, G., Kawai, H., Ogihara, T., Structure and Thermal/Mechanical Properties of Poly (l-lactide)-Clay Blend. *Journal of Applied Polymer Science: Part B: Polymer Physics*, 1997. **35**: p. 389-396.
94. Ray, S.S., Yamada, K., Okamoto, M., Ueda, K., Polylactide-Layered Silicate Nanocomposites:A Novel Biodegradable Material. *Nano Letters*, 2002. **2**: p. 1093-1096.
95. Ray, S.S., Maiti, P., Okamoto, M., Yamada, K., Ueda, K., New polylactide/layered silicate nanocomposites. 1. Preparation, characterization and proerties. . *Macromolecules*, 2002. **35**: p. 3104-3110.

96. Ray, S.S., Yamada, K., Ogami, A., Okamoto, M., Ueda, K., New polylactide layered silicate nanocomposites: nanoscale control of multiple properties. *Macromol Rapid Commun*, 2002. **23**: p. 493-497.
97. Ray, S. S., Yamada, K., Okamoto, M., Ueda, K., Control of biodegradability of polylactide via nanocomposite technology. *Macromolecular Materials and Engineering*, 2003. **288**(3): p. 203-208.
98. Ray, S.S., Okamoto, M., Biodegradable Polylactide and Its Nanocomposites: Opening a New Dimension for Plastics and Composites. *Macromol. Rapid Commun.* , 2003. **24**: p. 815-840.
99. Ray, S.S., Yamada, K., Okamoto, M., Ueda, K., New polylactide-layered silicate nanocomposites. 2. Concurrent improvements of material properties, biodegradability and melt rheology. *Polymer*, 2003. **44**: p. 857-866.
100. Ray, S.S., Yamada, K., Okamoto, M., Ogami, A., Ueda, K., New Polylactide/Layered Silicate Nanocomposites. 3. High-Performance Biodegradable Materials. *Chem. Mater.*, 2003. **15**: p. 1456-1465.
101. Ray, S.S., Yamada, K., Okamoto, M., Fujimoto, M., Ogami, A., Ueda K., New polylactide/layered silicate nanocomposites. 5. Designing of materials with desired properties. *Polymer*, 2003. **44**: p. 6633–6646.
102. Ray, S.S., Yamada, K., Okamoto, M., Ogami, A., Ueda K., New polylactide/layered silicate nanocomposites, 4. Structure, properties and biodegradability *Composite Interfaces*, 2003. **10**(4-5): p. 435-450.
103. Ray, S.S., Yamada, K., Okamoto, M., Ueda, K., Biodegradable polylactide/montmorillonite nanocomposites *Journal of Nanoscience and Nanotechnology*, 2003. **3**(6): p. 503-510.
104. Ray, S. S., Okamoto, M., New Polylactide/Layered Silicate Nanocomposites, 6a Melt Rheology and Foam Processing. *Macromol. Mater. Eng.*, 2003. **288**: p. 936–944.
105. Fujimoto, Y., Ray, S.S., Okamoto M, Ogami, Yamada, K., Ueda, K., Well-Controlled Biodegradable Nanocomposite Foams: From Microcellular to Nanocellular. *Macromol Rapid Commun*, 2003. **24**: p. 457–461.
106. Di, Y., Iannace, S., Maio, E. D., Nicolaisi, L., Poly(lactic acid)/Organoclay Nanocomposites: Thermal, Rheological Properties and Foam Processing. *Journal of Polymer Science: Part B: Polymer Physics*, 2005. **43**: p. 689–698.

107. Maiti, P., Yamada, K., Okamoto, M., Ueda, K., Okamoto, K., New Poly(lactide)/Layered Silicate Nanocomposites: Role of Organoclays. *Chem. Mater.*, 2002. **14**: p. 4654-4661.
108. Nam, J. Y., Ray, S. S., Okamoto, M., Crystallization Behavior and Morphology of Biodegradable Poly(lactide)/Layered Silicate Nanocomposite. *Macromolecules*, 2003. **36**: p. 7126-7131.
109. Shibata, M., Someya, Y., Orihara, M., Miyoshi, M., Thermal and Mechanical Properties of Plasticized Poly(L-lactide) Nanocomposites with Organo-Modified Montmorillonites. *Journal of Applied Polymer Science*, 2006. **99**: p. 2594–2602.
110. Wu, T. M., Chiang, M. F., Fabrication and Characterization of Biodegradable Poly(Lactic Acid)/Layered Silicate Nanocomposites. *Polymer Engineering and Science*, 2005: p. 1615-1621.
111. Chen, G. X., Kim, H. S., Shim, J. H., Yoon, J.S., Role of Epoxy Groups on Clay Surface in the Improvement of Morphology of Poly(L-lactide)/Clay Composites. *Macromolecules*, 2005. **38**: p. 3738-3744.
112. Hasook, A., Tanoue, S., Iemoto, Y., Characterization and Mechanical Properties of Poly(lactic acid)/Poly(ϵ -caprolactone)/Organoclay Nanocomposites Prepared by Melt Compounding. *Polymer Engineering and Science*, 2006: p. 1001-1007.
113. Pluta, M., Paul, M. A., Alexandre, M., Dubois, P., Plasticized poly(lactide)/clay nanocomposites. I. The role of filler content and its surface organo-modification on the physico-chemical properties. *Journal of Polymer Science Part B: Polymer Physics*, 2005. **44**(2): p. 299 - 311.
114. Pluta, M., Paul, M. A., Alexandre, M., Dubois, P., Plasticized poly(lactide)/clay nanocomposites. II. The effect of aging on structure and properties in relation to the filler content and the nature of its organo-modification. *Journal of Applied Polymer Science: Part B Polymer Physics*, 2005. **44**(2): p. 312 - 325.
115. Pluta, M., Melt Compounding of Poly(lactide)/Organoclay: Structure and Properties of Nanocomposites. *Journal of Polymer Science: Part B: Polymer Physics*, 2006. **44**: p. 3392–3405.
116. Lewitus, D., McCarthy, S., Ophir, A., Kenig, S., The Effect of Nanoclays on the Properties of PLLA-modified Polymers Part 1: Mechanical and Thermal Properties. *J Polym Environ*, 2006. **14**: p. 171–177.
117. Paul, M. A., Alexandre, M., Dege'e, P., Henrist, C., Rulmont, A., Dubois, P., New nanocomposite materials based on plasticized poly(-lactide) and organo-modified montmorillonites: thermal and morphological study *Polymer*, 2003. **44**(2): p. 443-450.

118. Paul, M. A., Delcourt, C., Alexandre, M., Dege' e, P., Monteverde, F., Rulmont, A., Dubois, P., (Plasticized) Polylactide/(Organo-)Clay Nanocomposites by in situ Intercalative Polymerization. *Macromol. Chem. Phys.* 484–498, 2005. **206**: p. 484–498.
119. Thellen, C., Orroth, C., Froio, D., Ziegler, D., Lucciarini, J., Farrell, R., D'Souza, N. A., Ratto, J. A., Influence of montmorillonite layered silicate on plasticized poly(L-lactide) blown films. *Polymer*, 2005. **46**: p. 11716–11727.
120. Tanoue, S., Hasook, A., Iemoto, Y., Preparation of Poly(lactic acid)/Poly(ethylene glycol)/Organoclay Nanocomposites by Melt Compounding. *Polymer Composites*, 2006: p. 256-263.
121. Chang J. H., An Y. U., Cho D. H., Giannelis E. P. , Poly(lactic acid) nanocomposites: comparison of their properties with montmorillonite and synthetic mica(II) *Polymer*, 2003. **44**(13): p. 3715-3720.
122. Chang, J. H., Yeong, U. A., Sur, G.S., Poly(lactic acid) Nanocomposites with Various Organoclays. I. Thermomechanical Properties, Morphology, and Gas Permeability. *Journal of Applied Polymer Science: Part B Polymer Physics*, 2003. **41**: p. 94-103.
123. Gorrasi, G., Tammaro, L., Vittoria, V., Paul, M. A., Alexandre, M., Dubois, P. , Transport properties of water vapor in polylactide/montmorillonite nanocomposites *Journal of Macromolecular Science- Physics* 2004. **B43**(3): p. 565-575
124. Lagaron, J. M., Cabedo, L., CAVA, D., Feijoo, J. L., Gavara, R., Gimenez, E., Improving packaged food quality and safety. Part 2: Nanocomposites. *Food Additives and Contaminants*, 2005. **22**(10): p. 994–998.
125. Mathew, A. P., Chakraborty, A., Oksman, K., Sain, M., The structure and mechanical properties of cellulose nanocomposites prepared by twin screw extrusion *ACS symposium series* 2006. **938** p. 114-131.
126. Oksman, K., Mathew, A. P., Bondesona, D., Kviena, I. , Manufacturing process of cellulose whiskers/polylactic acid nanocomposites *Composite Science and Technology*, 2006. **66**(15): p. 2776-2784
127. Petersson, L., Oksman, K., Preparation and properties of biopolymer-based nanocomposite films using microcrystalline cellulose. *Acs Symposium Series*, 2006. **938**: p. 132-150.
128. Petersson, L., Oksman, K., Biopolymer based nanocomposites: Comparing layered silicates and microcrystalline cellulose as nanoreinforcement. *Composites Science and Technology*, 2006. **66**(13): p. 2187-2196.

129. Tomalia, D. A., Frechet, J. M., Introduction to "Dendrimers and dendritic polymers". *Progress in Polymer Science*, 2005. **30**(3-4): p. 217-219.
130. Tomalia, D. A., Frechet, J. M. J., *Dendrimers and Other Dendritic Polymers*. Ed. Frechet, J. M. J, Tomalia, D. A. in Wiley Series in Polymer Science, ed. J. Scheirs. 2001, Chichester: John Wiley and Sons.
131. Tomalia, D. A., Frechet, J. M. J., Discovery of dendrimers and dendritic polymers: A brief historical perspective. *Journal of Polymer Science Part a-Polymer Chemistry*, 2002. **40**(16): p. 2719-2728.
132. Tomalia, D. A., Birth of a new macromolecular architecture: dendrimers as quantized building blocks for nanoscale synthetic polymer chemistry. *Prog. Polym. Sci.* , 2005. **30**: p. 294-324.
133. Seiler, M. , Dendritic Polymers-Interdisciplinary Research and Emerging Applications from Unique Structural Properties. *Chem. Eng. Technol*, 2002. **25**(3): p. 237-253.
134. Redrawn after <http://www.hyperpolymers.com/prodinf.html> (Accesses on November 2, 2007).
135. Pettersson, B. , *Hyperbranched Polymers - Unique design tools for multi property controls in resins and coatings*. http://www.perstorp.com/upload/hyperbranched_polymers.pdf, Date Accessed: January 5, 2007.
136. Hult, A., Johansson, M., Malmström, E., Hyperbranched Polymers. *Advances in Polymer Science*, 1999. **143**.
137. Mezzenga, R., Boogh, L., Manson, J. A. E., A review of dendritic hyperbranched polymer as modifiers in epoxy composites. *Composites Science and Technology*, 2001. **61**(5): p. 787-795.
138. Wu, H., Xu, J., Liu, Y., Heiden, P., Investigation of readily processable thermoplastic-toughened thermosets. V. Epoxy resin toughened with hyperbranched polyester. *Journal of Applied Polymer Science*, 1999. **72**(2): p. 151-163.
139. Boogh, L., Pettersson, B., Kaiser, P., Manson, J. A., Novel tougheners for epoxy-based composites. *Sampe Journal*, 1997. **33**(1): p. 45-49.
140. Jannerfeldt, G., Boogh, L., Manson, J.A.E. , Tailored interfacial properties for immiscible polymers by hyperbranched polymers. *Polymer*, 2000. **41**: p. 7627-7634.

141. Jannerfeldt, G., Boogh, L., Manson, J. A. E., The morphology of hyperbranched polymer compatibilized polypropylene/polyamide 6 blends. *Polymer Engineering and Science*, 2001. **41**(2): p. 293-300.
142. Jannerfeldt, G., Tornqvist, R., Rambert, N., Boogh, L., Manson, J. A. E., Matrix modification for improved reinforcement effectiveness in polypropylene/glass fibre composites. *Applied Composite Materials*, 2001. **8**(5): p. 327-341.
143. Wong, S., Shanks, R. A., Hodzic, A., Mechanical Behavior and Fracture Toughness of Poly(L-lactic acid)-Natural Fiber Composites Modified with Hyperbranched Polymers. *Macromol. Mater. Eng.*, 2004. **289**: p. 447-456.
144. Zhang, J. F., Sun, X., Mechanical properties and crystallization behavior of poly(lactic acid) blended with dendritic hyperbranched polymer. *Polymer International* 2004. **53**: p. 716-722.
145. Bucknall, C. B., *Toughened Plastics*. 1977, London: Applied Science Publishers.
146. Michler, G. H., Adhikari, R., Hennings, S., Toughness enhancement of nanostructured amorphous and semicrystalline polymers. *Macromol. Symp.*, 2004. **214**: p. 47-71.
147. Liang, J. Z., Li, R. K. Y., Rubber toughening in polypropylene: A review. *Journal of Applied Polymer Science*, 2000. **77**(2): p. 409-417.
148. Bucknall, C. B., Quantitative approaches to particle cavitation, shear yielding, and crazing in rubber-toughened polymers. *Journal of Polymer Science Part B-Polymer Physics*, 2007. **45**(12): p. 1399-1409.
149. Zhou, C., Si, Q. B., Ao, Y. H., Tan, Z. Y., Sun, S. L., Zhang, M. Y., Zhang, H. X., Effect of matrix composition on the fracture behavior of rubber-modified PMMA/PVC blends. *Polymer Bulletin*, 2007. **58**(5-6): p. 979-988.
150. Sjoerdsma, S. D., The Tough-Brittle Transition in Rubber-Modified Polymers. *Polymer Communications*, 1989. **30**(4): p. 106-108.
151. Guild, F. J., Young, R. J., A Predictive Model for Particulate Filled Composite-Materials .2. Soft Particles. *Journal of Materials Science*, 1989. **24**(7): p. 2454-2460.
152. Merz, E. H., Claver, G. C., Baer, M., Studies on Heterogeneous Polymeric Systems. *Journal of Polymer Science*, 1956. **22**(101): p. 325-341.
153. Orowan, E., Fracture and Strength of Solids. *Reports on Progress in Physics*, 1948. **12**: p. 183-&.

154. Sue, H. J., Huang, J., Yee, A. F., Interfacial Adhesion and Toughening Mechanisms in an Alloy of Polycarbonate Polyethylene. *Polymer*, 1992. **33**(22): p. 4868-4871.
155. Maspoch, M. L., Tafzi, A., Ferrando, H. E., Velasco, J. I., Benasat, A. M., Filled PMMA: Mechanical properties and fracture behaviour. *Macromolecular Symposia*, 2001. **169**: p. 159-164.
156. Yang, J., Liu, J. J., Initiation and termination of crazes in high impact polystyrene. *Acta Polymerica Sinica*, 2000(3): p. 361-363.
157. Burford, R. P., Benson, C. M., Crazing in polymers. *Materials Forum*, 1995. **19**: p. 129-144.
158. Michler, G. H., Bucknall, C. B., New toughening mechanisms in rubber modified polymers. *Plastics Rubber and Composites*, 2001. **30**(3): p. 110-115.
159. Socrate, S., Boyce, M. C., Lazzeri, A., A micromechanical model for multiple crazing in high impact polystyrene. *Mechanics of Materials*, 2001. **33**(3): p. 155-175.
160. Lee, L. H., Mandell, J. F., McGarry, F. J., Multiple Crazing at Crack Tips in PVC under Plane-Strain Conditions. *Polymer Engineering and Science*, 1986. **26**(9): p. 626-632.
161. Wu, S. H., Impact Fracture Mechanisms in Polymer Blends - Rubber-Toughened Nylon. *Journal of Polymer Science Part B-Polymer Physics*, 1983. **21**(5): p. 699-716.
162. Wu, S. H., Phase-Structure and Adhesion in Polymer Blends - a Criterion for Rubber Toughening. *Polymer*, 1985. **26**(12): p. 1855-1863.
163. Wu, S. H., A Generalized Criterion for Rubber Toughening - the Critical Matrix Ligament Thickness. *Journal of Applied Polymer Science*, 1988. **35**(2): p. 549-561.
164. Margolina, A., Wu, S. H., Percolation Model for Brittle-Tough Transition in Nylon Rubber Blends. *Polymer*, 1988. **29**(12): p. 2170-2173.
165. Wu, S. H., Margolina, A., Percolation Model for Brittle Tough Transition in Nylon Rubber Blends - Reply. *Polymer*, 1990. **31**(5): p. 972-974.
166. Klempner, D., Interpenetrating Polymer Networks. *Angewandte Chemie-International Edition in English*, 1978. **17**(2): p. 97-106.

167. Sperling, L. H., Mishra, V., The current status of interpenetrating polymer networks. *Polymers for Advanced Technologies*, 1996. **7**(4): p. 197-208.
168. Lin, M. S., Liu, C. C., Lee, C. T., Toughened interpenetrating polymer network materials based on unsaturated polyester and epoxy. *Journal of Applied Polymer Science*, 1999. **72**(4): p. 585-592.
169. Subramaniam, R., McGarry, F. J., Toughened polyester networks. *Journal of Advanced Materials*, 1996. **27**(2): p. 26-35.
170. Blanco, I., Cicala, G., Lo Faro, C., Recca, A., Development of a toughened DGEBS/DDS system toward improved thermal and mechanical properties by the addition of a tetrafunctional epoxy resin and a novel thermoplastic. *Journal of Applied Polymer Science*, 2003. **89**(1): p. 268-273.
171. Shaker, Z. G., Browne, R. M., Stretz, H. A., Cassidy, P. E., Blanda, M. T., Epoxy-toughened, unsaturated polyester interpenetrating networks. *Journal of Applied Polymer Science*, 2002. **84**(12): p. 2283-2286.
172. Kai, W. H., Zhao, L., Zhu, B., Inoue, Y., Enforcing effect of double-fullerene end-capped poly(ethylene oxide) on mechanical properties of poly(L-lactic acid). *Macromolecular Rapid Communications*, 2006. **27**(2): p. 109-113.
173. Kai, W. H., Zhao, L., Zhu, B., Inoue, Y., Mechanical properties of blends of double-fullerene end-capped poly(ethylene oxide) and poly(L-lactic acid). *Macromolecular Chemistry and Physics*, 2006. **207**(8): p. 746-754.
174. Pernot, H., Baumert, M., Court, F., Leibler, L., Design and properties of co-continuous nanostructured polymers by reactive blending. *Nature Materials*, 2002. **1**(1): p. 54-58.
175. Hu, G. H., Cartier, H., Reactive Extrusion: Toward Nanoblends. *Macromolecules*, 1999. **32**: p. 4713-4718.
176. Ruzette, A. V., Leibler, L., Block copolymers in tomorrow's plastics. *Nature Materials*, 2005. **4**: p. 19-31.
177. Shimizu, H., Li, Y., Kaito, A., and Sano, H. , Formation of Nanostructured PVDF/PA11 Blends Using High-Shear Processing. *Macromolecules*, 2005. **38**: p. 7880-7883.
178. Bhardwaj, R., Mohanty, A. K. , *New Materials from Polylactide Bioplastics*, in *SPE-ANTEC*. 2007: Cincinnati, Ohio.

Chapter 3: Modification of Brittle Polylactide (PLA) by Novel Hyperbranched Polymer based Nanostructures

3.0 Introduction

There is an increased emphasis on the enhancement of material properties by means of structures engineered at the nanometer length scales. The inherently high surface area to volume ratio of nanometer sized materials plays a key role in enhancing the desired properties. Recently, nanostructure polymer blends having a minority polymer phase with nanoscale dimensions, offered much promise because of the enhanced thermo-mechanical properties, optical transparency and toughness in comparison to conventional polymer blends. Reactive blending, utilizing the concept of in-situ polymerization, graft and block copolymerization leads to creation of nanostructure blends^[1,2]. So far the nanostructure blending is restricted to a handful of petroleum based polymers, i.e. polyamide (PA), polypropylene (PP), and poly(vinylidene fluoride) (PVDF)^[1-3]. In the midst of these polymers, polylactide (PLA) or polylactic acid is emerging as promising thermoplastic polyester due to its renewable resource based origin along with its biodegradability and biocompatibility^[4]. PLA can exist in three stereochemical forms: poly(L-lactide) (PLLA), poly(D-lactide) (PDLA), and poly(DL-lactide) (PDLLA)^[5]. The inherent brittleness of PLA has been a major bottleneck for its large-scale commercial applications. Numerous approaches such as plasticization, block copolymerization, blending with tough polymers, and rubber toughening have been adopted to improve the toughness of brittle polylactide bioplastic^[6-9]. The major drawbacks of these methods are the substantial decreases in the strength and modulus of

the toughened polylactide. So, a polylactide based material having good stiffness-toughness balance along with high biobased polylactide content is still elusive.

Previous research suggested that the brittleness of PLA is due to low entanglement density (V_e) and the high value of characteristic ratio (C_∞), a measure of chain stiffness^[10-12]. The enantiomerically pure PLAs, such as PLLA and PDLA as well as amorphous PLA deform in brittle fashion due to the formation of crazes^[13]. Crazes are microcracks bridged by small fibrils and often lead to the catastrophic failure of a polymer. In conventional polymers, polystyrene (PS) is a classical example of a craze forming polymer^[14]. Micron scale rubber particles are usually dispersed in the PS matrix to enhance its toughness. In conventional rubber toughening, some of the major drawbacks are incompatibility between rubber particles and the polymer phase, requirement of high shear processing and increased melt viscosity.

In the midst of polymers having conventional molecular architecture such as linear, branched and crosslinked, hyperbranched polymers (HBP) are emerging additives, which fall in the category of dendritic polymers and are gaining attention due to their unique structures and properties. Hyperbranched polymers encompass highly branched nanoscopic structures having high peripheral functionalities^[15]. They are polydisperse and can be prepared in a one-pot synthesis unlike dendrimers, making the former less costly. Reported roles of hyperbranched polymers include processing aids, branching agents, compatibilizers and tougheners for conventional thermoplastics and thermosets^[16-19]. However, the unique physical properties and high peripheral functionalities of HBP offer many other pathways for polymer modification. HBP can play a role of novel

building blocks for generating new nanostructures inside a polymer matrix ranging from core-shell to highly networked morphologies. In our recent findings^[20], crosslinking of hydroxyl functional hyperbranched polyester in PLA matrix is demonstrated as a new method to overcome its brittleness, and the modified PLA showed promise in various applications.

In this chapter, we report the creation of a novel polylactide (PLA) based nanoblend by in-situ generation of new hyperbranched polymer (HBP) based nanostructures in the matrix polymer prepared via an environmentally friendly melt processing technique. Fourier transform infrared (FTIR), low temperature dynamic mechanical thermal analysis (DMTA), parallel plate rheology, transmission electron microscopy (TEM), atomic force microscopy (AFM), tensile testing and scanning electron microscopy (SEM) were used to characterize the blends.

3.1 Experimental Section

3.1.1 Materials

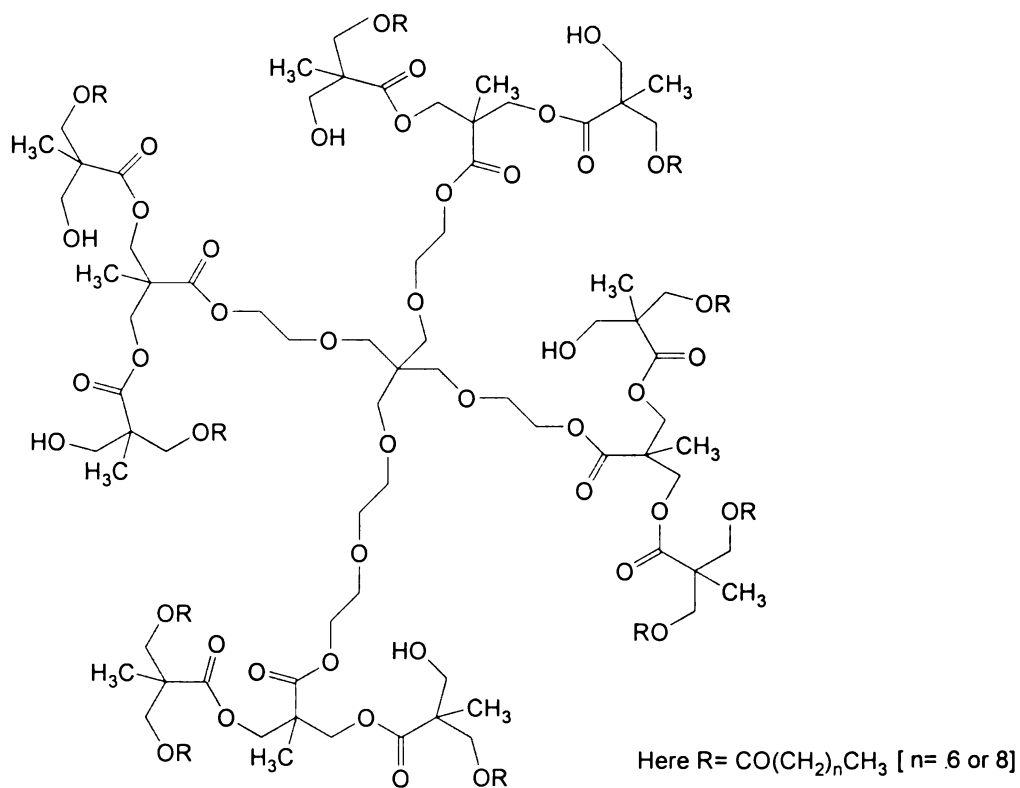
Poly(lactic acid), PLA (BIOMER® L9000) (Mol. Wt.: 188 kDa from GPC) was obtained from Biomer, Germany. The PLA was the L-form of poly(lactic acid). The hyperbranched polymer (HBP), a biodegradable dendritic polymer having the trade name BOLTORN® H2004^[21], mol. wt.-3200 g/mol was procured from Perstorp, Sweden. BOLTORN®H2004 has 6 primary hydroxyl groups, with a hydroxyl value of 110-135 mg KOH/g and maximum acid number of 7 mg KOH/g. Polyamide, trade name PA-18 (LV) having an average molecular weight ~ 22500 g/mol was obtained from Chevron-

Phillips, USA. Here, LV stands for low viscosity. The PA is a linear polyanhydride resin having a 1:1 mole ratio of 1-octadecene and maleic anhydride.

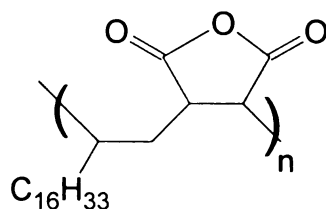
3.1.2 Reactive Extrusion

The PLA was dried for 4 h at 40°C in a vacuum oven before processing. The HBP was dried for 4 h at 80°C in a convection oven. The blends were prepared by melt mixing in a microcompounder/microextruder (DSM Research, Netherlands). The instrument is a co-rotating twin-screw microcompounder having a screw length of 150 mm, L/D of 18, and barrel volume of 15 cm³. The test specimens were prepared with the help of a mini-injection molder. mini-injection molder. All compositions are reported on a weight basis. Initially, PLA was melted in the microcompounder. The hyperbranched polymer (HBP) was added, followed by addition of an appropriate amount of polyanhydride (PA). The chemical structures of the polyanhydride (PA) and the chief constituent of HBP are depicted in Figure 3.1^[22, 23]. The hyperbranched polymer was a second generation of dendritic aliphatic polyester having alkyl and hydroxyls group at the periphery. It was synthesized from an AB₂ type monomer and a B₄ type core. The hyperbranched polyester was based on 2,2-bis-methylolpropionic acid (bis-MPA) as a chain extender with a pentaerythritol derivative core. There were 6 primary hydroxyl groups (–OH) groups at the periphery of this HBP. The glass transition temperature (T_g) of the HBP was around –40°C. A multifunctional polyanhydride (PA) was selected as a cross-linking agent for hyperbranched polymer. PA was a copolymer of octadecene and maleic anhydride having 1:1 molar ratio. The hydroxyl functionality of HBP was exploited to cause interparticle cross-linking of HBP to obtain new highly networked morphologies inside the PLA matrix. The reactivity of hydroxyl (–OH) functional compounds with

anhydride groups containing copolymer is well known^[24]. The molar ratio of hydroxyl (-OH) to anhydride group was 1:2. The molar ratio was calculated on the basis of hydroxyl and anhydride equivalent weight of hyperbranched polymer (HBP) and polyanhydride



(A)



(B)

Figure 3.1: (A) Chemical structure of the chief constituent of hyperbranched polymer (HBP). (B) Chemical structure of polyanhydride (PA).

(PA), respectively. Figure 3.2^[25] schematically depicts the in-situ crosslinking of HBP with PA in PLA matrix performed during melt processing of PLA. The details of processing parameters and material types are given in Table 3.1. The processing cycle time of different blends were obtained with the help of variation of extruder force with cycle time. Here, the cycle time represent the duration of time used for the mixing of polymers after material feeding and before removal of material from the microcompounder. In the case of neat PLA, the extruder force increased until the PLA pellets melted and then dropped with the cycle time. For, PLA/HBP (92/08) blend, the force dropped remarkably due to the lubricating effect of HBP, which resulted in the decrease in the melt viscosity of PLA. The addition of polyanhydride (PA) in the PLA/HBP system caused the extruder force to increase with cycle time until it stabilized

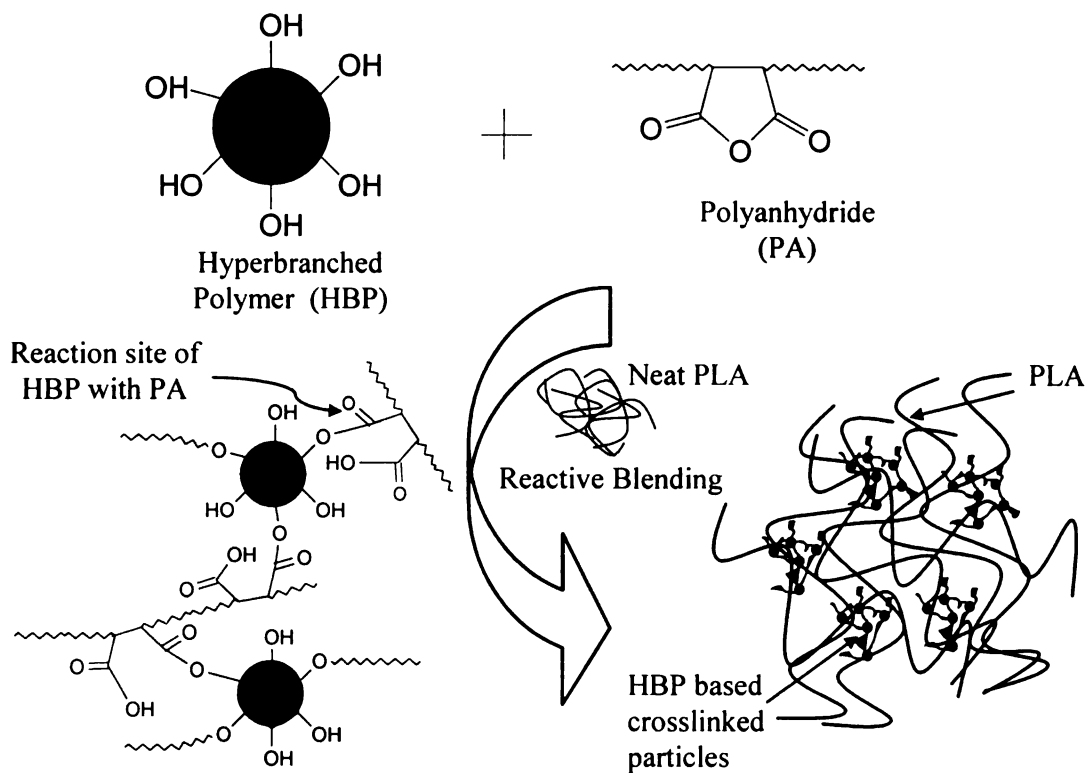


Figure 3.2: Schematic illustrations of in-situ crosslinking of hyperbranched polymer (HBP) in PLA melt with the help of a polyanhydride (PA). (After ref. 25)

around 10 minutes of cycle time. This cycle time represented the time for which PLA, HBP and PA were mixed in microcompounder at a screw speed of 100 rpm. The overall composition for this blend was PLA/HBP/PA (92/5.4/2.6). The increase in the force was attributed to the crosslinking reaction of HBP with PA in the PLA matrix. A control sample of PLA/PA (97.3/2.7) blend was also fabricated at the same processing conditions as that of PLA/HBP/PA (92/5.4/2.6) blend. This blend had a similar ratio of PLA to PA concentration as the PLA/HBP/PA blend. The purpose of this blend was to investigate the possible interaction of PA with PLA and its effect on the resulting properties of PLA.

Table 3.1: Processing parameters of neat PLA and its blend with hyperbranched polymer (HBP), in-situ crosslinked HBP and polyanhydride (PA)

Material System (wt.%/wt.%)	Processing temperature (°C) at three zones of mini-extruder				Cycle time (Minutes)	Screw Speed (rpm)	Mold Temp. (°C)
	Top	center	Bottom	Melt			
Neat PLA	185	185	185	178	3	100	50
PLA/HBP (92/08)	185	185	185	178	3	100	50
PLA/HBP/PA (92/5.4/2.6)	185	185	185	178	10	100	50
PLA/PA (97.3/2.7)	185	185	185	178	10	100	50

3.1.3 Testing and Characterization

3.1.3.1 Ultracentrifugation

Solvent extraction and ultracentrifugation technique was used to determine the insoluble component in neat PLA and its blends. 0.5 gram of processed blends was dissolved in 30 ml of methylene dichloride (CH₂Cl₂) (Jade Scientific) and stirred for 4 hrs at room temperature. The solutions were observed for their physical appearance. The insoluble fraction of the PLA/HBP/PA (92/5.4/2.6) blend was extracted with repeated cycles of centrifugation (3000 rpm, 30 minutes) and solvent wash. The weight fraction of the insoluble crosslinked HBP particles formed by the reaction of HBP and PA was calculated using following equation:

$$W_{cHBP} = \frac{W_{ins}}{W_{HBP} + W_{PA}} \dots\dots\dots 3.1$$

Where,

W_{cHBP} = Weight fraction of crosslinked HBP particles.

W_{ins} = Final weight of insoluble fraction after extraction and drying.

W_{HBP} = Initial weight of HBP in PLA composition.

W_{PA} = Initial weight of PA in PLA composition.

3.1.3.2 Fourier Transform Infrared Microscopy (FTIR)

The chemical composition of the insoluble fraction of crosslinked HBP and other materials was evaluated with the help of Perkin Elmer system 2000 FTIR spectrometer having an ATR assembly.

3.1.3.3 Dynamic Mechanical Thermal Analysis (DMTA)

The dynamic mechanical thermal analysis (DMTA) of the neat polymers and their blends was performed with DMA Q800, TA Instruments, DE. The test was carried out at a heating rate of 3°C/min from -90 to 150°C in the single cantilever mode. The drive amplitude was 15 µm, while, the oscillating frequency was 1 Hz.

3.1.3.4 Parallel Plate Rheology

Rheological studies of neat PLA and its blends were conducted with an ARES parallel plate rheometer in dynamic strain frequency sweep mode. The plates had 25 mm diameter. The gap between plates was 0.5 mm during testing. Testing was conducted in the frequency range of 0.1 to 100 rad/sec at a strain rate of 1% and at a testing temperature of 175°C.

3.1.3.5 Transmission Electron Microscopy (TEM)

A transmission electron microscope (TEM) (JEOL 100 CX) was used to analyze the morphology of PLA based blends at an accelerating voltage of 100 kV. Microtomed ultra-thin film specimens with thickness of less than 100 nm were used for TEM observation. The microtomy was carried out at room temperature using a diamond blade on a RMC microtome station. The PLA based blend samples were stained with ruthenium tetroxide (RuO₄) before examination.

3.1.3.6 Atomic Force Microscopy (AFM)

Atomic force microscopy (AFM) of microtomed surfaces of modified PLA was performed on an AFM microscope (Digital Instrument MultiMode SPM with Nanoscope IV controller, Digital Instruments, NY) in tapping mode. Scan sizes of 10 and 5 µm at a

scan rate of 0.5044 Hz were used for AFM analysis. Contrast enhancement of pictures was also performed.

3.1.3.7 Tensile Properties

Tensile properties of neat PLA and its blends were measured using a United Calibration Corp SFM 20 testing machine as per ASTM D638. Specimens having a gage length of 2.54 mm were tested at a strain rate of 15.4 mm/mm-min.

3.1.3.8 Scanning Electron Microscopy (SEM)

A scanning electron microscope, JEOL (model JSM-6400) was used to evaluate the morphology of and extracted hyperbranched polymers and tensile-fractured surfaces of the neat PLA and its blends. An accelerating voltage of 15kV was used to produce the SEM photomicrographs. The samples were sputter coated with gold before SEM analysis.

3.2 Results and Discussion

3.2.1 Solvent Extraction, Morphology and Fourier Transform Infrared Spectroscopy

The physical observation of solutions of PLA and its blends in methylene dichloride are depicted in Table 3.2. All of the solutions were clear in physical appearance except that of the PLA/HBP/PA (92/5.4/2.6) blend, which was turbid in appearance. The turbidity was attributed to the scattering of light by the suspended particles in continuous PLA solution. Methylene dichloride is a reported as a good

Table 3.2: The solution behavior of PLA and its blends after dissolving in methylene dichloride.

Material Compositions (wt. %/wt. %)	Appearance
Neat PLA	Clear
PLA/HBP (92/08)	Clear
PLA/HBP/PA (92:5.4:2.6)	Turbid
PLA/PA (97.3/2.7)	Clear

solvent for PLA^[26]. So it was likely that the particles were the reaction product of HBP and PA. The reaction of HBP and PA could form a crosslinked network due to their multi-functionality and make them insoluble in a solvent. The insoluble mass was dried and characterized with SEM and FTIR. The scanning electron microscopy (Figure 3.3) of extracted crosslinked HBP revealed particle morphology of the extracted insoluble fraction. The particles were fused with each other after solvent removal. Most of these particles had dimensions less than 100 nm. The photomicrograph also revealed a large size distribution of crosslinked particles. In order to confirm the reaction of HBP with PA, HBP was allowed to react with polyanhydride (PA) in a laboratory flask in the absence of PLA for 10 minutes at 185°C. The molar ratio of OH to anhydride was 1:2. There was gelation and formation of a solid mass as a result of the reaction between HBP and PA. Figure 3.4 represents the FTIR spectrum of PLA, HBP-PA particles (extracted), HBP-PA particles (reacted in absence of PLA), neat HBP and PA. The FTIR spectrum of

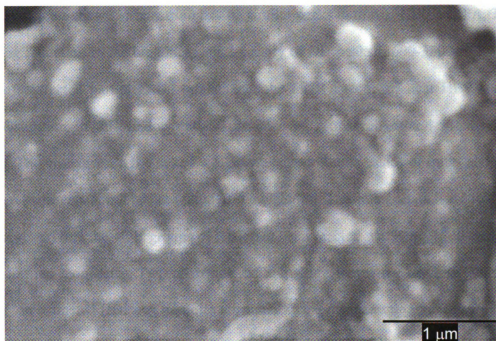


Figure 3.3: SEM photomicrographs of extracted crosslinked HBP particles from the PLA matrix.

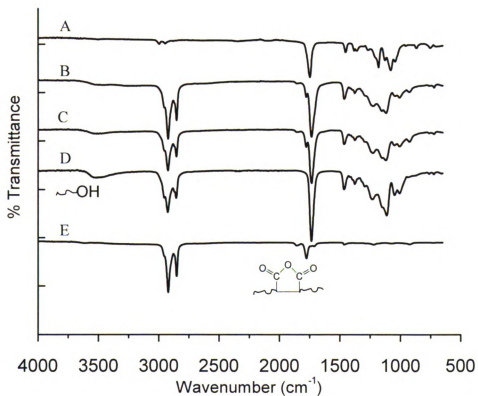


Figure 3.4: FTIR spectrum: A: Neat PLA; B: HBP-PA particles (Extracted), C: HBP-PA particles (Outside); D: Hyperbranched polymer (HBP); E: polyanhydride (PA)

extracted particles showed a spectrum having similar peaks to that of HBP and PA. There was strong reduction in the broadness and intensity of OH peaks ($3600\text{-}3500\text{cm}^{-1}$) in the spectra of extracted particles. On other hand, the FTIR spectra of neat HBP showed strong absorption in this region due to presence of primary hydroxyl groups in its structure. The broadness in the peak for HBP was due to the presence of inter- and intra-molecular hydrogen bonding between HBP molecules. The interpretation of hydroxyl peaks suggested that the -OH groups of HBP had been reacted with anhydride groups of PA and formed monoester. Two characteristic anhydride frequency bands at 1855 and 1777 cm^{-1} in extracted HBP-PA particles attributed to the coupled vibration of symmetric and asymmetric stretching of two >C=O groups in the anhydride group of the polyanhydride. These bands attributed to the presence of unreacted anhydride groups in the extracted particles. The molar ratio of OH to anhydride was 1:2 in the PLA/HBP/PA blend so it was quite expected that there would be unreacted anhydride groups. The characteristic anhydride frequency bands of extracted particle matched perfectly with that of polyanhydride (PA). The fingerprint region ($< 1500\text{ cm}^{-1}$) of the spectra of extracted particles was in coherence with that of HBP. There were no characteristic bands of PLA in the spectra of extracted particles. This suggested that the main reaction occurred between HBP and PA in the PLA matrix, while the PLA chains were physically entangled in the network of HBP and PA. PLA has functional groups (-OH and -COOH) only at the chain ends, which might not able to react with OH and anhydride group of HBP and PA, respectively. A further confirmation of the reaction of HBP with PA in the PLA matrix was performed by comparing the FTIR spectra of reaction product of HBP and PA in absence of PLA. The FTIR spectra of extracted particles were in complete

agreement with that of particle prepared outside. This result confirmed that polyanhydride had successfully caused the crosslinking of HBP in the PLA matrix. The weight fraction of extracted crosslinked HBP particles was calculated as per equation 3.1 and was ~ 0.89 i.e. 89%. So there was high reactivity of HBP with PA in PLA matrix. The presence of some unreacted HBP and PA was primarily due to steric hindrance created by the large amount of PLA media.

3.2.2 Dynamic Mechanical Thermal Analysis

Low temperature dynamic mechanical thermal analysis (DMTA) was conducted to observe the crosslinking of HBP, phase separation and molecular interaction of PLA with HBP and crosslinked HBP (cHBP). The temperature dependence of the loss modulus (E'') of neat PLA, PLA/HBP (92/08) blend and PLA/HBP/PA (92/5.4/2.6) is shown in Figure 3.5. In the PLA/HBP (92/08) blend, there were two loss modulus (E'') relaxation peaks at $-40\text{ }^{\circ}\text{C}$ and $58\text{ }^{\circ}\text{C}$ respectively, corresponding to the glass transition temperatures (T_g) of HBP and PLA, respectively. There was slight depression in the T_g of PLA in the presence of HBP. This suggested that there was some molecular interaction between PLA and HBP but this system was dominated by phase separation. Phase separation has also been a major problem in most of the plasticized PLA systems^[27]. The creation of free volume in plasticized PLA enhances its molecular mobility facilitating the increase in its crystallinity, which result in the expulsion of plasticizer molecules from the amorphous region.

On the other hand, the PLA/HBP/PA (92/5.4/2.6) composition revealed two peaks at -31 and $58\text{ }^{\circ}\text{C}$ representing the glass transition temperature (T_g) of crosslinked HBP (cHBP) and PLA respectively. There was a shift in glass transition temperature from -40

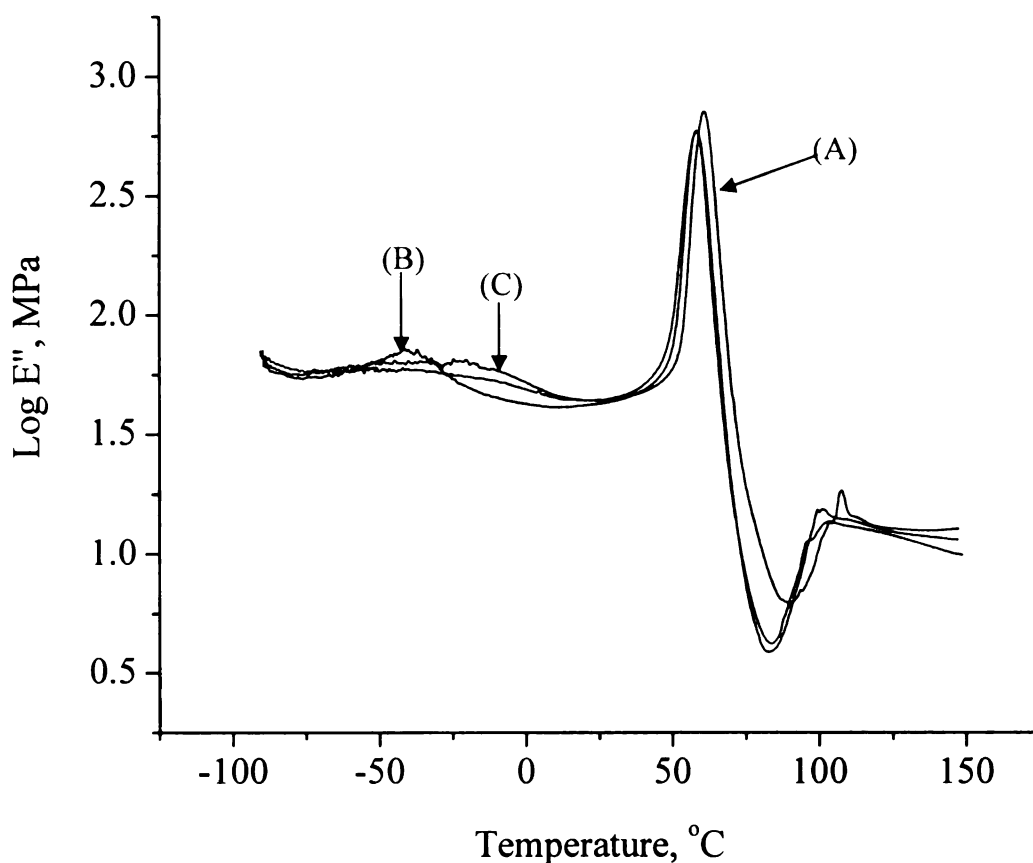


Figure 3.5: Temperature dependence of the loss modulus (E'') of: (A) neat PLA, (B) PLA/HBP (92/08), and (C) PLA/HBP/PA (92/5.4/2.6) blends.

°C for HBP in PLA/HBP blend to -31 °C for cHBP in PLA/HBP/PA blend. This suggested that polyanhydride (PA) had selectively caused the crosslinking of HBP in PLA matrix. The increase in the glass transition temperature of crosslinked HBP was attributed to the restricted segmental mobility and increase in the molecular weight of HBP after cross linking. It is known that cross-linking helps in reducing the macro-phase separation in polymer blends^[28]. The present system could be considered as a pseudo-semi-interpenetrating network system. Here, in the presence of a linear PLA chain, the hyperbranched polymer was crosslinked and thus leads to the formation of highly branched networked domains in the PLA matrix. The growing network of HBP during in-situ reaction could cause physical interlocking with PLA chains and thus helped in

reducing the macro-phase separation of HBP from the PLA phase. It is likely that physical interlocking of the PLA chain with the growing network of HBP occurred at the phase boundaries between PLA and crosslinked HBP only, primarily due to the limited miscibility of PLA with HBP.

3.2.3 Rheological Evidence of Networked Interface between PLA and Crosslinked HBP

The variation of storage modulus, G' with small-amplitude oscillatory frequency for the neat PLA and its blends is given in Figure 3.6. There was a distinct formation of a rubbery plateau of highest length in the case of PLA/HBP/PA (92/5.4/2.6) blend unlike that of neat PLA, PLA/HBP (92/08) and PLA/PA (97.3/2.7) blend in lower frequency region. The rubbery plateau is determined by the presence of crosslinks and entanglement

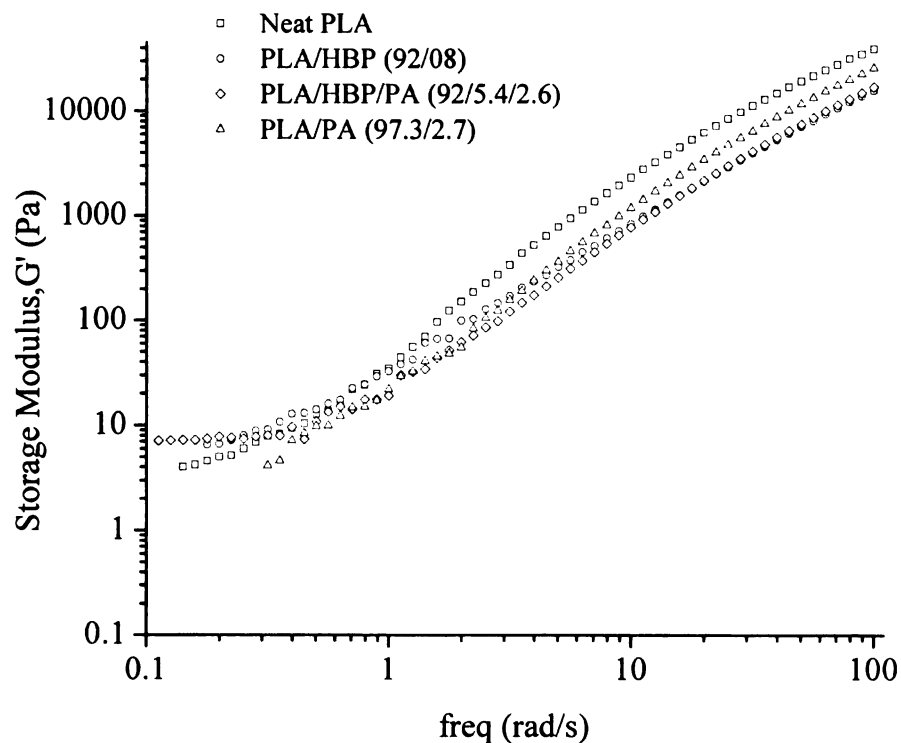


Figure 3.6: Behavior of storage modulus, G' of neat PLA and its blend as a function of oscillatory frequency (ω)

in a polymer^[29]. When observing the lowest frequency region of all curves, it is found that the PLA/HBP/PA (92/5.4/2.6) blend had the highest value of plateau modulus. Such increase in plateau modulus is caused by the presence of crosslinks or entangled networks in a polymer melt^[29]. So it is believed that the presence of crosslinked HBP network caused the upward shift in the plateau modulus. On the other hand, the in-situ crosslinking of HBP with PA in PLA melt caused the formation of crosslinked particles, which had tendency to form an entangled network with PLA chain preferably at the interface. The terminal slope of the $G'-\omega$ curve approached zero for PLA/HBP/PA (92/5.4/2.6) system reflecting its pseudo-solid like behavior. The relaxation and motion of PLA chains, which was a major fraction in the blend, would have a prominent effect on rheological properties in the low shear regime. The longer relaxation of PLA chain in the presence of the HBP-PA particles caused the frequency independence of the storage modulus in lower shear regime. This behavior also strongly indicated towards formation of a physical network of PLA chains with HBP/PA particles during their in-situ reaction in PLA matrix.

3.2.4 Complex Viscosity

Figure 3.7 represents the dependency of the complex viscosity on the oscillatory frequency for neat PLA, PLA/HBP (92/08) and PLA/HBP/PA (92/5.4/2.6) blends obtained at 175°C. The neat PLA tended to show shear thinning behavior with increase in the shear rate. In a previous study, shear thinning behavior of PLA is also reported^[30]. There was strong reduction in the complex viscosity of PLA with the addition of hyperbranched polymer. Kim et al.^[31] showed that blends of hyperbranched polyphenylene and polystyrene exhibit a reduced viscosity at high temperatures as

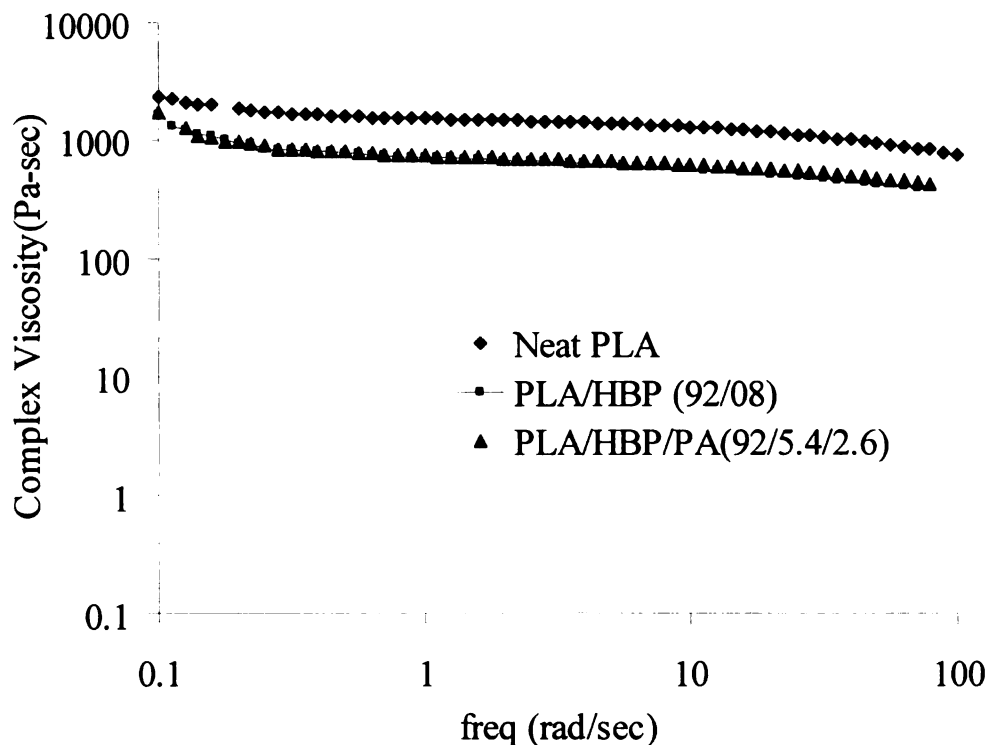


Figure 3.7: Variation of complex viscosity, η^* , of neat PLA and its blend as function of oscillatory frequency (ω).

compared to pure polystyrene. In a recent study^[32], a strong decrease in the melt viscosity of polylactide is reported in the presence of a biodegradable hyperbranched poly(ester amide). The reduction in melt viscosity of polylactide is attributed to the globular shape of HBP molecules, which don't entangle with each other. Their lubrication effect can separate the PLA chain and introduce large free volume in the PLA. This effect can lower the frictional forces between the PLA chains and they can slip past each other leading to the reduction in its melt viscosity. It was interesting to note that in-situ crosslinking of HBP phase in the PLA matrix did not diminish the viscosity modifier effect of HBP as the networked structure of crosslinked HBP maintained a good amount of free volume between the PLA chains.

3.2.5 Transmission Electron Microscopy (TEM)

Transmission electron microscopy (TEM) was carried out to evaluate the morphology and dispersion of pristine and crosslinked HBP particles in the PLA matrix. The ultra microtomed samples of PLA/HBP (92/08) and PLA/HBP/PA (92/5.4/2.6) blend were stained with ruthenium tetroxide (RuO_4) before TEM observation. Ruthenium tetroxide selectively stained the ether moiety present in the hyperbranched polymer and appeared darker than the PLA phase in the TEM photomicrographs. The TEM photomicrograph (Figure 3.8) of PLA /HBP (92/08) blend revealed the nanoscopic dimension of HBP (4-6 nm) but the particles were not well distributed in the PLA matrix and rather appeared as agglomeration. This was attributed to the limited miscibility of HBP with PLA and presence of strong intermolecular hydrogen bonding between HBP molecules due to their high peripheral hydroxyl functionalities. Figure 3.9A and 3.9B revealed the nanoscale phase separated sea-island morphology of the PLA/HBP/PA (92/5.4/2.6) blend, in which crosslinked HBP particles (dark patches) had heterogeneous size distribution having dimensions ranging from 50-100 nm. The multi-functionalities of HBP and PA and random effective collisions of HBP molecules with PA molecules during their reaction in the large sea of PLA are the possible reasons behind the random size distribution. The heterogeneity in the morphologies of crosslinked HBP particles would also arise from the polydispersity of pristine HBP itself and uncontrolled crosslinking reactions. The variation in stain intensity of crosslinked HBP particles also indicated the random crosslinking of HBP particles. The phase boundaries of all of the crosslinked particles were diffused and devoid of any sharp demarcation, which is an indication of formation of a network between PLA and crosslinked HBP chains. Such

networked structures at an interface would increase the compatibility between the two phases.

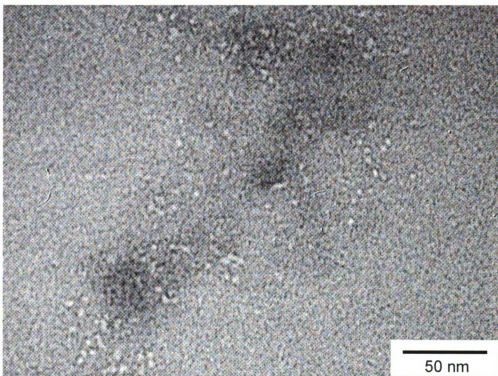


Figure 3.8: Transmission electron micrographs of PLA having 8 wt.% of pristine HBP. (Scale bar: 50 nm).

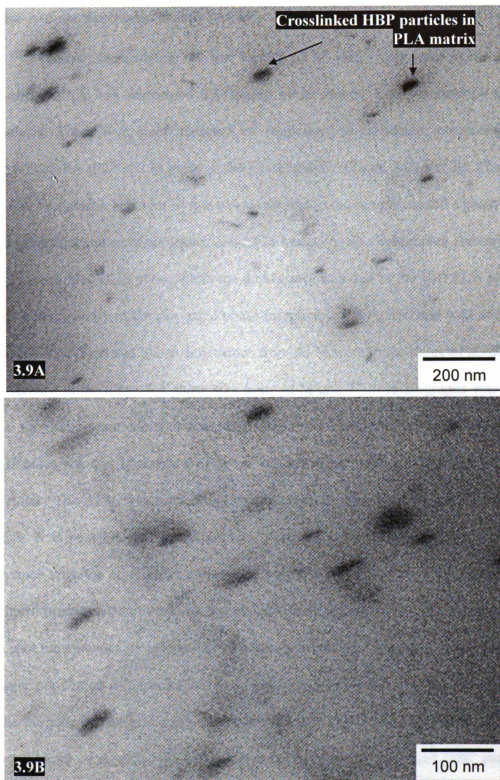


Figure 3.9: Transmission electron micrographs of PLA having crosslinked HBP. 3.9A: Scale bar: 200 nm; 3.9B: Scale bar: 100 nm.

3.2.6 Atomic Force Microscopy (AFM)

Further confirmation of the formation of HBP based nanoscale particles in modified PLA was performed by tapping mode atomic force microscopy (TM-AFM) analysis. There was clear evidence of formation of nanoscale morphologies in the PLA/HBP/PA (92/5.4/2.6) blend in the phase images (Figure 3.10A & B). The difference in the viscoelastic behavior of two phases present in the sample caused a phase lag, which led to an appearance of contrast in the AFM image^[33]. The lighter area corresponds to the soft crosslinked HBP phase while the darker area was due to the stiff PLA phase. There was heterogeneity in the dispersed phase morphology that correlated well with the TEM images. The dispersed phase dimensions from AFM were in the range of 80-200 nm. The difference in the dispersed phase size from AFM and TEM micrographs was obvious as the tip radii, scan rate and scan size affect the resolution in AFM. Another major difference was the appearance of lesser number of particles in AFM pictures than TEM pictures. The AFM was carried out in tapping mode over a smooth surface of modified PLA. It is possible that some particles were not being exposed to the surface of the scanned area. On other hand, a thin cross section (~70 nm) of modified PLA was stained with ruthenium tetroxide and looked at under the electron microscope. So, it was possible to spot these stained crosslinked HBP particles more easily. So, the TEM can estimate the larger population of particles and their sizes more accurately than AFM for this sample. The purpose of characterizing modified PLA with AFM was to validate the two-phase morphology of modified PLA and the softer nature of crosslinked HBP particles. The presence of depressions around crosslinked HBP particles in the AFM images was a

microtomy artifact. The knife cut the softer crosslinked HBP particle deeper as compared to the surrounding stiff PLA matrix and therefore left a depression.

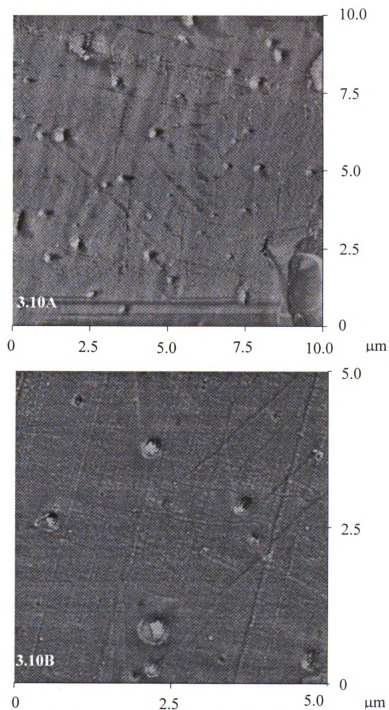


Figure 3.10: Tapping mode AFM phase image of PLA/HBP/PA (92/5.4/2.6) blend 3.10A: Scan size: 10 μm; 3.10B: Scan size: 5 μm

3.2.7 Tensile Properties

Stress-strain curves of neat PLA, PLA/HBP (92/08) and PLA/HBP/PA (92/5.4/2.6) blends are shown in Figure 3.11, while the detail of the measured tensile properties is provided in Table 3.3. The PLA and PLA/HBP (92/08) blends underwent strain softening and deformed in brittle fashion. On other hand, PLA/HBP/PA (92/5.4/2.6) blend showed initial strain softening after yielding and then underwent considerable cold drawing. The stress-strain curve after the yield point showed a combination of strain softening and cold drawing. In this region there was competition

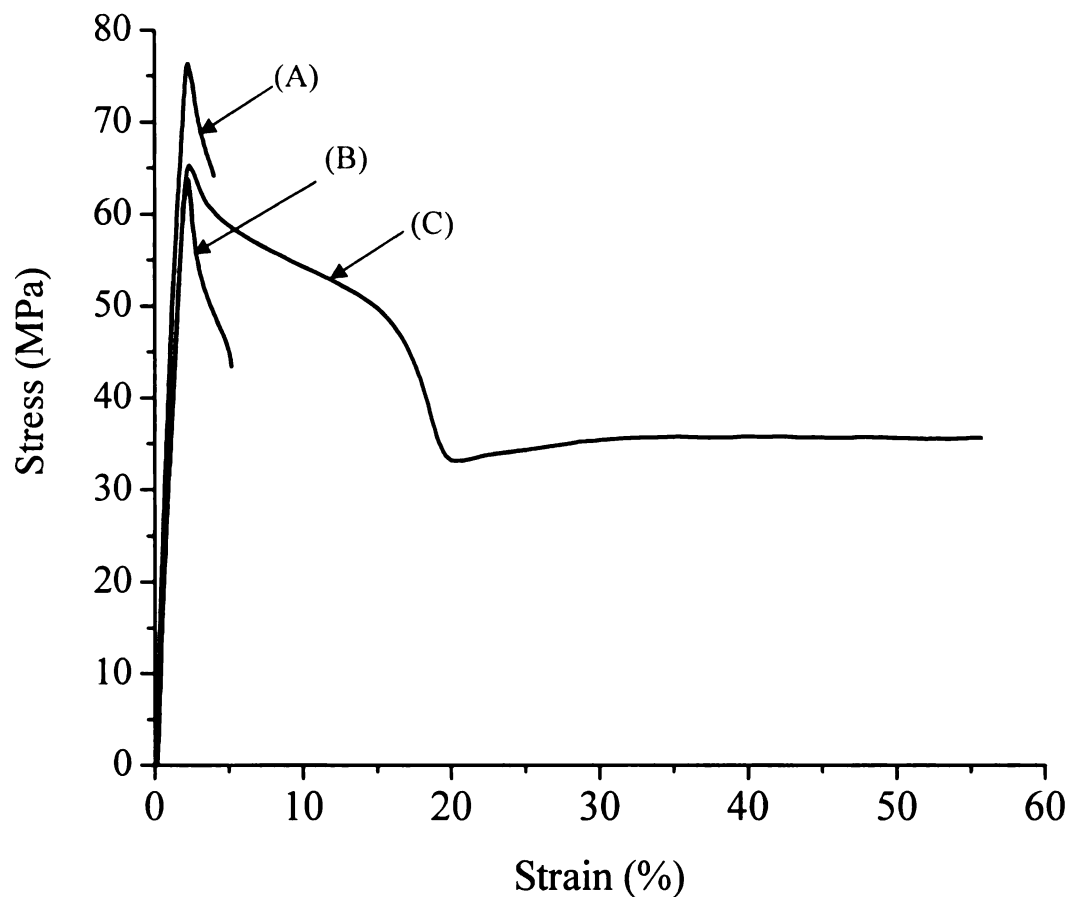


Figure 3.11: Stress-strain curves obtained at a cross head speed of 15.4 mm/min: (A) neat PLA; (B) PLA/HBP (92/08); (C) PLA/HBP/PA (92/5.4/2.6)

Table 3.3: Mechanical properties of neat PLA and its blends

Properties Materials (wt./wt.)	Tensile Modulus (GPa)	Tensile Strength at Yield (MPa)	Elongation at Break (%)	Toughness (MJ/m ³)
PLA (100/00)	3.6 ±0.07	76.5 ±1.45	5.1 ±1.7	2.6 ±0.9
PLA/HBP (92/08)	3.4 ±0.05	64.2 ±0.8	5.1 ±1.0	1.6 ±0.7
PLA/HBP/PA (92/5.4/2.6)	2.8 ±0.2	63.9 ±1.7	48.3 ±6.3	17.4 ±1.5
PLA/PA (97.3/2.7)	2.6±0.1	76.2±0.5	3.3±0.2	1.5±0.6

between PLA chain orientation and crack formation. Hence, there was drop in stress with increasing strain. After 15% of strain, cold drawing dominated with a constant stress. This suggested that there was large energy dissipation occurred in the presence of crosslinked HBP particles in the PLA/HBP/PA (92/5.4/2.6) blend. The toughness, calculated as the area under the stress-strain curve, declined in the PLA/HBP (92/08) blend as compared to the neat PLA, while it increased dramatically from 2.6 MJ/m³ for neat PLA to 17.4 MJ/m³ for the PLA/HBP/PA (92/5.4/2.6) blend. This was quite an unusual result, as the modified PLA maintained a quite high tensile modulus value of 2.8 GPa. The result was very significant in obtaining a biobased material having remarkable

stiffness-toughness balance. The tensile strength of modified PLA decreased to 63.9 MPa from 76.5 MPa for neat PLA. These result suggested that the nanoscale crosslinked HBP particles behaved like rubber particles and were effective in improving the toughness of PLA at low concentration (8 wt.%) with a minimal sacrifice of tensile strength and modulus.

3.2.8 Mode of Deformation of PLA-crosslinked HBP Blend under Tensile Loading

In such a multi-phase system having a dispersed rubbery phase, inelastic deformation occurs via the phenomena of shear yielding, multiple crazing and cavitation in the softer dispersed phase^[34]. PLA is an example of a semi-crystalline glassy polymer and undergoes brittle deformation via craze formations^[13]. The craze volume fraction (V_f) plays a crucial role in determining the propensity of a craze for catastrophic failure. The true stress σ_t , acting on the craze fibrils, is inversely proportional to the volume fraction of craze, which is given by the equation 3.2^[14]:

$$\sigma_t = \frac{\sigma_\infty}{v_f} = \lambda \sigma_\infty \dots\dots\dots 3.2$$

Here σ_∞ is the applied stress and λ is the craze extension ratio. So increasing the volume fraction, v_f , of craze can reduce the true stress on an individual craze.

Dispersing an elastic second phase and plasticization with low molecular weight molecules can provide control over nucleation and growth of crazes and can increase craze plasticity in glassy polymers leading to a decrease in the brittleness^[35-38]. In the PLA/HBP/PA (92/5.4/2.6) blend, the nanoscale rubbery crosslinked HBP ($T_g \sim -30^\circ\text{C}$) particles were formed in a continuous PLA matrix. During tensile testing, there was

stress-whitening in the sub-fracture region in PLA/HBP (92/08) and PLA/HBP/PA (92/5.4/2.6) blends (Figure 3.12). The stress whitening was more pronounced in PLA samples having crosslinked HBP (cHBP) particles i.e. the PLA/HBP/PA (92/5.4/2.6) blend. There was possibility of the creation of numerous tiny stable crazes nucleated by crosslinked HBP (cHBP) in the PLA matrix. The stress-whitening occurred due to the scattering of light by these tiny crazes. Such intense stress whitening was absent in the

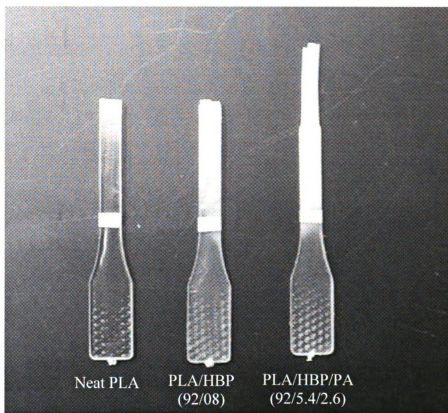


Figure 3.12: Tensile specimen after testing to failure at 15.4 mm/min under uniaxial tension.

neat PLA sample (Figure 3.12). The neat PLA deformed by craze formation, the crazes were several microns long and formed normal to the direction of tensile loading (Figure 3.13). The catastrophic deformations of these crazes were the primary reason for the brittle failure of unmodified PLA. The phenomenon of matrix crazing and shear yielding were likely the possible energy dissipation mechanisms behind the toughening of modified PLA bioplastic. It is also possible that the tiny crosslinked HBP particles can be incorporated into craze fibrils and can help in the extension of these fibrils under tensile loading.



Figure 3.13: TEM photomicrograph of deformed region of neat PLA.

The arrow indicates the tensile load direction(Scale bar: 2 μ m)

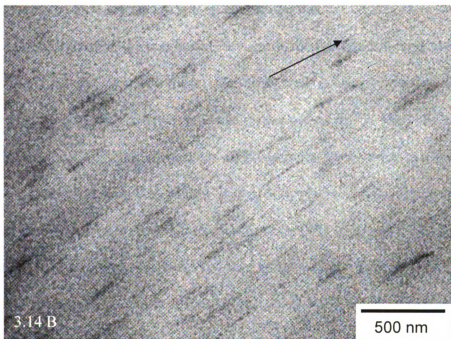
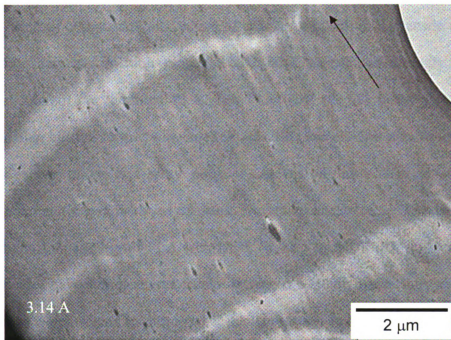


Figure 3.14: TEM photomicrograph of deformed region of modified PLA; 3.14 A: Extension of crazes; 3.14 (scale bar: 2 μm); 3.14B: Extension of crosslinked HBP. The arrow indicates the tensile load direction. (scale bar: 500nm)

The TEM photomicrograph of a deformed region of modified PLA revealed large extension of crazes and deformation of crosslinked HBP in the tensile direction (Figure 3.14). These deformation modes would have contributed strongly towards energy dissipation in the modified PLA. The PLA/HBP (92/08) blend also exhibited stress whitening but the sample was failed in a brittle manner. The stability of crazes initiated by a rubbery phase in a brittle polymer depends on the level of adhesion between the polymer matrix and dispersed particles. The crazes nucleated by HBP were not stable due to the incompatibility of PLA with HBP. In the PLA/HBP (92/08) blend, pristine HBP molecules have strong intermolecular hydrogen bonding due to their abundant hydroxyl groups, which seems to promote their aggregation in the PLA matrix and resulted in macroscopic phase separation and inferior properties.

The deformation in the toughened PLA can be divided in following stages:

Stage I: Stress concentration: The dispersed rubbery crosslinked hyperbranched particles in PLA matrix acted as stress concentrators due to their different visco-elastic behavior. Primarily, the crosslinked HBP particles have lower modulus than the PLA matrix at ambient temperature due to their low glass transition temperature. This stress concentration can help in relieving a triaxial stress state in the neighboring PLA matrix.

Stage II: Matrix Crazing/shear yielding: In this stage, the crosslinked HBP can initiate multiple crazes in the matrix leading to reduction in the stress on the single craze in PLA matrix. At the same time the thin ligament between two particles can shear yield and can eliminate the formation of large crazes. There was no observation of cavitation in the crosslinked particles as seen in TEM of deformed regions of modified PLA. It was

observed that the crosslinked particles tend to extend in the tensile direction. By this mechanism they can absorb considerable strain energy.

Stage III: Necking: After reaching at a critical strain, the stress fields associated with crosslinked HBP particles can overlap, causing the yield strength to decrease and facilitating the cold drawing by formation of neck until the sample fails.

The above mentioned mechanical deformation stages were previously reported by Kim et al.^[39] in PMMA nanocomposite nanofibers prepared from electron spinning process. A schematic illustration of the mechanical deformation process of PLA in the presence of crosslinked HBP particles is shown in Figure 3.15.

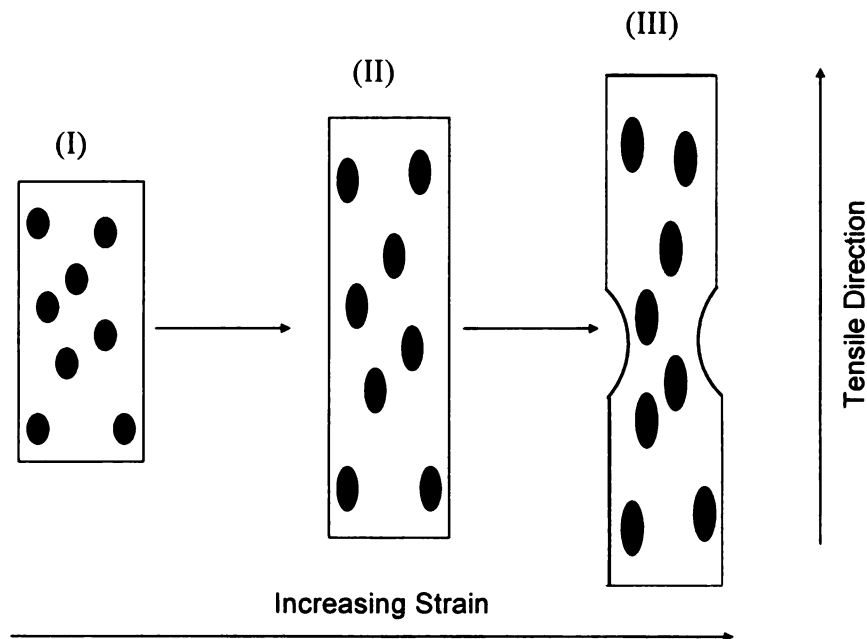


Figure 3.15: Schematic illustration of different stages of mechanical deformation process of PLA in presence of crosslinked HBP particles.

3.2.9 Scanning Electron Microscopy (SEM)

Figure 3.16 represents the scanning electron micrographs of the tensile fractured surfaces of neat PLA, PLA/HBP (92/08) and PLA/HBP/PA (92/5.4/2.6) blends. The surface of neat PLA was extremely flat, indicating the brittle failure of PLA under tensile loading. The tensile fractured surface of PLA/HBP (92/08) revealed inhomogeneity, formation of voids and absence of ductile tearing. This was an indication of phase separation, incompatibility between the PLA and HBP, and brittle failure under tensile loading. The in-situ crosslinking of HBP in PLA matrix dramatically changed its surface characteristics after deformation. The tensile fractured surface of PLA/ HBP/PA (92/5.4/2.6) blend exhibited considerable ductile tearing, surface roughness and surface integrity. The increased surface area of fractured surface of PLA/ HBP/PA (92/5.4/2.6) blend suggested that the crack paths were highly bifurcated and crack propagation absorbed considerable strain energy before failure. This led to a conclusion that the in-situ crosslinking of HBP was instrumental in improving the compatibility between PLA and HBP phases and resulted in significant toughness enhancement of PLA bioplastic.

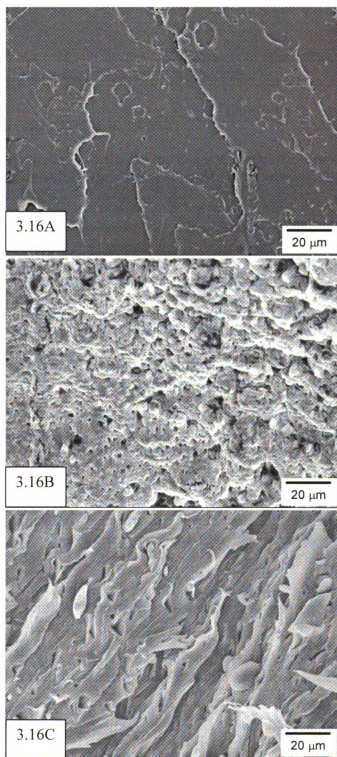


Figure 3.16: Scanning electron micrographs of tensile fractured surfaces: 3.16A: Neat PLA; 3.16B: PLA/HBP (92/08); 3.16C: PLA/HBP/PA (92/5.4/2.6).

3.3 References

1. Hu, G. H., Cartier, H. Reactive Extrusion: Toward Nanoblends. *Macromolecules* 1999. 32: p. 4713-4718.
2. Ruzette, A. V., Leibler, L., Block copolymers in tomorrow's plastics. *Nature Materials*, 2005. 4, p. 19-31.
3. Shimizu, H., Li, Y., Kaito, A., and Sano, H. Formation of Nanostructured PVDF/PA11 Blends Using High-Shear Processing. *Macromolecules*, 2005, 38, 7880-7883.
4. Ragauskas, A.J., Williams, C. K., Davison, B. H., Britovsek, G., Cairney, J., Eckert, C. A., Frederick Jr., W. J., Hallett, J. P., Leak, D. J., Liotta, C. L., Mielenz, J. R., Murphy, R., Templer, R., Tschaplinski, T., The Path Forward for Biofuels and Biomaterials. *Science*, 2006. 311: p. 484-489.
5. Drumright, R.E., Gruber, P.R., Henton, D.E., Polylactic Acid Technology. *Advanced Materials*, 2000. 12(23), p. 1841 – 1846.
6. Ljungberg N., Wesslen, B., Preparation and Properties of Plasticized Poly(lactic acid) Films. *Biomacromolecules*, 2005. 6: p. 1789-1796.
7. Wang, Y., Hillmyer, M.A., Polyethylene-Poly(L-lactide) Diblock Copolymers: Synthesis and Compatibilization of Poly(L-lactide)/Polyethylene Blends. *Journal of Polymer Science Part A: Polymer Chemistry*, 2001. 39: p. 2755-2766.
8. Shibata, M., Inoue, Y., Miyoshi, Y., Mechanical properties, morphology, and crystallization behavior of blends of poly(L-lactide) with poly(butylene succinate-co-L-lactate) and poly(butylene succinate). *Polymer*, 2006. 47: p. 3557-3564.
9. Jin, H.J., Chin, I. J., Kim, M. N., Kim, S. H., Yoon, J. S., Blending of poly(L-lactic acid) with poly(cis-1,4-isoprene). *European Polymer Journal*, 2000. 36: p. 165-169.
10. Tonelli, A.E., Flory, P.J., The Configuration Statistics of Random Poly (lactic acid) Chains. I. Experimental Results'. *Macromolecules*, 1969. 2(3): p. 225-227.
11. Joziasse, C.A.P., Veenstra, H., Grijpma, D. W., Pennings, A. J., On the chain stiffness of poly(lactide)s. *Macromol. Chem. Phys.*, 1996. 197: p. 2219-2229.
12. Grijpma, D.W., Penning, J.P., Pennings, A.J., Chain entanglement, mechanical properties and drawability of poly(lactide). *Colloid Polym. Sci.*, 1994. 271: p. 1068-1081.
13. Grijpma, D.W., Pennings, A.J., (Co)polymers of L-lactide, 2a) Mechanical Properties. *Macromol. Chem. Phys.*, 1994. 195: p. 1649-1663.

14. Donald, A. M. in *Physics of glassy polymers*, Edn: Harward, R. N., Young, R. J., Chapman & Hall, 1997.
15. Seiler, M., *Dendritic Polymers-Interdisciplinary Research and Emerging Applications from Unique Structural Properties*. *Chem. Eng. Technol*, 2002. 25 (3).
16. Hong, Y., Coombs, S.J., Cooper-White, J.J., Mackay, M.E., Hawker, C.J., Malmström, E., Rehnberg, N., Film blowing of linear low-density polyethylene blended with a novel hyperbranched polymer processing aid. *Polymer* 2000. 41: p. 7705–7713.
17. Jannerfeldt, G., Boogh, L., Manson, J.A.E., Tailored interfacial properties for immiscible polymers by hyperbranched polymers. *Polymer*, 2000. 41: p. 7627–7634.
18. Kil, S.B., Augros, Y., Leterrier, Y., Manson, J.A.E., Rheological Properties of Hyperbranched Polymer/Poly(ethylene Terephthalate) Reactive Blends. *Polymer Engineering and Science*, 2003. 43(2).
19. Mezzenga, R., Boogh, L., Manson, J. A. E., A review of dendritic hyperbranched polymer as modifiers in epoxy composites. *Composites Science and Technology*, 2001. 61(5): p. 787-795.
20. Mohanty, A.K., Bhardwaj, R., Hyperbranched polymer modified biopolymers, their biobased materials and process for the preparation thereof. US20060247387A1 (Pending), 2006.
21. Boltorn[®] H2004, Safety Data Sheet, <http://www.perstorppolyols.com/Products/MSDS.aspx> (Accessed on November 1, 2007).
22. Structure drawn after reference from “Perstorp Specialty Chemicals, TSCA-Exempted Polymers Structures (January 22, 2001)”.
23. http://www.cpchem.com/enu/specialty_chemicals_polyanhydride_resins.asp (Accessed on February 2, 2007)
24. Orr, C.A., Cernohous, J. J., Guegan, P., Hirao, A., Jeon, H. K., Macosko, C. W., Homogeneous reactive coupling of terminally functional polymers. *Polymer*, 2001. 42(19): p. 8171-8178.
25. Bhardwaj, R., Mohanty, A. K., Modification of Brittle Polylactide by Novel Hyperbranched Polymer-Based Nanostructures. *Biomacromolecules*, 2007. 8: p. 2476-2484.
26. Agrawal, A., Saran, A. D., Rath, S. S., Khanna, A., Constrained nonlinear optimization for solubility parameters of poly(lactic acid) and poly(glycolic acid)—validation and comparison. *Polymer*, 2004, 45: p. 8603–8612

27. Ljungberg, N., Wesslen, B., The effects of plasticizers on the dynamic mechanical and thermal properties of poly(lactic acid) *Journal of Applied Polymer Science*, 2002. 86: p. 1227-1234.
28. Klempner, D., Sperling, L. H., Utracki, L. A., in *Interpenetrating Polymer Networks*, Eds; *Advances in Chemistry Series No. 239*; American Chemical Society: Washington, DC, 1994.
29. Edwards, S.F., Takano, H., Terentjev, E. M., Dynamic mechanical response of polymer networks. *Journal of Chemical Physics*, 2000. 113(13): p. 5531-5538.
30. Ramkumar, D.H.S., Bhattacharya, M., Steady Shear and Dynamic Properties of Biodegradable Polyesters. *Polymer Engineering and Science*, 1998. 38(9): p. 1426-1435.
31. Kim, Y. H., Webster, O. W., Hyperbranched Polyphenylenes. *Macromolecules* 1992. 25 (21): p.5561-5572
32. Lin, Y., Zhang, K. Y., Dong, Z. M., Dong, L. S., Li, Y. S., " Study of Hydrogen Bonded Blends of Polylactide with Biodegradable Hyperbranched Poly(ester amide), *Macromolecules*, 2007. 40, p.6257-6267
33. Sa'nchez, M. S., Mateo, J. M., Colomer, J. S. R., Ribelles, J. L. G., Nanoindentation and tapping mode AFM study of phase separation in poly(ethyl acrylate-co-hydroxyethyl methacrylate) copolymer networks, *European Polymer Journal*, 2006. 46 1378–1383.
34. Bucknall, C. B. in *Physics of glassy polymers*, Edn: Harward, R. N., Young, R. J., Chapman & Hall, 1997.
35. Bucknall, C. B., *Toughened Plastics*, Applied Science Publication, London, 1977.
36. Kinloch, A. J., Young, R. J., *Fracture Behavior of Polymers*, Applied Science Publication, London, 1983.
37. Gabizlioglu, O. S., Beckham, H.W., Argon, A. S., Cohen, R. E., Brown, H. R., A New Mechanism Of Toughening Glassy-Polymers .1. Experimental Procedures. *Macromolecules* 1990. 23(17): p.3968-3974.
38. Argon, A. S., Cohen, R. E., Gabizlioglu, O. S., Brown, H. R., Kramer, E. J., A New Mechanism Of Toughening Glassy-Polymers. 2. Theoretical Approach *Macromolecules* 1990. 23(17): p.3975-3982.
39. Kim, G. M., Lach, R., Michler, G. H., Potschke, P., Albrecht, K., Relationships between Phase Morphology and Deformation Mechanism in Polymer Nanocomposite Nanofibers Prepared by an Electrospinning Process. *Nanotechnology* 2006. 17: p.963-972.

Chapter 4: Effect of the Concentration of Crosslinker on the Properties of PLA/in-situ Crosslinked HBP Blends

4.0 Introduction

Dispersing rubbery particles in polymeric matrices is a popular approach for improving the toughness of brittle polymers. Rubber, being an excellently elastic and tough material, is the most effective toughening agent for amorphous as well as semi-crystalline brittle thermoplastics^[1, 2]. Polylactide can be amorphous or crystalline depending upon the stereochemistry of its repeat unit. PLA behaves as a glassy and brittle polymer at ambient conditions due to its high glass transition temperature. Rubber toughening of PLA is mentioned in the literature to overcome its brittleness^[3]. In chapter 3, we reported a new modification technique to overcome the brittleness of polylactide without a substantial sacrifice in strength and modulus of the material^[4]. In this approach, rubbery nanoscale domains of crosslinked hyperbranched polymer were in-situ created during the melt processing of PLA. The technique is analogous to rubber modification, where micron or submicron scale particle are usually dispersed in a brittle polymer.

The well established energy dissipating mechanisms of rubber toughened polymers are shear yielding, multiple crazing and cavitation in rubber particles. Wu^[5] put forward the concept of matrix ligament thickness (surface to surface distance between two neighboring rubber particles) as an important parameter for the brittle to ductile transition in rubber toughened blends. A smaller average matrix ligament thickness than a critical value, will make a blend tough, while it will be brittle in the opposite case. Phase

morphology, polydispersity, particle size, flocculation and particle volume fraction have a direct effect on the matrix ligament thickness^[5].

In this chapter, in-situ crosslinking of hyperbranched polymer is carried out by using different molar ratio of polyanhydride in the PLA matrix. The effect of extent of crosslinking of hyperbranched polymer on the mechanical properties of PLA–crosslinked HBP (cHBP) blends is studied. The size, polydispersity and distribution of crosslinked hyperbranched polymer in PLA matrix are evaluated. Contact angle measurements of PLA, HBP and crosslinked HBP are correlated with the dispersion of particles. The effects of processing, presence of HBP and cHBP on the molecular weight of PLA are also determined.

4.1 Experimental Section

4.1.1 Materials

Poly(lactic acid), PLA (BIOMER® L9000) (Mol. Wt.: 188 kDa from GPC) was obtained from Biomer, Germany. The PLA was L-form of poly(lactic acid). The hyperbranched polymer (HBP), a dendritic polymer having the trade name BOLTORN® H2004, mol. wt.-3200 g/mol was procured from Perstorp, Sweden. BOLTORN®H2004 has 6 primary hydroxyl groups, with a hydroxyl value of 110-135 mgKOH/g and maximum acid number of 7 mg KOH/g. Polyanhydride, trade name PA-18 (LV) having an average molecular weight ~22500 gm/mol was obtained from Chevron-Phillips, USA. The PA is a linear polyanhydride resin having 1:1 mole ratio of 1-octadecene and maleic anhydride.

4.1.2 Preparation of PLA-cHBP Blends

In this part of research, HBP was crosslinked with varying molar ratios of polyanhydride. The detail of processing parameters is given in Table 4.1. The PLA was dried for 4 hours at 40°C in a vacuum oven before processing. The HBP was dried for 4 hours at 80°C in a convection oven. The blends were prepared by melt mixing in a microcompounder/micro-extruder (DSM Research, Netherlands). The instrument is a co-

Table 4.1: Processing parameters of neat PLA and its blends

Material Type (wt.%/wt.%)	Processing temperature (°C) of screw zones and melt				Cycle time (Minutes)	Screw Speed (rpm)	Mold Temp. (°C)
	Top	center	Bottom	Melt			
Neat PLA	185	185	185	178	3	100	50
PLA/HBP/PA (92:7.55:0.45) OH to anhydride 4:1	185	185	185	179	10	100	50
PLA/HBP/PA (92:7.4:0.6) OH to anhydride 3:1	185	185	185	178	10	100	50
PLA/HBP/PA (92:7.1:0.9) OH to anhydride 2:1	185	185	185	176	10	100	50
PLA/HBP/PA (92:6.4:1:6) OH to anhydride 1:1	185	185	185	178	10	100	50
PLA/HBP/PA (92:5.4:2.6) OH to anhydride 1:2	185	185	185	177	10	100	50

rotating twin-screw microcompounder having screw length of 150 mm, L/D of 18 and barrel volume of 15 cm³. The test specimens were prepared with help of a mini-injection molder. The mold temperature was 50°C.

4.1.3 Testing and Characterization

4.1.3.1 Dynamic Mechanical Analysis

The dynamic mechanical thermal analysis (DMTA) of the neat polymers and their blends was performed with DMA Q800, TA Instruments, DE. The test was carried out at a heating rate of 3°C/min from -90 to 150°C in the single cantilever mode. The drive amplitude was 15 µm, while the oscillating frequency was 1 Hz.

4.1.3.2 Ultracentrifugation and Fourier Transform Infrared Spectroscopy

Ultracentrifugation technique was used to determine the insoluble component or the crosslinked HBP in PLA based blends. 0.5 gram of processed blends were dissolved in 30 ml of methylene dichloride (CH₂Cl₂) (Jade Scientific) and stirred for 4 hrs at room temperature. The solutions were observed for their physical appearance. The insoluble fraction of the blends was extracted with repeated cycles of centrifugation (3000 rpm, 30 minutes) and solvent wash. The insoluble fraction was dried for 24 hrs at 40°C before characterization. The chemical composition of insoluble fraction was evaluated with help of Perkin Elmer system 2000 FTIR spectrometer having ATR assembly. The weight fraction of the insoluble crosslinked HBP particles formed by the reaction of HBP and PA was calculated by equation 4.1:

$$W_{cHBP} = \frac{W_{ins}}{W_{HBP} + W_{PA}} \dots\dots\dots 4.1$$

W_{cHBP} = Weight fraction of crosslinked HBP particles.

W_{ins} = Final weight of insoluble fraction after extraction and drying.

W_{HBP} = Initial weight of HBP in PLA composition.

W_{PA} = Initial weight of PA in PLA composition.

4.1.3.3 Tensile Testing

Tensile properties were measured using a United Calibration Corp SFM 20 testing machine as per ASTM D638. The specimens having a gage length of 2.54 mm, were tested at a cross-head speed of 15.4 mm/mm-min. At least five replications were done for each sample.

4.1.3.4 Transmission Electron Microscopy

A transmission electron microscope (TEM) (JEOL 100 CX) was used to analyze the morphology of PLA based blends at an accelerating voltage of 100 kV. Microtomed ultra thin film specimens with thickness of less than 100 nm were used for TEM observation. The PLA based blend samples were stained with ruthenium tetroxide (RuO₄) by dipping the bulk specimens in the solution for 3 hrs. The microtomy was carried out at room temperature using a diamond blade on a RMC microtome station after staining the samples.

4.1.3.5 Contact Angle Measurements

Water contact angles of neat PLA, HBP, PA and crosslinked HBP were measured with the help of N.R.L. C. A. Goniometer, ramé-hart instrument co., NJ, USA. Compression molded film having uniform surfaces were used for neat PLA and PA. In

the case of HBP, a thin film of semi-solid HBP was spread on a glass slide and used for measurements. In the case of crosslinked HBP, the extracted particles were annealed at 100°C and pressed into thin films. HPLC grade water was used for drop formation. The drop volume was 50 µl. The contact angle of the drop with the substrate was measured using an Olympus Microscope. At least 10 repetitions were conducted for each sample.

4.1.3.6 Gel Permeation Chromatography (GPC)

GPC was used to determine the molecular weight of neat PLA, processed PLA and PLA extracted from PLA-crosslinked HBP blends. A 600 Multisolvant delivery system equipped with 717 autosampler and 2410 RI detector procured from Waters (Milford, MA) was used to determine the molecular weight of samples. Initially 20 mg of sample was dissolved in 30 ml of inhibitor free tetrahydrofuran (THF) solution (Sigma Aldrich, Milwaukee, WI). 1 ml of the filtered solution (filtered with 0.2 mm pore size, 13mm disposable PTFE (polytetra-fluoroethylene) filter procured from Whatman (Florham Park, NJ) was transferred to the 1 ml clear glass shell vials and capped with polyethylene snap caps. The glass vials were placed on an autosampler stage. The injection volume was 100 µl and flow rate of solvent was 1 ml/min. The three replications for each sample were done.

4.2 Results and Discussion:

4.2.1 Dynamic Mechanical Thermal Analysis

Behavior of loss modulus with respect to temperature was evaluated to observe the crosslinking of hyperbranched polymer in the presence of polyanhydride in the PLA matrix. Hydroxy (-OH) to anhydride group molar ratio in the PLA/HBP/PA blends were

varied from 4:1, 3:1, 2:1, 1:1 and 1:2. Figure 4.1 represents the effect of molar ratio of OH to anhydride on the glass transition temperature of crosslinked HBP phase in PLA/cHBP blends. It is found that with increase in the anhydride molar ratios, there was an increase in the glass transition temperature of the HBP phase in the PLA matrix (Figure 4.1). The glass transition temperature of the HBP phase in the PLA/HBP (92/08) blend was -40°C , while the glass transition temperature of polyanhydride was -27°C as observed from loss modulus peak of dynamic mechanical analysis. It is found that there was an increase in the glass transition temperature of cHBP phase with an increase in the molar concentration of polyanhydride (PA). There was a marginal increase in the glass

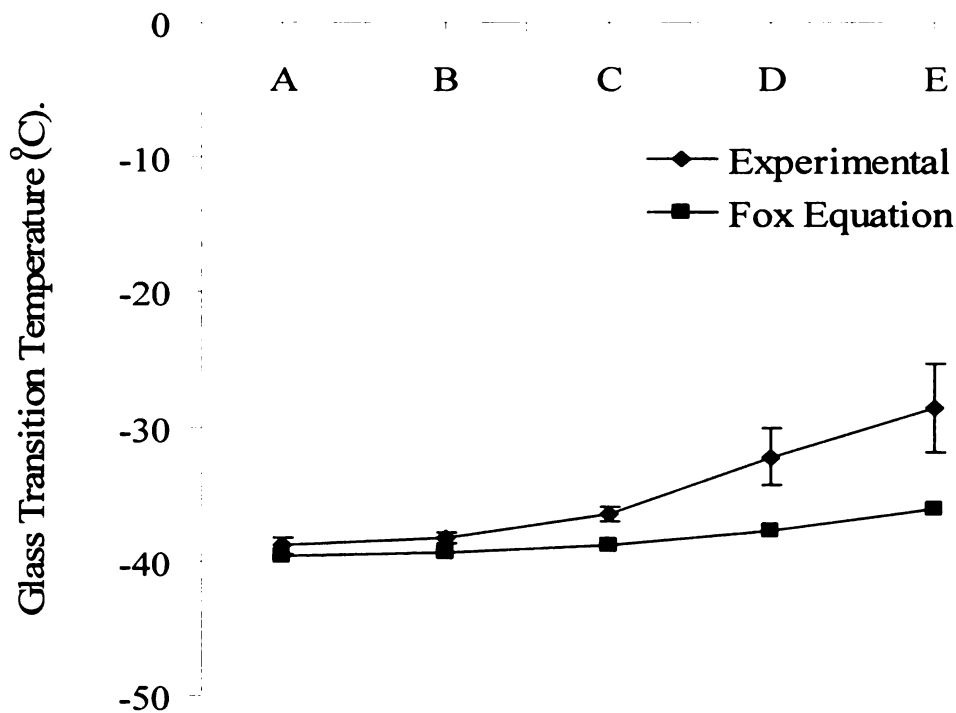


Figure 4.1 Effect of OH to anhydride molar ratio on the glass transition temperature of crosslinked HBP phase in PLA blends where, A: OH/anhydride (4:1); B: OH/anhydride (3:1); C: OH/anhydride (2:1); D: OH/anhydride (1:1) and E: OH/anhydride (1:2).

transition temperature when the OH to anhydride ratios were 4:1 and 3:1, but increased to larger extent when the OH to anhydride ratio was 2:1, 1:1 and 1:2. The maximum glass transition temperature was -29°C when OH to anhydride ratio was 1:2. The experimental values of glass transition temperature of crosslinked HBP were compared with the theoretical values obtained from the Fox equation. The Fox equation^[6] is used to estimate the glass transition temperature (T_g) for miscible blends, random copolymers and plasticized polymer systems in a bulk state. The Fox equation for the present system can be represented by the equation 4.2.

$$1/T_{g\ cHBP} = \frac{W_{HBP}}{T_{g\ HBP}} + \frac{W_{PA}}{T_{g\ PA}} \dots\dots\dots 4.2$$

Here W_{HBP} and W_{PA} are the mass fraction of HBP and PA while $T_{g\ HBP}$ and $T_{g\ PA}$ are the glass transition temperature of HBP and PA in Kelvin. Figure 4.1 represents the comparison of experimental and theoretical values of glass transition temperature of the cross linked HBP as a function of OH to anhydride ratio. It is observed that the crosslinked HBP tended to follow the concept of simple mixture when the OH to anhydride ratio was more towards the hydroxyl group i.e. 4:1 and 3:1. There were considerable deviations from Fox prediction in the values of glass transition temperature for blends when the OH to anhydride ratios were 2:1, 1:1 and 1:2. This was due the higher extent of crosslinking reaction between HBP and PA functionalities that led to the formation of networks in the crosslinked HBP phase at these molar ratios. The extent of deviation from theoretical values was more pronounced when the molar concentration of polyanhydride was sufficiently high. This result suggested that crosslinking of HBP occurred by reaction of its hydroxyl functionality with the anhydride functionality of

polyanhydride (PA). The behavior of the loss modulus with respect to temperature for neat PLA and some selected blends is shown in Figure 4.2. It is interesting to note that there was no significant increase in the glass transition temperature of crosslinked HBP. It suggested that the crosslinking of HBP with polyanhydride resulted in a networked structure, where a sufficient molecular mobility can occur at low temperature. The low glass transition temperature of crosslinked HBP showed its rubbery nature at ambient

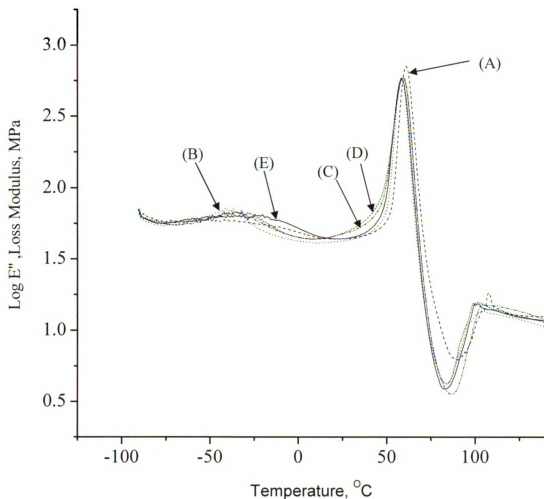


Figure 4.2: Temperature dependency of loss modulus of neat PLA and its blend with HBP and in- situ crosslinked HBP; (A) Neat PLA; (B) PLA/HBP (92/08); (C) PLA/HBP/PA (92:7.1:0.9) OH to anhydride 2:1; (D) PLA/HBP/PA (92:7.1:0.9) OH to anhydride 1:1; (E) PLA/HBP/PA (92:7.1:0.9) OH to anhydride 1:2

conditions. On the other hand, there was small decrease in the glass transition temperature of PLA with addition of hyperbranched polymer. This result indicated the presence of a small interaction of HBP with PLA. The in-situ crosslinking of HBP did not bring any further change in the glass transition temperature of PLA.

The glass transition temperature of hyperbranched polymers is reported to depend on the nature of the chain ends^[7]. The lower polarity of the end group lowers the glass transition temperature of a particular HBP. It is well established that glass transition temperature of polymers is primarily due to the segmental mobility of the polymer chains. But for HBP, it has been proposed that the glass transition occurs due to a translational movement of the entire molecule instead of a segmental movement^[7]. In present case, the end hydroxy group of HBP reacted with anhydride groups of PA to form crosslinks between different HBP molecules thus restricting their translation motion and resulted in the increase in the glass transition temperature of HBP after crosslinking. It is well known that the crosslinking reduces the molecular mobility of networked systems consisting of reactive polymers^[8]. On the other hand, the extent of depression of glass transition suggests that there was crosslinked HBP particles were in rubbery state in the PLA matrix at room temperature for all hydroxy to anhydride ratios.

4.2.2 Ultra-Centrifugation and Fourier Transform Infrared Spectroscopy of Crosslinked HBP

Table 4.2 represents estimation of reaction product of HBP and PA in the PLA matrix. It was observed that the weight fraction of tightly crosslinked particles, which were insoluble in methylene dichloride solution, increased until the OH to anhydride ratio reached to 1:1 and then it leveled off. There was less formation of highly networked

particles, when the OH to anhydride ratio was more towards hydroxy group, i.e. 4:1 and 3:1. In these two compositions, there was partial crosslinking of HBP molecules with polyanhydride, which were still soluble in methylene dichloride. It is well established that a polymer system becomes insoluble in solvents after having sufficient crosslinking. This result suggested that OH to anhydride ratio of 2:1, 1:1 and 1:2 were most effective in

Table 4.2: Estimation of amount of crosslinked hyperbranched polymer (using equation 4.1) formed in various PLA blends after in-situ crosslinking of hyperbranched polymer with different concentration of polyanhydride.

Material System	Initial wt.% of HBP in blend	Initial wt.% of PA in Blend	Weight Fraction of Insoluble Crosslinked HBP Particles	Actual wt.% of Crosslinked HBP particles
Neat PLA	-	-	-	-
PLA/HBP/PA (92:7.55:0.45) OH /anhydride 4:1	7.55	0.45	0.41±0.09	3.3
PLA/HBP/PA (92:7.4:0.6) OH/anhydride 3:1	7.4	0.6	0.55±0.07	4.4
PLA/HBP/PA (92:7.1:0.9)OH/ anhydride 2:1	7.1	0.9	0.70±0.08	5.6
PLA/HBP/PA (92:6.4:1:6) OH/anhydride 1:1	6.4	1.6	0.88±0.08	7.0
PLA/HBP/PA (92:5.4:2.6) OH /anhydride 1:2	5.4	2.6	0.90±0.05	7.2

generating sufficient crosslinking of hyperbranched polymers.

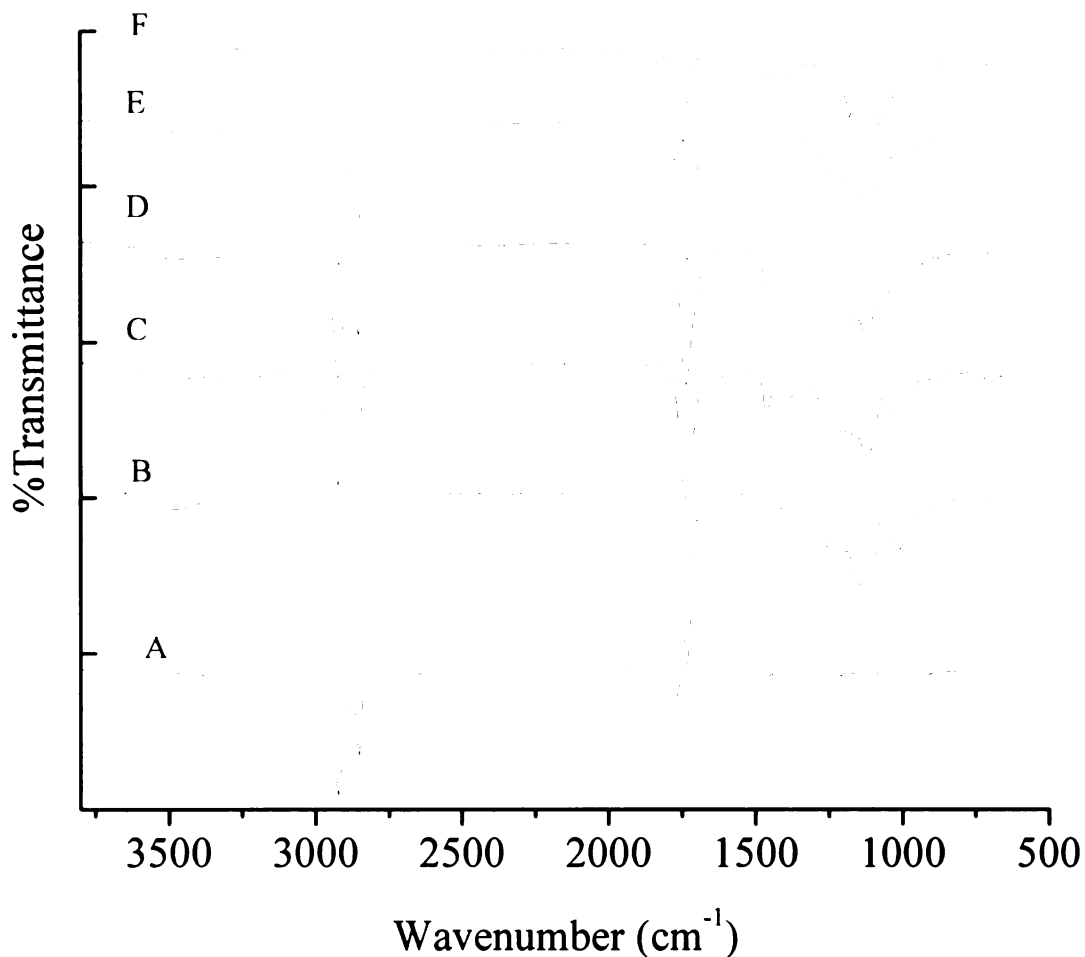


Figure 4.3: FTIR spectrum: A: Polyanhydride; B: HBP, C: Extracted HBP-PA (2:1); D: Extracted HBP-PA (1:1); E: Extracted HBP-PA (1:2); F: Neat PLA.

The FTIR spectrum of neat PLA, neat polyanhydride, neat HBP and extracted crosslinked hyperbranched polymers from the PLA matrix having OH to anhydride ratios i.e. 2:1, 1:1 and 1:2 are shown in Figure 4.3. The FTIR spectra suggested that the -OH groups of HBP readily reacts with anhydride functionalities of polyanhydride as a result there was a strong reduction in the absorption due to hydroxyl group in crosslinked HBP to that of HBP only. In case of extracted HBP particles, where OH to anhydride ratio was 2:1 and 1:1, there was no presence of unreacted anhydride group, while in case of

cHBP (OH to anhydride 1:2), there was absorption corresponding to anhydride peaks. So it is found that in PLA/cHBP blend, the presence of unreacted anhydride functionality can be minimized by using a lower amount of polyanhydride as a crosslinking agent or in other words, the HBP can be easily crosslinked by keeping low molar ratio of polyanhydride. It is expected that there might be a formation of a pseudo semi-interpenetrating network by in-situ crosslinking of HBP in the PLA phase. A perfect semi-interpenetrating network is usually formed by swelling a linear polymer with a monomer, followed by its polymerization and subsequent crosslinking^[9]. The formation of a semi-interpenetrating network also depends on the solubility of monomer in the linear polymer and the kinetics of the crosslinking reaction. In a previous research, brittle polylactide (PLA) was toughened by a poly(l-caprolactone)(PCL) diol- and triol-based polyurethane (PU) semi-interpenetrating network^[10]. In the present case, there were no characteristic FTIR absorption peaks of PLA in the FTIR spectra of the extracted crosslinked particles. This suggests that there was no true interpenetrating network between PLA and crosslinked HBP particles. There is possibility of an entangled network between crosslinked HBP and PLA, preferably at the interface of two phases.

4.2.3 Tensile Properties

The effect of varying HBP to PA weight contents, determined on the basis of OH/anhydride molar ratios, on the tensile properties of PLA is shown in Table 4.3. It is observed that a HBP to PA molar ratio as low as 2:1 was effective in improving the elongation at break of PLA. The PLA/HBP/PA (92:7.1:0.9) blend, where the OH/anhydride molar ratio was 2:1, showed about 620% improvement in the elongation at break as compared to neat PLA, while in the case of PLA/HBP/PA (92:6.4:1:6) blend

Table 4.3: Effects of HBP/ PA ratio on the tensile properties of PLA-cHBP blends.

Material Type	Tensile Modulus, GPa	Tensile Strength at Yield, MPa	Elongation at Break, %
Neat PLA	3.6±0.1	77 ±1.5	5 ±1.7
PLA/HBP/PA (92:7.55:0.45) OH to anhydride 4:1	3.3 ±0.1	60 ±1.3	9 ±1.2
PLA/HBP/PA (92:7.4:0.6) OH to anhydride 3:1	3.2 ±0.2	59 ±0.4	18 ±1.2
PLA/HBP/PA (92:7.1:0.9) OH to anhydride 2:1	3.2 ±0.1	59 ±1.5	37 ±8.5
PLA/HBP/PA (92:6.4:1:6) OH to anhydride 1:1	3.2 ±0.2	60 ±1.1	50 ±1.6
PLA/HBP/PA (92:5.4:2.6) OH to anhydride 1:2	2.8 ±0.2	64 ±1.7	48 ±6.3

(OH/anhydride, 1:1) and PLA/HBP/PA (92:5.4:2.6) (OH/anhydride, 1:2), the percent improvement was 877% and 847%, respectively. The tensile modulus and strength values of these blends were not statistically different from each other. Figure 4.4 represents the variation of elongation at break with respect to the actual amount of crosslinked HBP particles in the blend. It was found that elongation at break increased with increase in the weight % of crosslinked particles and reached a plateau for the PLA-cHBP Blends, where OH to anhydride ratio was 1:1 and 1:2. The amount of polyanhydride cross linker tend to affect the elongation at break value of PLA-cHBP blend. The crosslinked HBP particles

could be have sufficient crosslinked density and its concentration when the amount of polyanhydride was above a certain value, which is 0.9 wt.% in the composition where OH to anhydride ratio was 2: 1. Among all these compositions, the OH to anhydride ratio of 1:1 in a PLA-cHBP blend is likely to be the best optimization of OH/anhydride molar ratio. The reason for this selection is not the elongation at break only but there were minimum unreacted hydroxyl groups as well as anhydride groups in crosslinked HBP particles at this molar ratio.

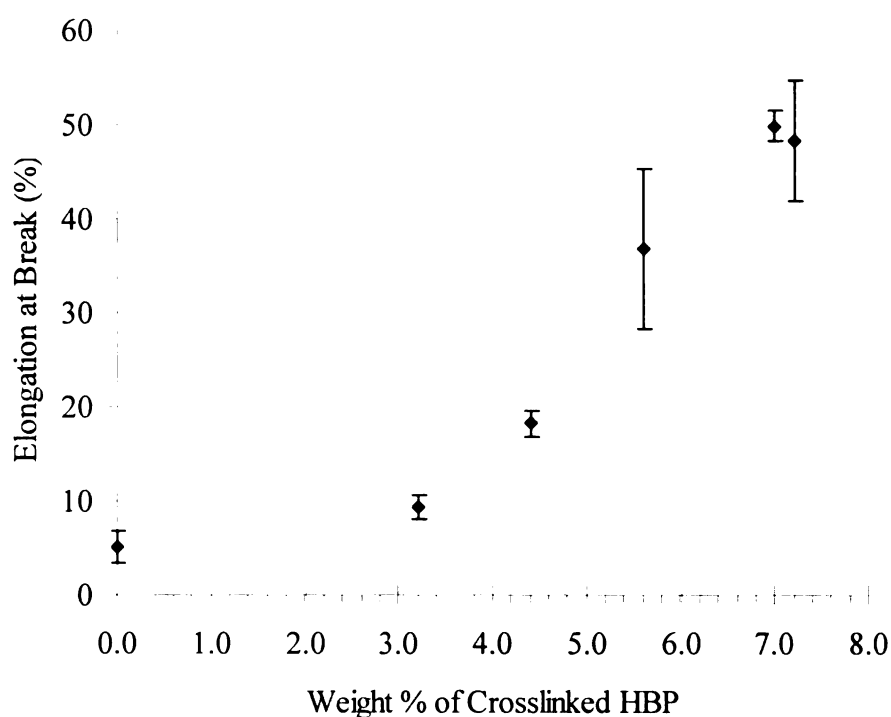


Figure 4.4: Effect of weight% of crosslinked HBP particles on the elongation at break value of PLA-cHBP blends

4.2.4 Transmission Electron Microscopy

Transmission electron microscopy (TEM) was used to study the effect of OH to anhydride ratio on the size and dispersion of crosslinked HBP in the PLA blends. It is observed that with an increase in the polyanhydride molar ratio, there was an increase in the dispersion of crosslinked HBP particles in PLA-cHBP blends. TEM photomicrographs (Figure 4.5) of PLA/HBP/PA (92:7.55:0.45) OH to anhydride, 4:1 and PLA/HBP/PA (92:7.4:0.6) OH to anhydride, 3:1 blends showed low concentration and sparse distribution of the crosslinked HBP particles, but there was an increase in the concentration of particles when the OH to anhydride ratio were 2:1, 1:1 and 1:2 (Figure 4.6, 4.7). This trend suggests that the increase in the concentration of polyanhydride provided more HBP molecules to crosslink with each other. There was evidence of better particle distribution with an increase in the polyanhydride concentration in PLA-cHBP blends. There was polydispersity in the domain size of crosslinked hyperbranched polymer in all blends, which vary from 50 nm to 400 nm. In term of mechanical properties, the PLA-cHBP blends having 2:1, 1:1 and 1:2, OH to anhydride ratio, showed better ductility as compared to those of having 4:1 and 3:1 ration. So the presence of significant number of particles in these blends helped in the energy dissipation of PLA-cHBP blends. It is well established in other parallel toughening methodologies such as rubber toughening that a critical concentration of rubber particles is required for the brittle to ductile transition^[11, 12].

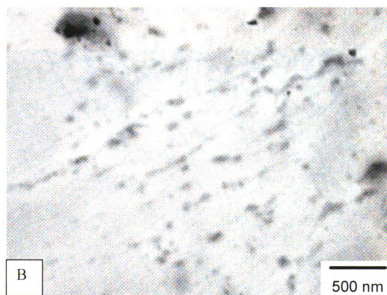
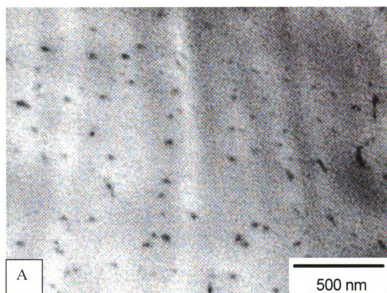


Figure 4.5: TEM photo-micrographs

A: PLA/HBP/PA (92:7.55:0.45) OH to anhydride, 4:1

B: PLA/HBP/PA (92:7.4:0.6) OH to anhydride, 3:1

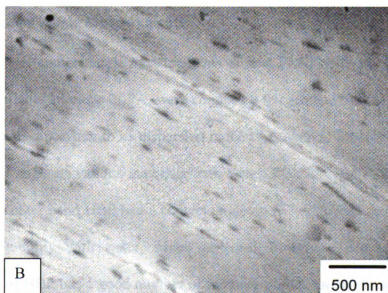
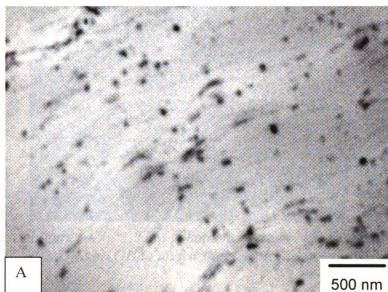


Figure 4.6: TEM photo-micrographs

A: PLA/HBP/PA (92:7.1:0.9) OH to anhydride 2:1

B: PLA/HBP/PA (92:6.4:1:6) OH to anhydride 1:1

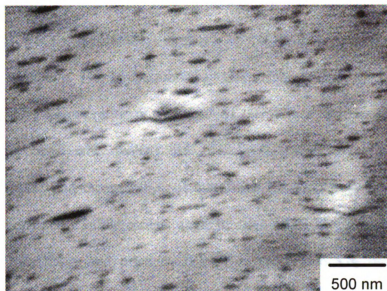


Figure 4.7: TEM photomicrograph of PLA/HBP/PA (92/5.4/2.6). OH to anhydride ratio 1:2.

4.2.5 Contact Angle Measurements

Water contact angle measurements of neat PLA, HBP, PA and crosslinked HBP having variable amounts of PA, were conducted to correlate the extent of crosslinking of hyperbranched polymer to its dispersion in the PLA matrix. Table 4.4 provides the values of contact angle of various materials with water. PLA showed a contact angle 60° with water; on other hand HBP had a contact angle of 13° only. This suggested that HBP had more wettability with water, which reflected its hydrophilic nature. The chemical structure of HBP has a good number of hydroxy groups on its periphery, which makes it hydrophilic in nature. There was a large difference in the contact angle of HBP and PLA reflecting the differences in the surface energy of two materials. When HBP was crosslinked with polyanhydride, there was considerable increase in the value of water

contact angle. The water contact angle of polyanhydride film was 88°. The polyanhydride has a polar anhydride group in its structure. So it is like that it should have a good affinity with water. However, the chemical structure of PA has a long hydrocarbon (-C₁₈H₃₃) stretch in its backbone. This hydrocarbon tail was responsible for the high water contact angle of PA. The incorporation of PA changed the surface characteristic of HBP from hydrophilic to considerably hydrophobic. This was attributed to the increase in the crosslinked density and incorporation of more hydrophobic PA in the crosslinked HBP network. The difference in the contact angle of crosslinked HBP and neat PLA was less than that of neat PLA and pristine HBP. This result indicates that there was less difference in the surface energies of crosslinked HBP and PLA. This property of crosslinked HBP helped in improving its dispersion inside the PLA matrix.

Table 4.4: Contact angle of various materials with water.

Material Type	Contact angle, θ
Neat PLA	60±3
Hyperbranched Polymer (HBP)	13±2
Polyanhydride	88±3
Extracted crosslinked HBP (2:1 OH/anhydride)	32±6
Extracted crosslinked HBP (1:1 OH/anhydride)	78±5
Extracted crosslinked HBP (1:2 OH/anhydride)	83±7

4.2.6 Effect of Processing, Presence of HBP and Crosslinked HBP on the Molecular Weight of PLA

Figure 4.8 represents the weight average molecular weight, number average molecular weight and polydispersity index of neat PLA, processed PLA, and PLA extracted from the blends of PLA-cHBP blends. The weight average molecular weight of PLA decreased by 2 and 7% with the processing cycle of 3 and 10 minutes, respectively. On the other hand, the number average molecular weight of PLA was unaffected at 3 minute of cycle time but it decreased by about 13% when PLA was processed for 10 minutes. The polydispersity index was unaffected at 3 minutes of processing cycle time

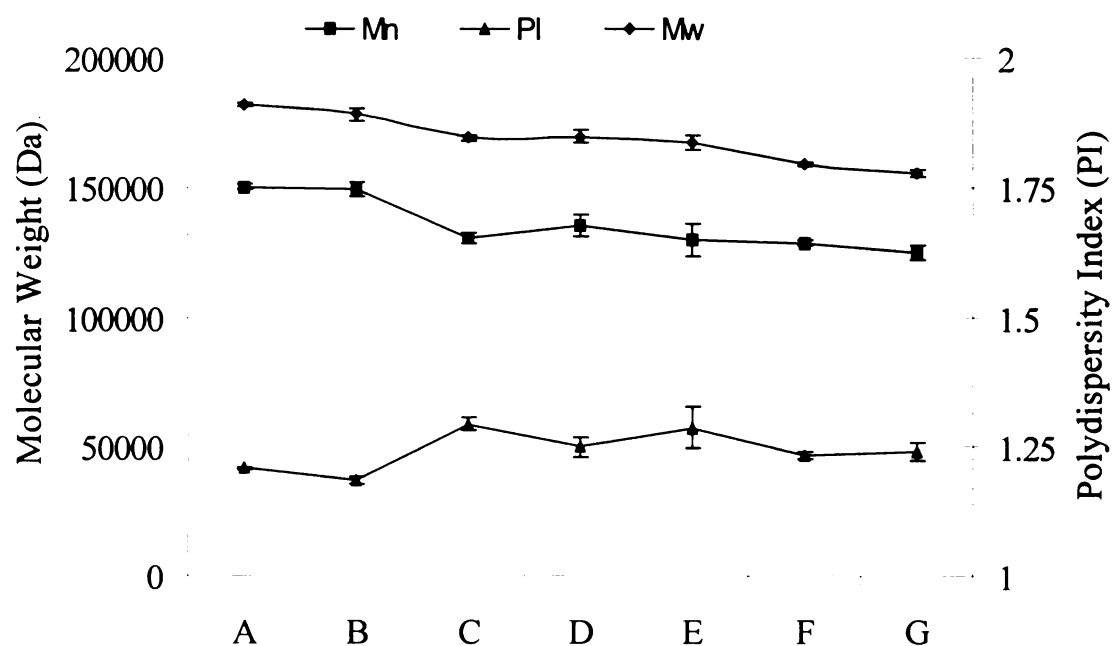


Figure 4.8: Molecular weight and polydispersity of PLA in various processing conditions, and in presence of HBP and crosslinked HBP: A: Neat PLA; B: PLA (3 min.); C: PLA (10min.); D: PLA/HBP (92/08); E: PLA/HBP/PA (92:7.1:0.9) OH to anhydride 2:1; F: PLA/HBP/PA (92:7.1:0.9) OH to anhydride 1:1; G: PLA/HBP/PA (92:7.1:0.9) OH to anhydride 1:2

but increased from 1.21 to 1.29 when PLA was processed for 10 minutes. In previous research, a decrease in the molecular weight of PLA was observed after melt processing^[13]. The molecular weight of the PLA decreased to some extent in the presence of HBP and crosslinked HBP but it was not drastic in nature. The blends of PLA with HBP and cHBP were processed for 10 minutes. The melt processing of PLA in the presence of pristine HBP caused 7% loss in weight average molecular weight and 13% loss in number average molecular weight. The presence of hydroxyl functional compounds is found to reduce the molecular weight of biopolyesters such as polyhydroxybutyrate^[14, 15]. So, it is likely that the presence of hydroxyl groups in hyperbranched polymer contributed to the reduction in the molecular weight of PLA. It was observed that there was a decrease in weight and number average molecular weight of PLA when polyanhydride crosslinker was introduced in the PLA-HBP blend. There was around 6-7 % loss in weight average molecular weight and 12-14% decrease in the number average molecular weight of PLA in the presence of cHBP having 1:1 and 1:2 OH to anhydride ratio when compared to the molecular weight of the processed PLA (10 minutes). In the case of PLA-cHBP blend where HBP to OH ratio was 2:1, there was no significant decrease in the molecular weight. The polydisperse index (PI) of these blends was not significantly different from each other. The polydispersity index (PI) was increased in the processed blend as compared to neat PLA.

4.3 References

1. Bucknall, C. B., *Rubber Toughening*. 2nd ed. Physics of glassy polymers, ed. R.N. Harward, Young, R. J. 1997, London: Chapman & Hall.
2. Liang, J. Z., Li, R. K. Y, Rubber Toughening in Polypropylene: A Review. *Journal of Applied Polymer Science*, 2000. **77**: p. 409-417.
3. Jin, H. J., Chin, I. J., Kim, M. N., Kim, S. H., Yoon, J. S., Blending of poly(L-lactic acid) with poly(cis-1,4-isoprene). *European Polymer Journal*, 2000. **36**: p. 165-169.
4. Bhardwaj, R., Mohanty, A. K., Modification of Brittle Polylactide by Novel Hyperbranched Polymer-Based Nanostructures. *Biomacromolecules*, 2007. **8**: p. 2476-2484.
5. Wu, S., A Generalized Criterion for Rubber Toughening: The Critical Matrix Ligament Thickness. *Journal of Applied Polymer Science*, 1988. **35**: p. 549-561.
6. Fox, T. G. , *Bull. Am. Phys. Soc.*, 1956. **1**: p. 123.
7. Kim, Y. H., Beckerbauer, R., Role of End-Groups on the Glass-Transition of Hyperbranched Polyphenylene and Triphenylbenzene Derivatives. *Macromolecules*, 1994. **27**(7): p. 1968-1971.
8. Gan, S., Seferis, J. C., Prime, R. B., A Viscoelastic Description of the Glass Transition-Conversion Relationship for Reactive Polymers. *Journal of Thermal Analysis*, 1991. **37**(3): p. 463-478.
9. Sperling, L. H., Mishra, V., The current status of interpenetrating polymer networks. *Polymers for Advanced Technologies*, 1996. **7**(4): p. 197-208.
10. Yuan, Y., Ruckenstein, E., Polyurethane toughened polylactide. *Polymer Bulletin* 1998. **40**: p. 485-490.
11. Bucknall, C. B., Cote, F. F. P., Partridge, I. K., Rubber Toughening of Plastics .9. Effects of Rubber Particle-Volume Fraction on Deformation and Fracture in HIPS. *Journal of Materials Science*, 1986. **21**(1): p. 301-306.
12. Bucknall, C. B., Davies, P., Partridge, I. K., Rubber Toughening of Plastics .10. Effects of Rubber Particle-Volume Fraction on the Kinetics of Yielding in HIPS. *Journal of Materials Science*, 1986. **21**(1): p. 307-313.
13. Gogolewski, S., Jovanovic, M., Perren, S. M., Dillon, J. G., Hughes, M. K., The Effect of Melt-Processing on the Degradation of Selected Polyhydroxyacids -

Poly lactides, Polyhydroxybutyrate, and Polyhydroxybutyrate-Co-Valerates. *Polymer Degradation and Stability*, 1993. **40**(3): p. 313-322.

14. Fernandes, E. G., Pietrini, M., Chiellini, E., Bio-based polymeric composites comprising wood flour as filler. *Biomacromolecules*, 2004. **5**(4): p. 1200-1205.
15. Chiellini, E.; Fernandes, E. G.; Pietrini, M.; Solaro, R., Factorial design in optimization of PHAs processing *Macromol. Symp*, 2003. **197**: p. 45-55.

Chapter 5: Phase Morphology and Brittle-to-Ductile Transition in PLA-crosslinked HBP Blends

5.0 Introduction

Toughness is a very important property of polymeric materials for many practical applications. Polymer modification techniques such as plasticization, copolymerization, rubber toughening, and polymer blends are commonly employed to improve the toughness of brittle polymers. One of the desired aims of polymer modification is to develop a polymeric system having high toughness and large plastic deformation at break, while retaining the other desirable properties such as stiffness and strength^[1]. Rubber toughening has been the most popular approach to overcome the brittleness of amorphous and semi-crystalline polymers. In such systems, rubber particles present as a dispersed phase in the continuous matrix of the brittle polymer and initiate the toughening of polymer by mean of shear yielding or multiple crazing of the matrix, and or cavitation in rubbery phase. The toughening mechanism is usually a complex combination of these events in the multi-phase polymer systems.

The semi-crystalline and amorphous polylactide fails under tensile loading by the formation of crazes^[2]. In conventional polymers, polystyrene (PS) deforms by formation of crazes. Catastrophic failures of such polymers usually occur by premature failure of crazes. Wu^[3] has correlated chain parameters such as characteristic ratio and entanglement density with craze formation in a polymer. On the other hand, various studies report that the toughness of glassy polymers can be improved considerably by incorporating rubbery particles that initiate a large density

of crazes^[4, 5]. High-impact polystyrene (HIPS) is a well known system, where multiple crazing is a well established toughening mechanism. The rubber particles can initiate crazes in the HIPS leading to reduction in the stress on a single craze and thus can prevent localized deformation as compared to neat polystyrene. Bubeck et al.^[6] found that in high-impact polystyrene (HIPS), cavitation in rubbery particles and deformation in the thin glassy ligament confined between rubber particles contribute significantly to the deformation mechanism, while the crazing is responsible for roughly half of the total plastic deformation. Wu^[7] put forward the concept of critical matrix ligament as an essential criterion for brittle to ductile transitions in rubber modified blends. Wu observed that for a brittle to ductile transition, the matrix ligament, i.e. region of matrix between two nearest rubber particles, must be equal or smaller than a critical matrix ligament thickness. The critical matrix ligament is found to be the characteristic of the matrix and influenced by the mode, temperature and rate of deformation. A percolation model for brittle –tough transition in the nylon-rubber blend was also proposed^[8], which was based on multiple connectivity of thin matrix ligaments and overlapping of stress field associated with rubber particles at particular matrix ligament thickness. In polylactide based systems, a matrix ligament thickness of 1 μ m was observed for PLA-LLDPE blend^[9].

In this chapter, different weight contents of crosslinked HBP particles having OH to anhydride ratio (1:1) were in situ synthesized in PLA-crosslinked HBP (cHBP) blends. The effects of the various weight contents of crosslinked HBP particles on the tensile properties of the blend were studied. Particle size, particle size distribution,

and interparticle distance were studied and correlated with the brittle-to-ductile transition in PLA-cHBP blends

5.1 Experimental Section

5.1.1 Reactive extrusion for fabrication of PLA-cHBP Blends

The PLA was dried for 4 hours at 40°C in a vacuum oven before processing. The HBP was dried for 4 hours at 80°C in a convection oven. The detail of all composition (wt.%/ wt.%) and their processing parameters are shown in Table 5.1. The blends were prepared by melt mixing in a microcompounder/micro-extruder

Table 5.1: Details of various PLA based compositions and their processing parameters

Material Type (wt.%/wt.%)	Processing temperature (°C) at three zones of mini-extruder				Cycle time (Minutes)	Screw Speed (rpm)	Mold Temp. (°C)
	Top	Center	Bottom	Melt			
Neat PLA	185	185	185	178	3	100	50
PLA/HBP/PA (98/1.6/0.4)	185	185	185	179	10	100	50
PLA/HBP/PA (96/3.2/0.8)	185	185	185	177	10	100	50
PLA/HBP/PA (92/6.4/1.6)	185	185	185	178	10	100	50
PLA/HBP/PA (88/9.7/2.3)	185	185	185	177	12	100	50
PLA/HBP/PA (84/12.9/3.1)	185	185	185	178	15	100	50

(DSM Research, Netherlands). The instrument is a co-rotating twin-screw microcompounder having screw length of 150 mm, L/D of 18 and barrel volume of 15cm³. The test specimens were prepared with help of a mini-injection molding machine. Initially, neat PLA was fed in to the microcompounder followed by a known amount of hyperbranched polymer (HBP) and polyanhydride (PA). The reaction was observed by monitoring the behavior of the extrusion force with time, and the appropriate cycle time was adopted depending the constancy or decrease in the force with time.

5.1.2 Testing and Characterization

5.1.2.1 Transmission Electron Microscopy (TEM)

A transmission electron microscope (TEM) (JEOL 100 CX) was used to analyze the morphology of PLA based blends at an accelerating voltage of 100 and 120 kV. Microtomed ultra thin film specimens with a thickness of less than 100 nm were used for TEM observation. Before microtomy, the bulk specimens of all blends were dipped in ruthenium tetroxide (RuO₄) solution for 3 hrs. The microtomy was carried out at room temperature using a diamond blade on a RMC microtome station.

5.1.2.2 Particle Size Analysis

The particle size analysis was performed with help of the Universal analysis software. The particle diameter, d , and interparticle distance were manually calculated using arbitrary distance measurements. This analysis was performed on at least 150 particles. The following equations^[10-12] were used for calculations.

$$\ln d = \frac{\sum_{i=1}^N n_i \ln d_i}{\sum_{i=1}^N n_i} \dots\dots\dots 5.1$$

Here, d_i is the diameter of i th particle.

$$\ln \sigma = \sqrt{\frac{\sum_{i=1}^N n_i (\ln d_i - \ln d)^2}{\sum_{i=1}^N n_i}} \dots\dots\dots 5.2$$

Here, σ represents the particle size distribution parameter, $\sigma=1$ for monodisperse system and $\sigma>1$ for polydisperse system.

5.1.2.3 Density and Volume Fraction of Crosslinked HBP Particles

The density of extracted crosslinked particles was calculated by dropping them in different concentrations of aqueous sodium chloride (NaCl) solutions. The particle were floating in salt solutions that have density more than 1.089 g/cc, while were sinking in solutions having density less than 1.059 g/cc. The density of solution, where HBP particles suspend in the solution was considered as density of particle. A table of density of various salt solutions is given in the appendix of the dissertation. The average density of the particles was found to be 1.073 gm/cc. The volume fraction of crosslinked HBP particles, ϕ_{cHBP} , was calculated from the equation 5.3.

$$\phi_{cHBP} = \rho_m w_{cHBP} / \{(\rho_m - \rho_{cHBP})w_{cHBP} + \rho_{cHBP}\} \dots\dots\dots 5.3$$

Here, ρ_m , ρ_{cHBP} are the density of polylactide, 1.25 gm/cc and the crosslinked HBP, 1.073 gm/cc. The weight fraction, W_{cHBP} , of actual crosslinked particles in each composition was calculated by equation 5.4 and the value was used in equation 5.3.

$$W_{cHBP} = \frac{W_{ins}}{W_{HBP} + W_{PA}} \dots\dots\dots 5.4$$

W_{cHBP} = Weight fraction of crosslinked HBP particles.

W_{ins} = Final weight of insoluble fraction after extraction and drying.

W_{HBP} = Initial weight of HBP in PLA composition.

W_{PA} = Initial weight of PA in PLA composition.

5.1.2.4 Tensile Properties

Tensile properties were measured using a United Calibration Corp SFM 20 testing machine as per ASTM D638. The specimens having a gage length of 2.54 mm, were tested at a strain rate of 15.4 mm/mm-min.

5.1.2.5 Scanning Electron Microscopy (SEM)

A scanning electron microscope, JEOL (model JSM-6400) was used to evaluate the morphology of tensile-fractured surfaces of the neat PLA and its blends. An accelerating voltage of 13 kV was used to produce the SEM photomicrographs.

5.2 Results and Discussions

5.2.1 Phase morphology of PLA-crosslinked HBP Blends

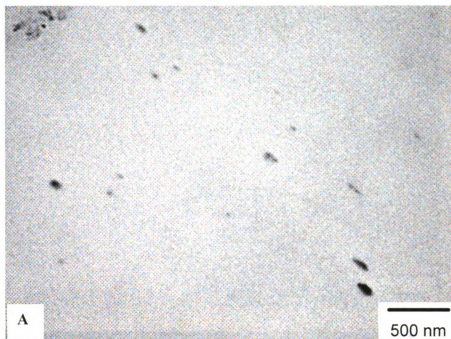


*Figure 5.1: Transmission Electron Photomicrograph (Scale bar: 500 nm); A: (PLA/HBP/PA(98/1.6/0.4)
B: PLA/HBP/PA(96/3.2/0.8)*

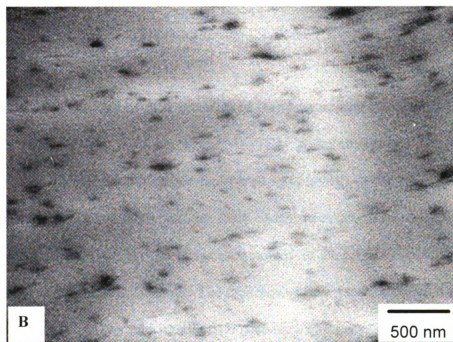
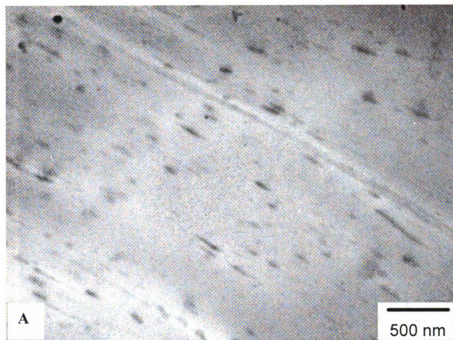


Figure 5.2: Transmission Electron Photomicrograph (Scale Bar: 500 nm); A: PLA/HBP/PA (92/6.4/1.6)
B: PLA/HBP/PA (88/9.7/2.3)

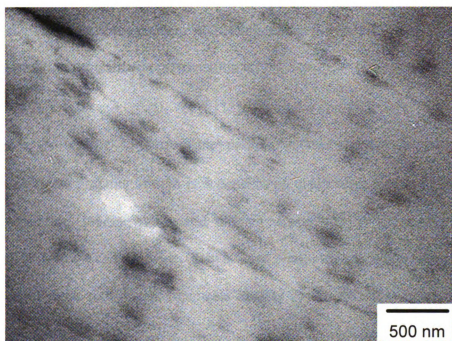


Figure 5.3: TEM photomicrograph (Scale bar: 500 nm) of PLA/HBP/PA (84/12.9/3.1)

The phase morphology of PLA-crosslinked blends were investigated with the help of transmission electron microscopy (TEM). TEM photomicrographs (Figure 5.1, 5.2 and 5.3) of all blends showed the two-phase morphology of the PLA-cHBP blends, where the cross linked HBP particles (dark phase) were present as a dispersed phase. Figure 5.1 A and B shows the phase morphology of PLA/HBP/PA (98/1.6/0.4), and PLA/HBP/PA (96/3.2/0.8) blends. The crosslinked HBP particles were well separated and there was considerable interparticle distance. The average particle size was 60 and 51 nm respectively, in these compositions. In the case of other blends i.e. PLA/HBP/PA (92/6.4/1.6) and PLA/HBP/PA (88/9.7/2.3), there was considerable increase in the particle concentration without having any significant aggregation. The interparticle distance was reduced quite significantly in these blends. The interparticle

distance, also known as matrix ligament thickness, has proven to play a significant role in the toughening mechanism of heterogeneous polymer systems. The critical criteria/condition for brittle/tough transition is ^[13]

$$\tau \leq \tau_c$$

Where τ is the surface- to- surface interparticle distance and τ_c is its critical value. The τ_c value of a polymer system is dependent on characteristic ratio of the matrix, rate, temperature, loading mode and internal stress^[14, 15]. If the matrix ligament thickness is below a critical value, then a local plane strain to plain stress transition can occur in these thin matrix ligaments leading to the reduction in the excessive hydrostatic stress^[7, 8, 13, 16, 17].

In another theory by Michler^[18], τ_c is related to the thickness of craze/bulk boundary layer. i.e.

$$\tau_c \sim 2t$$

Here t is the thickness of craze/bulk boundary layer, which is defined by the region of plastically deformed unvoided material, which consists of entanglement strands that are stretched from the undeformed state in the bulk to the deformed state in the craze interior (fibrils and voids). The thickness of this layer is found to be a characteristic of a material^[19]. It was suggested that if the matrix ligament is thinner the $2t$, shear yielding of the matrix occurs instead of crazing.

There was a polydispersity in the size (from spherical to elliptical) of crosslinked HBP particles in PLA/HBP/PA (92/6.4/1.6) and PLA/HBP/PA (88/9.7/2.3) blends. It is reported^[3] that uniform sized particles are more effective in toughening than polydisperse ones, while, asymmetric particles such as ribbons and

networks are more effective than spheroidal ones. The crosslinked particles were elliptical in shape due their orientation in the flow direction during melt processing as well as due to sample beam interaction during TEM observation, where PLA tends to expand due to high electron beam energy. The domain size of the particles varied from 50 nm to 200 nm (measuring axial length), a large population of particles were below 100 nm. The phase boundaries of crosslinked particles were highly indistinct suggesting the possibilities of a networked interface between PLA and crosslinked HBP particles. In the TEM photomicrograph of PLA/HBP/PA (84/12.9/3.1), where HBP and PA had a maximum concentration, the phase morphology was consisted of considerably larger particles (~200nm). This particular blend lacked the good distribution of particles as it was observed in the blends of (92/6.4/1.6) and PLA/HBP/PA (88/9.7/2.3). The potential reason for this difference could be the extensive phase separation of HBP from the PLA phase before its crosslinking, primarily due to the high concentration of HBP in this composition.

5.2.2 Mechanical Properties and Deformation Mechanism of PLA-crosslinked HBP Blends

In chapter 3 and 4, it was concluded that crosslinking of HBP in PLA matrix can be effectively used to improve its plastic deformation and toughness. The crosslinked HBP particles were effective, when there was a critical concentration of crosslinker i.e. 0.9 wt.% as well as of tightly crosslinked hyperbranched polymer, i.e. ~5.4 wt.%. Here, different combined weight (2, 4, 8, 12 and 16%) contents of HBP and PA at a OH to anhydride molar ratio of 1:1, were incorporated in the PLA matrix and their effect on tensile properties is studied. The detail of tensile properties of neat

PLA and PLA-cHBP blends is shown in Table 5.2, which also shows the amount of actual crosslinked particles in PLA-cHBP system, which was calculated by equation 5.4.

It was observed that the increasing weight content of crosslinked HBP improved the elongation at break of the blend. Elongation at break of PLA improve from 5.1 to 9.9 and 15.6%, respectively, when the weight content of crosslinked particles were 1.76 and 3.52% in the PLA/HBP/PA(98/1.6/0.4) and PLA/HBP/PA

Table 5.2: Effects of amount of crosslinked hyperbranched polymer of OH /anhydride ratio (1:1) on the tensile properties of PLA-cHBP blends.

Material Type (wt.%/wt%)	Wt.% of crosslinked HBP(eq. 5.4)	Tensile Modulus, GPa	Tensile Strength at Yield, MPa	Elongation at Break, %
Neat PLA	0	3.6±0.1	76.5 ±1.5	5.1 ±1.7
PLA/HBP/PA (98/1.6/0.4)	1.76	3.5 ±0.1	66.0 ±1.3	9.9 ±0.3
PLA/HBP/PA (96/3.2/0.8)	3.52	3.5 ±0.2	62.4 ±1.5	15.6 ±3.5
PLA/HBP/PA (92/6.4/1.6)	7.04	3.2 ±0.2	59.5 ±1.1	49.9±1.6
PLA/HBP/PA (88/9.7/2.3)	10.56	3.1 ±0.2	55.5 ±1.8	84.3 ±12.0
PLA/HBP/PA (84/12.9/3.1)	14.08	2.9 ±0.1	49.0 ±1.7	33.7 ±5.1

(96/3.2/0.8) blends. The critical concentration of crosslinked HBP particles for strong brittle-to-ductile transition in PLA-cHBP blends, was found to be 7.04 wt.% in the PLA/HBP/PA (92/6.4/1.6) blend, where the elongation at break of reached to 49.9%. The elongation at break reached a maximum value i.e. 84.3% for PLA/HBP/PA (88/9.7/2.3) blend but decreased for PLA/HBP/PA (84/12.9/3.1) to 33.7%. On the other hand, properties like tensile modulus and tensile strength at yield decreased with increasing amount of crosslinked hyperbranched polymer in the blend. For the highly ductile blend i.e. PLA/HBP/PA (88/9.7/2.3), the decrease in tensile modulus and tensile strength at yield was about 14% and 27% respectively, as compared with

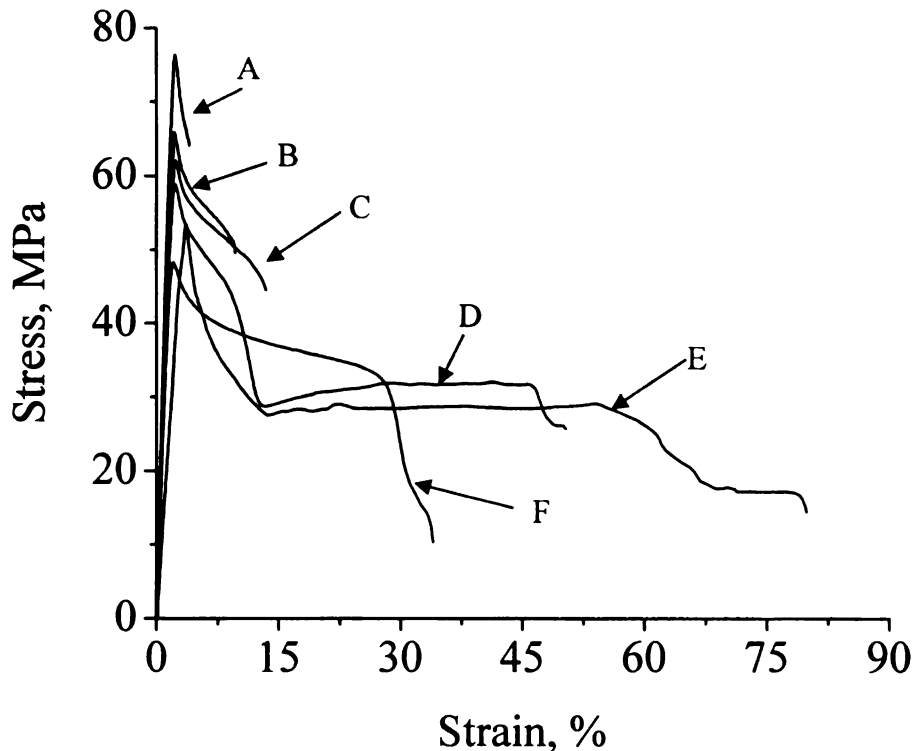


Figure 5.4: Stress – strain curves of neat PLA and various PLA-cHBP blends obtained at a strain rate of 15.4 mm/mm-min. A: Neat PLA; B: PLA/HBP/PA (98/1.6/0.4); C: PLA/HBP/PA (96/3.2/0.8); D: PLA/HBP/PA (92/6.4/1.6); E: PLA/HBP/PA (88/9.7/2.3); F: PLA/HBP/PA (84/12.9/3.1).

neat PLA. Figure 5.4 shows the stress- strain curves of the neat PLA and its blends with variable amount of crosslinked hyperbranched polymer having a similar OH to anhydride ratio of 1:1. The curves were obtained at room temperature, i.e. 23°C, at a strain rate of 15.4 mm/mm-min. It was observed that neat PLA failed in the brittle fashion after showing some strain softening behind its yield point. PLA used in this study, has a glass transition temperature of 55°C, it will be in a glassy state at room temperature. Its crystalline structure would be frozen-in at room temperature and its deformation would be primarily dictated by the amorphous region. There is an established conformity that crazes are the main precursor of failure of glassy polymers^[20,21]. In case of PLA, high chain stiffness and low entanglement density of can be the reasons for formation of crazes, leading to its catastrophic failure. A

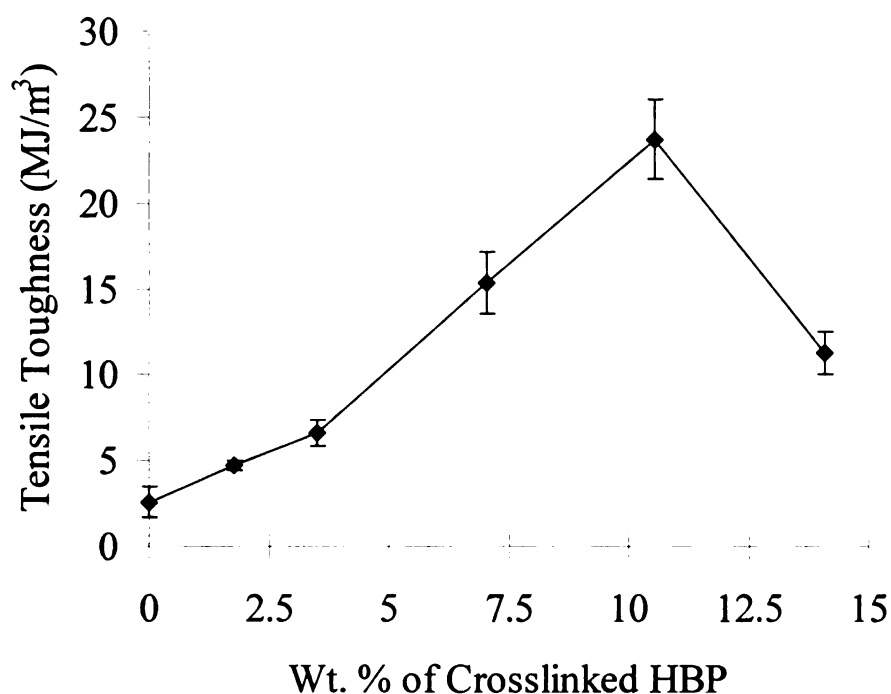


Figure 5.5: Effect of concentration of crosslinked hyperbranched polymer on the tensile toughness of neat PLA and PLA-cHBP blends

localized nature of crazes put a limitation on energy dissipation and leads to premature craze failure, causing the brittleness of a polymer.

In the present system, in-situ synthesis of crosslinked hyperbranched polymer particles in the PLA matrix was found to delay its premature craze/brittle failure (Figure 5.4). A considerable plastic deformation of the PLA/cHBP blend was observed when the weight contents of crosslinked particles were 7.04 and 10.56%. A minimum concentration of crosslinked HBP particles i.e. 7.04 wt% was found to be effective for brittle to ductile transition in the investigated PLA-cHBP blends. The ductile PLA-cHBP blends showed significant post yield deformation by the mechanism of strain softening and cold drawing. Figure 5.5 represents the variation of tensile toughness (area under the stress-strain curve) as a function of weight contents of cHBP particles. The tensile toughness showed an increasing trend from 2.3 MJ/m³ for neat PLA to a maximum of 23.7 MJ/m³ when 10.56 wt.% of cHBP particles i.e. for PLA/HBP/PA(88%/9.7%/2.3%) blend, was present and declined to 11.3 MJ/m³ for 14.08 wt.% of cHBP particles in PLA/HBP/PA (84%/12.9%/3.1%) blend. The flocculation of particles and loss of finely distributed particle morphology were the potential reasons for the decline in the tensile toughness at this concentration.

The SEM photomicrograph (Figure 5.6 and 5.7) revealed that the tensile fractured surface of neat PLA and various PLA-cHBP blends. The fracture surface of neat PLA was flat and showed its brittle nature (Figure 5.6 A). The surface characteristics of the tensile fractured surfaces changed progressively from flat to rougher, when the weight contents of cHBP increased in the blends. A marked change in the morphology of fractured surface was observed when the weight contents of

cHBP concentration were 7.04 and 10.56%. In these blends, the matrix was highly drawn and formed fibrils, which strongly indicated shear yielding of the polylactide matrix. This suggest that the onset of the brittle to ductile transition started at 7.04 wt.% of cHBP. The surface characteristics of PLA-cHBP blend having 14.08 wt.% of cHBP were not significantly different from the blends having 7.04 and 10.56 wt.% of cHBP.

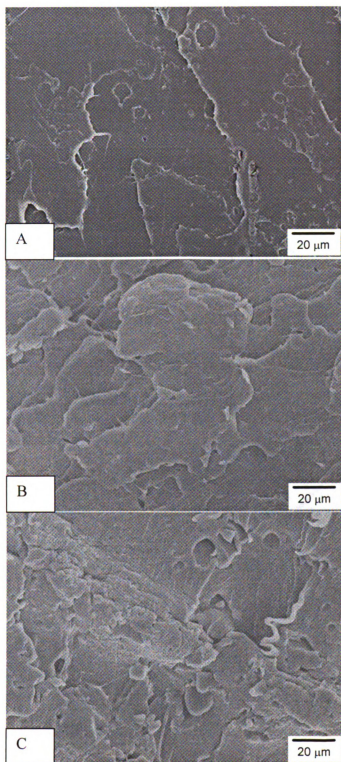


Figure 5.6: SEM photomicrograph of tensile fractured samples. A: Neat PLA
B: (PLA/HBP/PA (98/1.6/0.4)
C: PLA/HBP/PA(96/3.2/0.8)

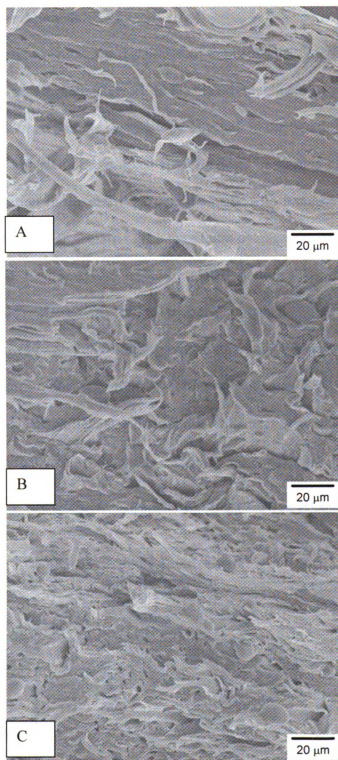


Figure 5.7: SEM photomicrograph of tensile fractured samples.

A: PLA/HBP/PA (92/6.4/1.6)

B: PLA/HBP/PA (88/9.7/2.3)

C: PLA/HBP/PA (84/12.9/3.1)

5.2.3 Particle Size Analysis

In the present section, the discussion of the PLA/HBP/PA (84/12.9/3.1) blend is omitted due to its anomalous effect on the tensile toughness of polylactide and an absence of well defined particle morphology of cHBP in the blend. Table 5.3 presents the particle size analysis of crosslinked HBP particles in various PLA-cHBP blends. There was a variation in the cHBP particle diameter with increase in the amount of crosslinked HBP in the PLA matrix. The maximum average particle diameter was 97 nm in the blend having 10.56 wt.% of cHBP particles i.e. for PLA/HBP/PA (8/9.7/2.3) blend . There was no clear trend obtained from the particle size distribution parameter value but it indicated towards polydisperse size of crosslinked HBP in PLA matrix. The minimum polydispersity occurred in the PLA/HBP/PA (88/9.7/2.3) blend. The particle size distribution parameter σ was found to 1.56 in the PLA/HBP/PA (92/6.4/1.6), while it was 1.31 in the PLA/HBP/PA (88/9.7/2.3) blend.

Table 5.3: Particle size characteristics of crosslinked HBP particles in PLA-cHBP blends.

Materials	Diameter (nm) of crosslinked HBP particles			Particle size distribution Parameter, σ
	Mean	Median	Mode	
PLA/HBP/PA (98/1.6/0.4)	60	40	54	1.45
PLA/HBP/PA (96/3.2/0.8)	51	49	49	1.39
PLA/HBP/PA (92/6.4/1.6)	86	72	50	1.56
PLA/HBP/PA (88/9.7/2.3)	97	90	68	1.31

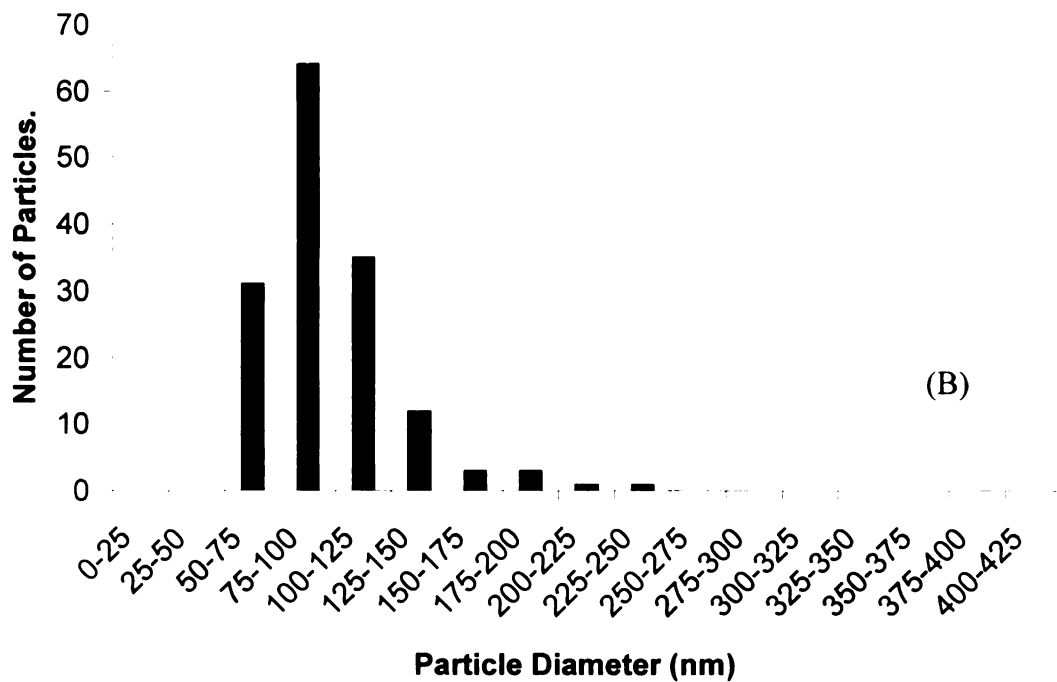
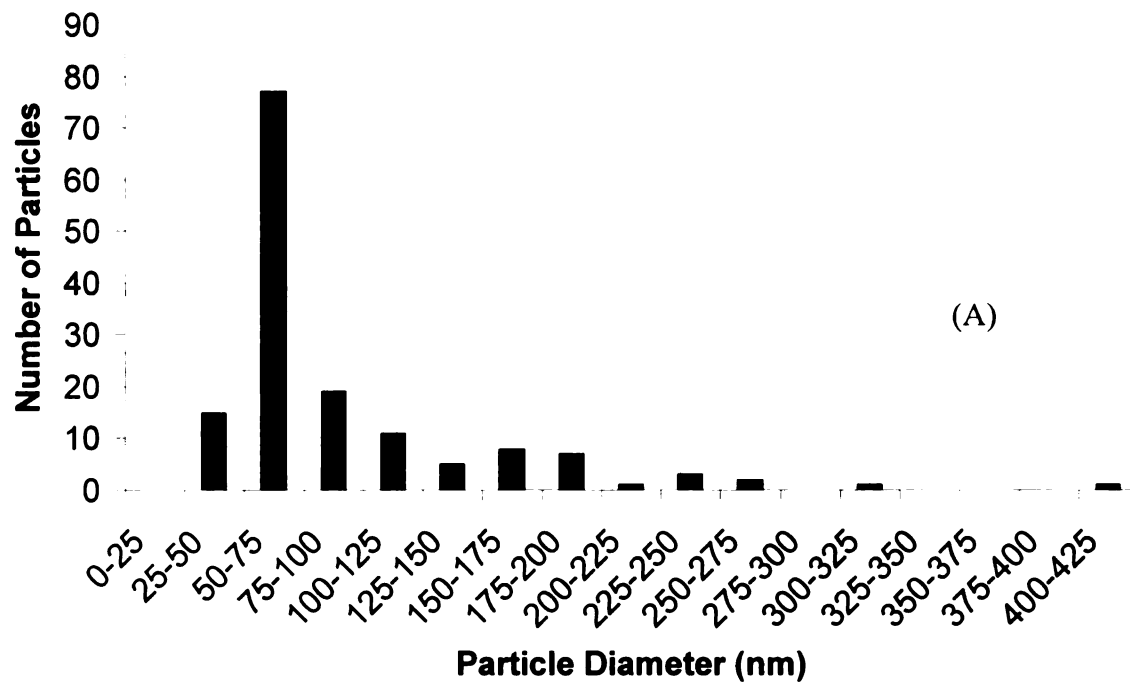


Figure 5.8: Particle size distribution of crosslinked HBP particles.
 (A) PLA/HBP/PA (92/6.4/1.6); (B) PLA/HBP/PA (88/9.7/2.3)

The histograms of cHBP particles in ductile blends, i.e. PLA/HBP/PA (92/6.4/1.6) and PLA/HBP/PA (88/9.7/2.3), are presented in Figure 5.8. The histograms showed the polydispersity of the crosslinked particles in these blends. In case of PLA/HBP/PA (92/6.4/1.6) blend, a major population of crosslinked HBP resided in the diameter interval of 50-75 nm, while in case of the PLA/HBP/PA (88/9.7/2.3) blend, the major population of particles had diameters between 75-100 nm. The particle size distribution spread was low in case of PLA/HBP/PA (88/9.7/2.3), compared to that of PLA/HBP/PA (92/6.4/1.6) blend. This suggested that the crosslinking reaction was more controlled in PLA/HBP/PA (88/9.7/2.3) blend and resulted in the particles having more uniform sizes.

5.2.4 Brittle-to-Ductile Transition in PLA-crosslinked HBP Blend

Wu et al.^[7, 13] suggested that a sharp brittle to ductile transition occurs in rubber modified plastics, when the inter-particle distance, also known as matrix ligament thickness, is smaller than a critical value. They observed this phenomenon in nylon-rubber blends^[13]. Figure 5.9 shows schematics of the matrix ligament

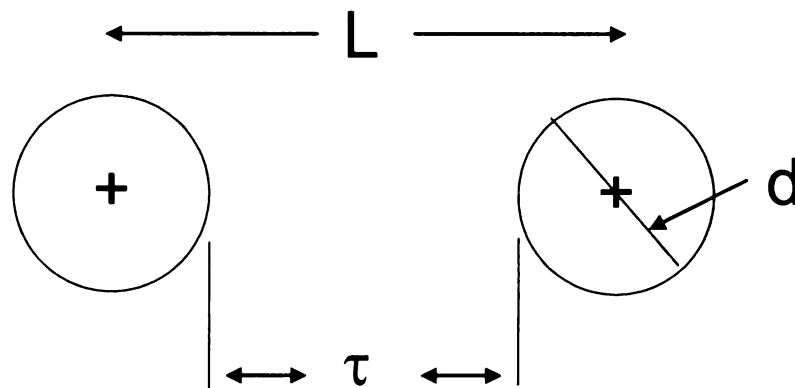


Figure 5.9: Schematic of Matrix Ligament Thickness. Redrawn after ref. 7.

thickness, where τ is the matrix ligament thickness, d is the diameter of particles and L , is the distance between the centers of the particles.

The condition of toughening in case the of brittle matrices is

$$\tau \leq \tau_c$$

Where τ is the surface- to- surface interparticle distance and τ_c is its critical value.

The matrix ligament thickness is correlated with the chain stiffness/or characteristic ratio of the polymer, where the critical matrix ligament thickness decreases with an increase in the characteristic ratio of the matrix^[3].

The theoretical calculation of matrix ligament thickness can be obtained from the following equations.

The matrix ligament thickness (T) of the monodisperse system can be related to particle diameter (d) and volume fraction (ϕ). Wu^[13] obtained an equation assuming that the particle occupies a cubic lattice in a system. The equation is given as

$$T(d, \phi) = d[(\pi / 6\phi)^{1/3} - 1] \dots\dots\dots 5.5$$

Wu^[7] later incorporated the parameter of particle size distribution parameter, σ , in equation 5.5 and obtained equation 5.6.

$$T = d[(\pi / 6\phi)^{1/3} - 1] \exp(\ln^2 \sigma) \dots\dots\dots 5.6$$

Equation 5.6 was further modified by Liu et al.^[12] for the calculation of matrix ligament thickness of a polymer blend having well dispersed polydisperse particle morphology. The equation 5.7 is as follows

$$T = d[(\pi / 6\phi)^{1/3} \exp(1.5 \ln^2 \sigma) - \exp(0.5 \ln^2 \sigma)] \dots\dots\dots 5.7$$

In PLA-crosslinked HBP blends, with increase in the volume fraction of crosslinked hyperbranched polymer, matrix ligament thickness or interparticle distance decreased (Figure 5.10). This was due to the increase in number density of crosslinked HBP particles with increase in the volume fraction of crosslinked HBP particles. The average matrix ligament thickness decreased from 461 nm to 72 nm, when the volume fraction of crosslinked HBP particles was increased from 0.02 i.e. in PLA/HBP/PA (98/1.6/0.4) blend to 0.12 i.e. in PLA/HBP/PA (88/9.7/2.3) blend. The decrease in the matrix ligament with increase in the volume fraction was evident from the TEM photomicrograph of various PLA-cHBP blends ((Figure 5.1, 5.2 and 5.3). The increase in the number of thinner matrix ligaments with increase in the volume fraction of crosslinked HBP particles was also observed from these TEM photomicrographs.

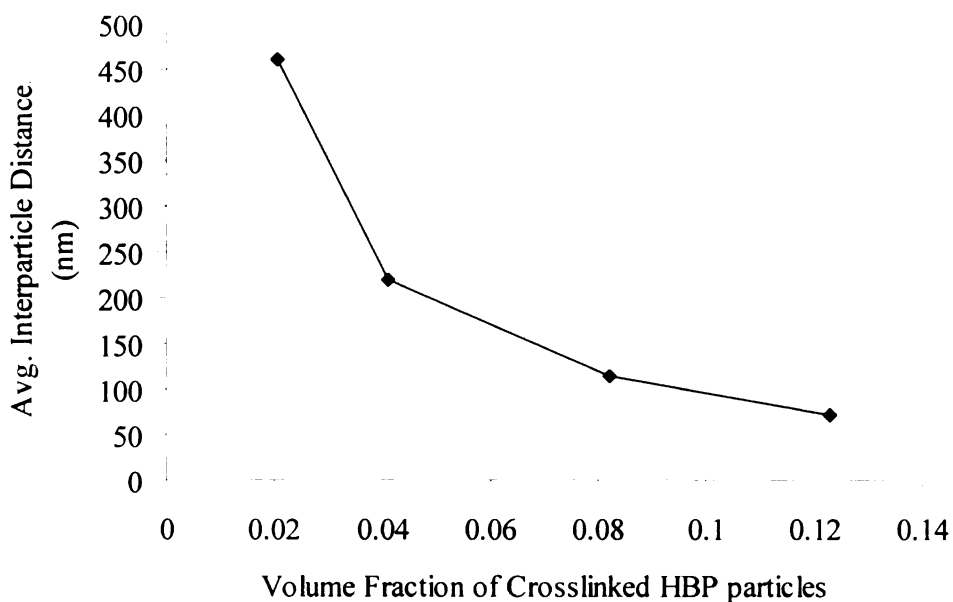


Figure 5.10: Effect of volume fraction on the inter-particle distance of crosslinked HBP particles in PLA-cHBP Blends

On the other hand, the tensile toughness was found to increase with decrease in the matrix ligament thickness (inter-particle distance) for various PLA–crosslinked HBP blends and the onset of brittle to ductile transition was observed for the PLA/HBP/PA (92/6.4/1.6) blend, where the matrix ligament thickness was 114 nm (Figure 5.11). The tensile toughness of this blend was 15.3 MJ/m³ as compared to 6.6 and 4.7 MJ/m³ for the blends of PLA/HBP/PA (96/3.2/0.8) and PLA/HBP/PA (98/1.6/0.4), where the average matrix ligament thickness was 219 and 461 nm, respectively. The tensile toughness further increased to 23.7 MJ/m³ when the average matrix ligament thickness decreased to 72 nm for PLA/HBP/PA (88/9.7/2.3) blends. This suggested that there was an increase in the number of thinner ligaments with increase in the volume fraction of crosslinked HBP particles. The experimental value of matrix ligament thickness in toughened blends, were compared with theoretical values obtained from equations 5.5, 5.6 and 5.7 and given in Table 5.4

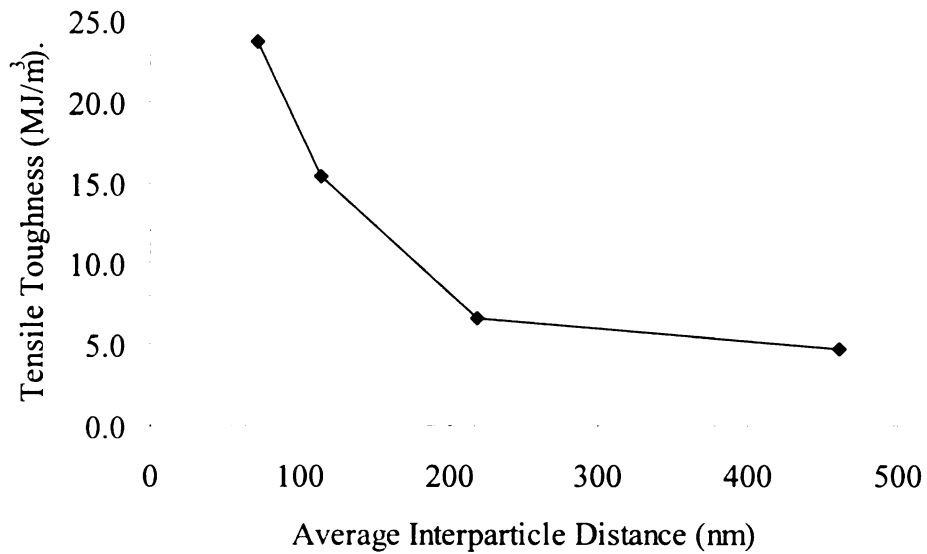


Figure 5.11: Effect of inter-particle distance on the tensile toughness of PLA-cHBP blends.

Table 5.4: Comparison of experimental matrix ligament thickness with theoretical values for toughened nanoblends; here type A: PLA/HBP/PA (88/9.7/2.3. type B: PLA/HBP/PA, (92/6.4/1.6).

Matrix Ligament Thickness	Particle Morphology	Type A	Type B
Experimental Matrix Ligament Thickness, nm		72	114
$T(d, \phi) = d[(\pi/6\phi)^{1/3} - 1]$, nm	Monodisperse	42	97
$T = d[(\pi/6\phi)^{1/3} - 1]\exp(\ln^2 \sigma)$, nm	Polydisperse	45	116
$T = d[(\pi/6\phi)^{1/3} \exp(1.5 \ln^2 \sigma) - \exp(0.5 \ln^2 \sigma)]$, nm	Polydisperse with well dispersion	54	145

Wu^[7, 13] suggested that shear yielding can take place in matrix ligaments, when their thickness is below a critical matrix ligament thickness. An essential condition for this to happen is that there should be a reduction in triaxial dilative stress in these thin ligaments. This is usually happen by the cavitation in rubber particles. It is also suggested that the cavitation is indeed not necessary to relieve the triaxial stress state; a dispersed phase having modulus lower than that of the matrix modulus can relieve this stress state in these thin ligaments^[7, 8]. This can facilitate a plane strain-to-plane stress transition in these ligaments leading to their shear yielding. In present PLA-crosslinked HBP blends, the dispersed phase i.e. crosslinked HBP has a low glass transition temperature, and expectedly low modulus than the PLA matrix. When these particles were present above a certain volume fraction, the extremely thin matrix ligaments formed in the PLA-cHBP blend. As shown in Chapter 3, the

crosslinked HBP particles tend to extend under tensile loading. By this mechanism, the triaxial stress state in thin matrix ligaments could be relieved and helped in their shear yielding. So, the inter-particle distance or matrix ligament thickness was found to be a critical parameter in the toughening of PLA-CHBP blends.

5.3 References

1. Michler, G. H., Adhikari, R., Henning, S., Toughness Enhancement of Nanostructured Amorphous and Semicrystalline Polymers. *Macromol. Symp.*, 2004. **214**: p. 47-71.
2. Kulinski, Z., Piorkowska, E., Crystallization, structure and properties of plasticized poly(L-lactide). *Polymer*, 2005. **46**(23): p. 10290-10300.
3. Wu, S., Chain structure, phase morphology, and toughness relationships in polymers and blends. *Polymer Engineering and Science*, 1990. **30**(13): p. 753-761.
4. Michler, G. H., The Role of Interparticle Distance in Maximizing the Toughness of High-Impact Thermoplastics. *Acta Polymerica*, 1993. **44**(3): p. 113-124.
5. Magalhaes, A. M. L., Borggreve, R. J. M., Contribution of the Crazing Process to the Toughness of Rubber-Modified Polystyrene. *Macromolecules*, 1995. **28**(17): p. 5841-5851.
6. Bubeck, R. A., Buckley, D. J., Kramer, E. J., Brown, H. R., Modes of Deformation in Rubber-Modified Thermoplastics During Tensile Impact. *Journal of Materials Science*, 1991. **26**(23): p. 6249-6259.
7. Wu, S. H., A Generalized Criterion for Rubber Toughening - the Critical Matrix Ligament Thickness. *Journal of Applied Polymer Science*, 1988. **35**(2): p. 549-561.
8. Margolina, A., Wu, S. H., Percolation Model for Brittle-Tough Transition in Nylon Rubber Blends. *Polymer*, 1988. **29**(12): p. 2170-2173.
9. Anderson, K. S., Lim, S. H., Hillmyer, M. A., Toughening of polylactide by melt blending with linear low-density polyethylene. *Journal of Applied Polymer Science*, 2003. **89**(14): p. 3757-3768.
10. Premphet, K., Paecharoenchai, W., Quantitative Characterization of Dispersed Particle Size, Size Distribution, and Matrix Ligament Thickness in Polypropylene Blended with Metallocene Ethylene-Octene Copolymers. *Journal of Applied Polymer Science*, 2001. **82**: p. 2140-2149.
11. Irani, R. R., Callis, F. C., *Particle Size: Measurement, Interpretation and Application*. 1963, New York: Wiley.
12. Liu, Z. H., Zhang, X. D., Zhu, X. G., Qi, Z. N., Wang, F. S., Effect of morphology on the brittle ductile transition of polymer blends: 1. A new

- equation for correlating morphological parameters. *Polymer*, 1997. **38**: p. 5267-5273.
13. Wu, S. H., Phase-Structure and Adhesion in Polymer Blends - a Criterion for Rubber Toughening. *Polymer*, 1985. **26**(12): p. 1855-1863.
 14. Borggreve, R. J. M., Gaymans, R. J., Luttmer, A. R., Influence of Structure on the Impact Behavior of Nylon-Rubber Blends. *Makromolekulare Chemie-Macromolecular Symposia*, 1988. **16**: p. 195-207.
 15. Flexman, E. A., New High-Impact Acetal Elastomer Has Broader Use Potentials. *Modern Plastics*, 1985. **62**(2): p. 72-76.
 16. Wu, S. H., Margolina, A., Percolation Model for Brittle Tough Transition in Nylon Rubber Blends - Reply. *Polymer*, 1990. **31**(5): p. 972-974.
 17. Wu, S. H., Impact Fracture Mechanisms in Polymer Blends - Rubber-Toughened Nylon. *Journal of Polymer Science Part B-Polymer Physics*, 1983. **21**(5): p. 699-716.
 18. Michler, G. H., *Private Communication*, in *32nd Microsymposium on Polymer Blends*. 1989: Prague, Czechoslovakia.
 19. Michler, G. H., Crazes in Amorphous Polymers .1. Variety of the Structure of Crazes and Classification of Different Types of Crazes. *Colloid and Polymer Science*, 1989. **267**(5): p. 377-388.
 20. Kramer, E. J., Microscopic and Molecular Fundamentals of Crazing. *Advances in Polymer Science*, 1983. **52-3**: p. 1-56.
 21. Kambour, R. P., Structure and Properties of Crazes in Polycarbonate and Other Glassy Polymers. *Polymer*, 1964. **5**(3): p. 143-155.

Chapter 6: Conclusions and Recommendations for Future Work

6.1 Conclusions

A nanostructure-controlled polylactide (PLA) was created by in-situ cross-linking of a hyperbranched polymer (HBP) in the PLA matrix through reactive melt blending. The generation of new HBP-based nanostructures in the PLA matrix improved the tensile toughness and elongation at break more than 500% and 800%, respectively, as compared to unmodified PLA. The modified PLA remarkably maintained high strength and modulus values. The cross-linking reaction of HBP was confirmed by the FTIR analysis and DMTA analysis. The transmission electron microscopy and atomic force microscopy observations of modified PLA confirmed the nanoscopic dimensions of cross-linked HBP particles in the PLA matrix. The scanning electron microscopy analysis clearly exhibited the toughening of PLA. The toughening mechanism of PLA was comprised of shear yielding and crazing. The TEM photomicrograph of deformed regions of neat PLA showed micron size crazes in neat PLA. On other hand, there was extension of craze fibrils in the modified PLA, which was correlated with the stabilization of these crazes. The crosslinked HBP particles were found to extend under tensile loading and helped in the energy dissipation mechanism. There was no cavitation observed in the crosslinked HBP particles. Rheological studies revealed that there was a network formation in PLA matrix after in-situ crosslinking of HBP. The HBP was found to reduce the melt viscosity of PLA dramatically and this effect was maintained even after its in-situ crosslinking in PLA matrix.

The effect of crosslinker concentration on the mechanical properties of PLA-crosslinked HBP blend was studied. It was found that the amount of crosslinked HBP synthesized inside the PLA matrix increased with the increase in the concentration of polyanhydride crosslinker. The increased weight fraction of crosslinked HBP in PLA matrix was found to have a promising effect on the elongation at break value of polylactide. The onset of the brittle to ductile transition for polylactide was observed when hydroxyl (OH) to anhydride ratio was 2:1 for a blend having 92 wt.% PLA/7.1 wt.%HBP/0.9 wt.% PA. The toughening effect originated from the amount of crosslinked HBP formed inside the PLA matrix. The crosslinking of HBP was observed with the help of dynamic mechanical thermal analysis by monitoring the glass transition temperature obtained from the relaxation peak associated with loss modulus. The glass transition temperature values of the crosslinked HBP phase were correlated with the Fox equation and found to deviate from it when OH to anhydride ratios were 2:1, 1:1 and 1:2 for crosslinked HBP. The hydrophilic nature of the hyperbranched polymer was altered to hydrophobic by incorporation of polyanhydride crosslinker, as demonstrated by the increase in the contact angle with water. Gel permeation chromatography (GPC) revealed that there was no dramatic decrease in the molecular weight of PLA in the presence of pristine as well as crosslinked HBP.

The concentration of crosslinked HBP having OH to anhydride ratio (1:1) was varied from 2 to 16 wt.% by in-situ synthesizing them in PLA matrix, for understanding the brittle-to-ductile transition in modified PLA. It was observed that toughness was dependent on the volume fraction of crosslinked HBP and matrix ligament thickness (inter-particle distance) in the modified blends. The tensile toughness was found to

increase with increase in volume fraction and decrease in the matrix ligament thickness. The maximum critical matrix ligament thickness was found to be 114 nm for PLA/HBP/PA (92wt.%/7.4wt.%/1.6wt.%), which further reduced to 72 nm for PLA/HBP/PA (88wt.%/9.7wt.%/2.3 wt.%) blend. The experimental matrix ligament thickness values were correlated with the values obtained from theoretical equations. Shear yielding in these thin ligaments was likely the most effective toughening mechanism in the toughened polylactide nanoblends.

Finally, hyperbranched polymer-based modification of polylactide resulted in a high performance polylactide based material having good mechanical and rheological properties. The current research unwraps new opportunities available to us from the unique physical and chemical properties of the highly functional hyperbranched polymers in generating new nanostructured multiphase polymer systems with enhanced properties.

6.2 Recommendations for Future Work

Polylactide has shown much promise towards building of a bioplastic regime, where it will play a pivotal role due to its affordable cost and useful property attributes. Unconventional research methodology must be encouraged to improve the PLA properties. The present work revealed that hyperbranched polymers can provide a gateway to such kind of research in the field of PLA based materials. There is still vast opportunity available to us for tailoring the architecture of HBP and study its influence on the PLA properties. HBP modified PLA can generate new materials, which can have applications ranging from packaging to automotives.

In the present system, structural modification of a second generation of hydroxyl functional aliphatic hyperbranched polymer is carried by in-situ crosslinking it in the

PLA matrix. This work can be extended to higher generation of hyperbranched polymers, which will have an effect on the size and molecular weight between crosslinks of crosslinked hyperbranched polymer. In this way, we can tailor the glass transition temperature and modulus of the crosslinked HBP particles. In present system, a polyanhydride is used for crosslinking of hyperbranched polymer. A crosslinker having better compatibility with polylactide base resin can be opted for the improved compatibilization effect in the PLA-cHBP blends. Interfacial adhesion of PLA-crosslinked HBP blend can be investigated to understand its local deformation mechanism.

Beside crosslinking, end capping of hyperbranched polymer with compounds compatible with polylactide can be attempted. This can generate new nano-size core-shell particles. Such particles can be studied for their toughening effect on polylactide. The hyperbranched polymers have been used for reducing interfacial tension in conventional polymer blends. Such approach can be used in bioplastics based blends.

The modified PLA can be used as a base resin for filler reinforcement such as talc and nano-clay. The functional nature of crosslinked HBP can provide compatibility between the filler and the PLA matrix. In this way, properties such as heat deflection temperature and gas barrier of the modified resin can be improved, along with preserving its toughness. Effects of rigid filler enhanced toughening in modified PLA can also be investigated. The lowered melt viscosity of PLA in presence of crosslinked HBP can provide ideal conditions for the filler dispersion. Such concepts can be extended to polymer-polymer blends and fiber reinforced composites.

7: Appendix: Density of NaCl Salt Solutions of Different Concentrations

Density Table of NaCl Salt Solutions of Different Concentrations

S.No	Wt of Nacl Salt, gm	Volume of Solution, ml	Weight of Solution, gm	Density of solution, gm/CC
1	5.3148	100	102.9609	1.0296
2	8.7154	100	105.0367	1.0503
3	9.3146	100	105.4965	1.0549
4	9.8930	100	105.9073	1.0590
5	11.5530	100	106.9443	1.0694
6	12.0067	100	107.2864	1.0728
7	14.6050	100	108.9893	1.0898
8	20.3524	100	113.7321	1.1373

MICHIGAN STATE UNIVERSITY LIBRARIES



3 1293 02956 6035